The Prevalence of Killer Yeasts in the Gardens of Fungus-Growing Ants and the Discovery of Novel Killer Toxin named Ksino.

Rodolfo Bizarria Jr.[a,b], Jack W. Creagh[a], Tanner J. Badigian[a], Renato A. Corrêa dos Santos[c], Sarah A. Coss[a], Rim T. Tekle[a], Noah Fredstrom[d], F. Marty Ytreberg[e.f], Maitreya J. Dunham[d], Andre Rodrigues[b]*, Paul A. Rowley[a,f]*

[a]Department of Biological Sciences, University of Idaho, Moscow, Idaho, USA.

[b]Department of General and Applied Biology, São Paulo State University (UNESP), Institute of Biosciences, Rio Claro, São Paulo, Brazil.

[c]Laboratory of Computational, Evolutionary, and Systems Biology, Center for Nuclear Energy in Agriculture, University of São Paulo (USP), Piracicaba, São Paulo, Brazil

[d]Department of Genome Sciences, University of Washington, Seattle, WA 98195, USA.

[e]Department of Physics, University of Idaho, Moscow, ID, 83844, USA.

[f]Institute for Modeling Collaboration and Innovation, University of Idaho, Moscow, ID, 83844, USA.

*Corresponding authors

Abstract

Killer toxins are proteinaceous antifungal molecules produced by yeasts, with activity against a wide range of human and plant pathogenic fungi. Fungus gardens of attine ants in Brazil were surveyed to determine the presence of killer toxin-producing yeasts and to define their antifungal activities and ecological importance. Our results indicate that up to 46% of yeasts isolated from specific fungal gardens can be killer yeasts, with an overall prevalence of 17% across all strains tested. Killer yeasts were less likely to inhibit the growth of yeasts isolated from the same environment but more effective at inhibiting yeast isolated from other environments, supporting a role for killer yeasts in shaping community composition. All

killer yeasts harbored genome-encoded killer toxins due to the lack of cytoplasmic toxin-encoding elements (i.e., double-stranded RNA satellites and linear double-stranded DNAs). Of all the killer yeasts identified, an isolate of *Candida sinolaborantium* showed a broad spectrum of antifungal activities against 57% of yeast strains tested for toxin susceptibility. The complete genome sequence of *C. sinolaborantium* identified a new killer toxin, Ksino, with primary and tertiary structure homology to the *Saccharomyces cerevisiae* killer toxin named Klus. Genome-encoded homologs of Ksino were found in yeast strains of *Saccharomycetes* and *Pichiomycetes*, as well as other species of Ascomycota and Basidiomycota filamentous fungi. This demonstrates that killer yeasts can be widespread in attine ant fungus gardens, possibly influencing fungal community composition and the importance of these complex microbial communities for discovering novel antifungal molecules.

Keywords: Killer yeasts, Killer toxins, Antifungals, Budding yeast, Fungus-growing ants

Importance

Attine ants perform essential ecosystem services through the harvesting of substrates for fungiculture. Cultured fungi are a food source for attine ants. Characterizing antifungal toxin-producing yeasts (killer yeasts) is vital to understanding how they might protect gardens from invasion by unwanted fungal species. This study describes a new toxin named Ksino from the yeast *Candida sinolaborantium*, a member of a new group of putative toxins found across many different species of fungi. This work supports the role of killer yeasts in the ecology of fungicultures and competition between fungi. The observed high prevalence of killer yeasts in fungal gardens also enables the discovery of novel antifungal molecules with the potential to be applied against disease-causing fungi.

1. Introduction

Killer yeasts were first described in *Saccharomyces cerevisiae* in the 1960s (Makower and Bevan, 1963; Woods and Bevan, 1968), after which many strains and species of yeasts and yeast-like fungi were also observed to secrete antifungal killer toxins (Woods and Bevan,

1968; Golubev et al., 2002; Pfeiffer et al., 2004; Koltin and Day, 1976; Castillo and Cifuentes, 1994). Killer toxins can have a range of antifungal activities ranging from narrow to broad specificities, affecting cells from close or distantly related fungal species (Boynton, 2019; Golubev, 1998; Golubev, 2006). The prevalence of killer yeasts in natural environments is mostly between 5% to 33% (Philliskirk and Young, 1975; Stumm et al., 1977; Starmer et al., 1987; Abranches et al. 1997, Abranches et al. 1998; Trindade et al. 2002; Pieczynska et al., 2013; Wojcik and Kordowska-Wiater, 2015) but can also be as high as 59% in yeast associated with wine production (Hidalgo and Flores, 1994). Killer toxins are known to be active against human and plant pathogenic yeasts (Middelbeek et al. 1980; Hodgson et al. 1995; Buzzini et al., 2001; Giovati et al., 2018) and can control spoilage organisms that are important for agriculture and food industry (Walker et al., 1995; Chessa et al., 2017). The rise in acquired drug resistance and the emergence of drug-resistant fungal pathogens justifies the search for novel antifungal killer toxins from diverse natural environments, including insect-associated fungal communities.

Killer yeast communities have been previously reported in fungus-growing ant colonies (Hymenoptera: tribe Attini: subtribe Attina, hereafter called ‘attine ants’). Attine ants established a long-term obligate mutualism with basidiomycete fungi in the *Agaricaceae* and *Pterulaceae* families, using them as the primary source of food for their colonies (Branstetter et al., 2017; Nygaard et al., 2016; Schultz and Brady, 2008, Möller, 1893; Weber, 1972). According to their cultivars and foraging substrates, each species approaches fungiculture differently, and these interactions are considered a model for studying the evolution of mutualisms (Schultz and Brady, 2008, Schultz et al., 2015). Moreover, attine ants are key ecological agents in the Neotropics as dominant herbivores, promoting nutrient cycling, soil fertility, and seed dispersal (Corrêa et al., 2010; Meyer et al., 2011, Farji-brener and Werenkraut, 2015; Sternberg et al., 2007; Leal and Oliveira, 1998). The foraging behavior of attine ants also contributes to the presence of a large and complex community of environmental yeasts in fungus gardens (Craven et al. 1970; Fisher et al., 1996; Pagnocca et al., 2008; Arcuri et al., 2014; Bizarria Jr. et al., 2022). Fungus gardens are likely an important source of new killer toxins due to the high concentration of simple sugars (Silva et al., 2003, Silva et al., 2006), a large density of yeasts and filamentous fungi (Fisher et al., 1996; Craven et al., 1970; Pagnocca et al., 1996; Rodrigues et al., 2008; Bizarria Jr. et al., 2022), and the hypothesized role on garden "immunity" by yeasts (Rodrigues et al. 2009) – all key elements for species competition (Boynton, 2019). Killer yeasts are primarily associated with the

basidiomycete fungus farmed by attine ants, the bodies of ants, and the leaves foraged by the ants (Carreiro et al. 2002; Robledo-Leal et al. 2016; Bizarria Jr. et. al. 2023). In prior studies, growth inhibition has been identified in 5.2 to 10.8% of the interactions between yeasts derived from attine ant fungus gardens (Carreiro et al. 2002; Bizarria Jr. et. al. 2023).

Killer toxins can modify the community composition of yeasts as an outcome of competition or cooperation between killer yeasts, killer toxin-susceptible yeasts, and killer toxin-resistant yeasts that are determined by spatial distribution, pH, and ploidy (Károlyi et al., 2005; McBride et al. 2008; Wloch-Salamon et al. 2008). Killer toxin production also plays a potential role in yeast dispersal, resource consumption among species, and invasion and protection of a community (Boynton, 2019; Buser et al., 2021; Pintar and Starmer, 2003; Ganter and Starmer, 1992; Travers-Cook et al., 2023). The coexistence of the different phenotypes is known to be affected by environmental parameters, including nutrient availability (Pintar and Starmer, 2003; Wloch-Salamon et al. 2008), cell density (Greig and Travisano 2008; Vadasz et al. 2003), pH, and temperature (Bussey et al. 1988; McBride et al. 2008; Magliani et al. 1997), which can reflect the production and distribution of killer toxins in spatially structured environments (Boynton, 2019; Giometto et al. 2021; Kerr et al. 2002; Libberton et al. 2015; Wloch-Salamon et al. 2008). On the other hand, killer toxins are often reported to play a role in interference competition in environments that enforce the interaction between toxin-producing and neighboring susceptible cells (such as well□mixed habitats like laboratory co-cultures and wine fermentation, changing the community structure and function, as an outcome of competition or cooperation between killer yeasts, killer toxin-susceptible yeasts, and killer toxin-resistant yeasts (Bussey et al., 1988; Hidalgo and Flores, 1994; Pieczynska et al., 2016; Boynton, 2019).

Killer toxins are encoded by different genetic elements, including chromosomal genes; extrachromosomal elements, such as non-autonomous double-stranded RNA (dsRNA) satellites that are maintained by mycoviruses; and autonomous linear double-stranded DNAs (dsDNA) (Bevan et al., 1973; Somers and Bevan, 1969; Magliani et al., 1997; Rowley, 2017). DsRNA satellites have been previously found to be associated with *Hanseniaspora uvarum*, *Pichia kluyveri*, *Saccharomyces* spp., *Torulaspora delbrueckii*, and *Zygosaccharomyces bailii* (Ivannikova et al 2006, Ivannikova et al 2007; Naumov et al., 2009; Schmitt and Neuhausen, 1994; Ramírez et al., 2015; Rodríguez-Cousiño et al., 2017; Zorg et al., 1988), while dsDNA plasmids have been identified in the genera *Babjevia*,

Debaryomyces, *Kluyveromyces*, *Millerozyma*, and *Pichia* (Klassen and Meinhardt 2007; Schaffrath et al. 2018; Klassen et al. 2017). The association of the killer phenotype with the presence of dsRNA satellites has been most thoroughly studied in *S. cerevisiae* (Crabtree et al., 2023; Vijayraghaven et al., 2023). For example, in a survey of 1,270 *S. cerevisiae* isolates, the frequency of killer yeasts was 50%, and 60% had dsRNA satellites (Crabtree et al., 2023). Killer toxin production by the remaining 40% of killer yeasts was closely correlated with the chromosomal killer toxin gene *KHS1*. Considering the many killer yeasts described, only a few studies have defined chromosomal genes that encode the toxins responsible for the observed antifungal effects. Chromosomally encoded killer toxins and their homologs, including K1-like (KKT killer toxins), KHR, KHS, SMKT, KP4-like, PMKT, and other *Pichia* toxins, have been described in many different species of fungi (Goto et al., 1990; Goto et al., 1991; Suzuki and Nikkuni, 1994; Belda et al., 2017, Fredericks et al. 2021, Brown 2011, Lu and Faris 2019). Despite the prevalence of genomic-encoded toxins, some dsRNA satellite-encoded toxins were observed to have genomic homologous in different Saccharomycotina lineages (Frank and Wolfe, 2009; Fredericks et al., 2021). However, the frequency of killer yeasts and the prevalence of dsRNA satellites and dsDNA extrachromosomal elements in different lineages of Saccharomycotina and yeast-like fungi is still understudied.

In this study, we explore the nature and prevalence of the killer phenotype in different Saccharomycotina lineages associated with attine ant fungus gardens, which are habitats that are rich in yeasts, shedding light on their putative ecological role in this environment (Bizarria Jr. et al. 2023). It was revealed that fungus gardens harbor diverse killer yeasts with narrow and broad antifungal activities. Unlike the well-studied killer yeasts of the *Pichia* and the *Saccharomyces* genera, attine ant-associated killer yeasts were devoid of cytoplasmic toxin-encoding elements such as linear dsDNA plasmids and dsRNA satellites (Magliani et al., 1997; Marquina et al., 2002). Therefore, to identify the gene(s) responsible for killer toxin production, a genome mining approach was used by determining the whole genome sequence of the killer yeast *Candida sinolaborantium* that displayed a broad spectrum of antifungal activities against many species of yeasts, including human pathogens. This approach identified a new killer toxin named Ksino. This novel killer toxin has homologs in both yeasts and filamentous fungi and shares a similar antifungal activity and predicted structure to an *S. cerevisiae* killer toxin named Klus. Collectively, it was found that fungus gardens of attine

ants can be used to explore the ecological role of killer yeasts and discover new killer toxins for possible future application as natural antifungals.

2. Results

Fungus gardens of attine ants harbor killer yeasts. To assess the diversity of yeasts associated with fungus-growing ants and their potential for antifungal toxin production, fungus gardens of four ant fungiculture systems were surveyed from 28 nests from four cities in Brazil (Fig. 1A; Table S1). The ant species included the leaf-cutting ant *Acromyrmex coronatus*, the non-leaf-cutting ant *Mycetomoellerius tucumanus*, and the lower attines *Mycetophylax* aff. *auritus* and *Mycocepurus goeldii* that cultivate Agaricaceae fungi, and *Apterostigma goniodes* that cultivates Pterulaceae fungi (Fig. 1B). Ants were selected to broadly represent different fungiculture systems, foraging and preparation behaviors, and the yeast microbiota associated with fungus gardens. Yeasts were isolated from fungus garden suspensions by culturing on synthetic growth media. Microsatellite amplification, sequencing of the D1/D2 domain of the large subunit ribosomal RNA gene, and phylogenetic reconstruction were used for taxonomy. The 180 isolated yeast strains comprised 59 species belonging to eight families and six orders from the Saccharomycotina subphylum previously characterized in a large study of yeasts and yeast-like fungi associated with fungus gardens of attine ants (Fig. 1C; Table S1) (Bizarria Jr. et al., 2023). Of the yeasts isolated, 91 were associated with *Acromyrmex coronatus*, 13 with *Mycetomoellerius tucumanus*, 42 with *Mycetophylax* aff. *auritus*, 25 with *Mycocepurus goeldii*, and nine with *Apterostigma goniodes* (Table S1) (Bizarria Jr. et al., 2023).

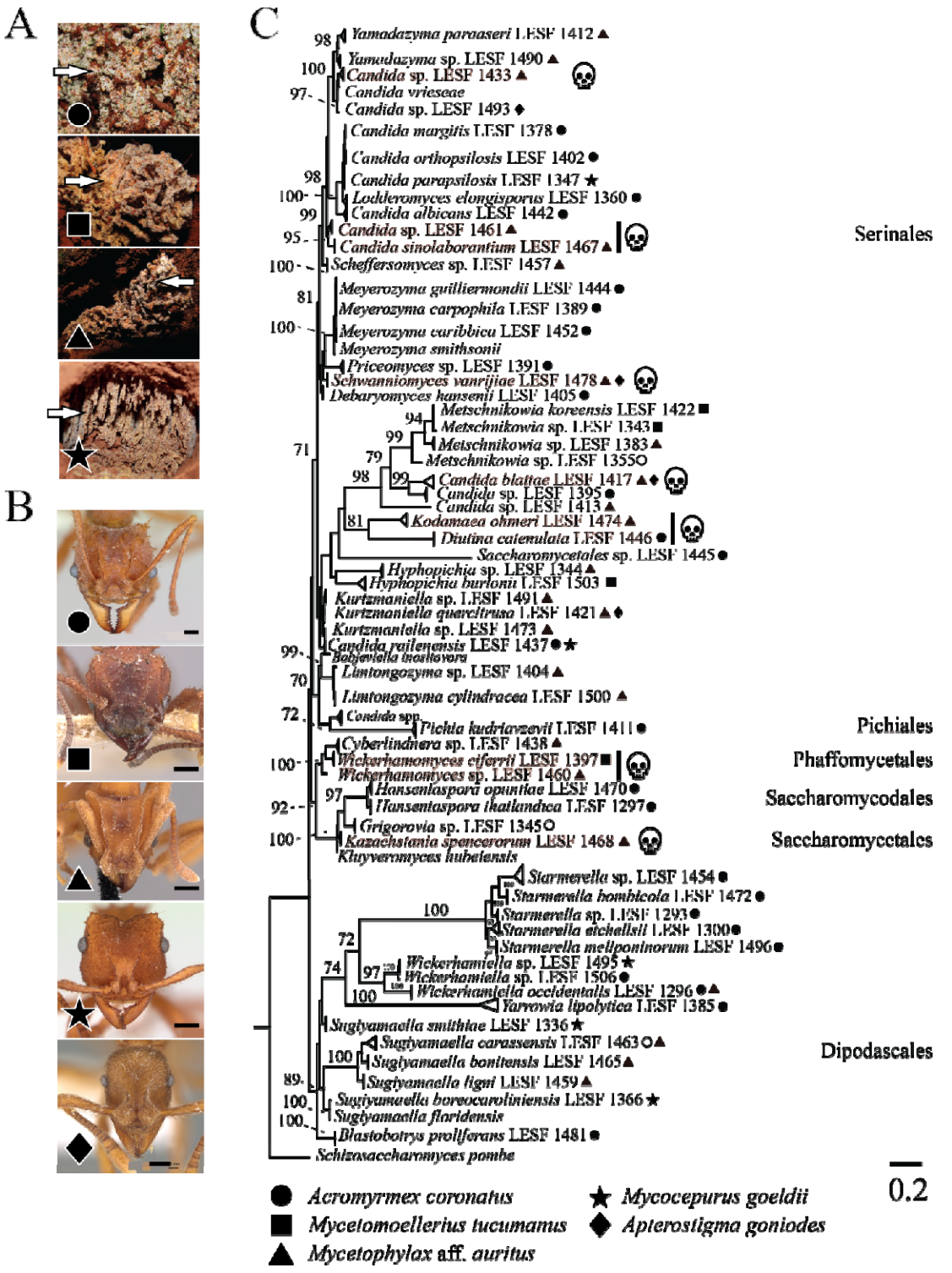

FIG 1. Fungus gardens of different attine ants harbor different killer yeasts. **A.** Images of fungus gardens of different ant species from which yeasts were isolated (arrowheads). The gardens of the leaf-cutting ant *Acromyrmex coronatus* (circle), the non-leaf-cutting ant *Mycetomoellerius tucumanus* (square), the lower attines *Mycetophylax* aff. *auritus* (triangle), and *Mycocepurus goeldii* (star). The fungus garden of *Apterostigma goniodes* is not represented. **B.** Representative images of attine ant species: *Acromyrmex coronatus* (CASENT0173791, April Nobile) (circle); *Mycetomoellerius tucumanus* (CASENT0909391, Will Ericson)

(square); *Mycetophylax auritus* (CASENT0901666, Ryan Perry) (triangle), *Mycocepurus goeldii* (CASENT0173988, April Nobile) (star), and *Apterostigma goniodes* (CASENT0922040, Michele Esposito (diamond). The scale bar on all images represents 0.2 mm. Photos of ants were downloaded from "www.antweb.org." **C**. Phylogenetic relationship of yeasts isolated from fungal gardens as inferred by maximum likelihood criteria and based on D1/D2 domain of the Large Subunit (LSU) ribosomal DNA. Symbols in tree leaves indicate the isolation source of yeasts, as depicted in panels A and B. Red shading and skulls denote the species confirmed as killer yeasts. The phylogenetic clades were highlighted by order following the updated classification for the Saccharomycotina proposed by Groenewald et al., (2023) and www.mycobank.org. *Schizosaccharomyces pombe* was positioned as an outgroup. The number on the branches are ultrafast bootstrap values (values higher than 70 are shown), and the scale bar denotes the number of nucleotide substitutions per site.

From the 59 yeast species identified that were associated with attine ant gardens, ten species had isolates that were able to produce killer toxins on killer assay agar plates (16.95% killer yeasts) (Fig. 1C). Killer toxin production was scored by the absence of growth around a killer yeast or the staining of the lawn yeast with the redox indicator methylene blue (as an indicator of cell death). These different killer yeasts were effective at inhibiting strains that were either previously determined to be susceptible to killer toxins (Fredericks et al., 2021), human pathogenic yeasts, or yeasts randomly selected from fungus gardens and other sources (Fig. 2A and S1; File S1). From the attine ant gardens, *Candida blattae*, *Candida sinolaborantium*, *Candida* sp. (closest to *Candida temnochilae*), *Candida* sp. (closest to *Candida membranifaciens*), *Diutina catenulata*, *Kazachstania spencerorum*, *Kodamaea ohmeri*, *Schwanniomyces vanrijiae*, *Wickerhamomyces ciferrii*, and *Wickerhamomyces* sp. (closest to *Wickerhamomyces rabaulensis*) were identified as killer yeasts, with unique antifungal activities when compared to other previously identified *Saccharomyces* killer toxins (K1, K1L, K2, K21, K28, K45, K62, K74, and Klus). Killer yeasts were only absent from the fungus gardens of *M. goeldii*. Still, they were recovered from the fungus gardens of *Acromyrmex coronatus* (6.59% killer yeasts, 6 out of 91 isolates), *Mycetomoellerius tucumanus* (46.15%, 6 out of 13), *Mycetophylax* aff. *auritus* (42.86%, 18 out of 42), and *Apterostigma goniodes* (22.22%, 2 out of 9) (Fig. 2B). Thirty-two out of 180 (17.78%) yeasts from attine ants were also capable of inhibiting the growth of susceptible yeasts, including human pathogenic yeasts such as *Candida albicans*, *Candida glabrata*, and *Candida auris* (Fig. S1). The attine ant-associated killer yeasts *K. spencerorum* LESF 1468 and *S. vanrijiae* LESF 1521 could only inhibit the growth of pathogenic yeasts tested (Fig. S1, File S1). Killer yeasts from the same attine-associated yeast species mostly had similar antifungal activities as demonstrated by their phenotypic clustering (see *Candida* sp. closest to *C. temnochilae*, *C. blattae*, *D. catenulata*, *S. vanrijiae*, *Wickerhamomyces* sp. closest to *W. rabaulensis*, and *W.*

ciferrii) (Fig. 2A). Specifically, *Candida blattae* killer yeasts had similar antifungal activities even when isolated from the fungicultures of different ant species (compare *Candida blattae* isolates from *Mycetophylax* aff. *auritus* and *Apterostigma goniodes*) (Fig. 2A). However, there were also *S. vanrijiae* killer yeasts from the fungiculture of *Mycetophylax* aff. *auritus* with strikingly different spectrums of antifungal activities, which suggests that isolates of the same species were not always clonal. *Candida sinolaborantium* (strain LESF 1467) had the broadest range of antifungal activity, inhibiting 56.52% of all 69 lawn strains tested (Fig. 2A and S1, File S1). Comparing interactions between ant-associated killer yeasts and susceptible lawn strains from fungus gardens and other environmental sources found that growth inhibition was more prevalent for yeasts from different sources (Chi-squared test, p-value < 0.01) (Fig. 2C; Table S2). Specifically, only 0.93% (6 of 647) of interactions between ant-associated yeasts from the same type of fungiculture resulted in growth inhibition. In contrast, 3.60% (301 of 8,353) of interactions between ant-associated killer yeasts and yeasts from fungus gardens and other environmental sources isolation sources resulted in growth inhibition.

The ability to produce killer toxins is often associated with the presence of linear dsDNA plasmids or mycovirus-associated dsRNA satellites. We assayed all attine ant-associated killer yeasts for the presence of these genetic elements using solvent extraction of nucleic acids, cellulose chromatography, and gel electrophoresis (Crabtree et al., 2019). In particular, the use of cellulose chromatography selectively enriches dsRNAs derived from mycoviruses and satellites, reducing the false negative rate compared to solvent extraction alone and without the bias of reverse-transcriptase PCR (Crabtree et al., 2023). However, we found that none of the attine ant-associated strains possess dsRNAs (i.e., viruses and satellites) or dsDNA cytoplasmic elements (i.e., plasmids). Double-stranded RNA viruses have been found in many different species of yeasts without satellite dsRNAs (Crucitti et al., 2021; Lee et al., 2022; Taylor et al., 2013); thus we broadened the survey to include all attine-associated yeasts but again did not identify any dsRNA viruses. This suggested that the killer toxins associated with yeasts from fungus gardens are genome-encoded and that dsRNA viruses, dsRNA satellites, and DNA plasmids were not observed in yeasts associated with attine ant species in the geographical area sampled.

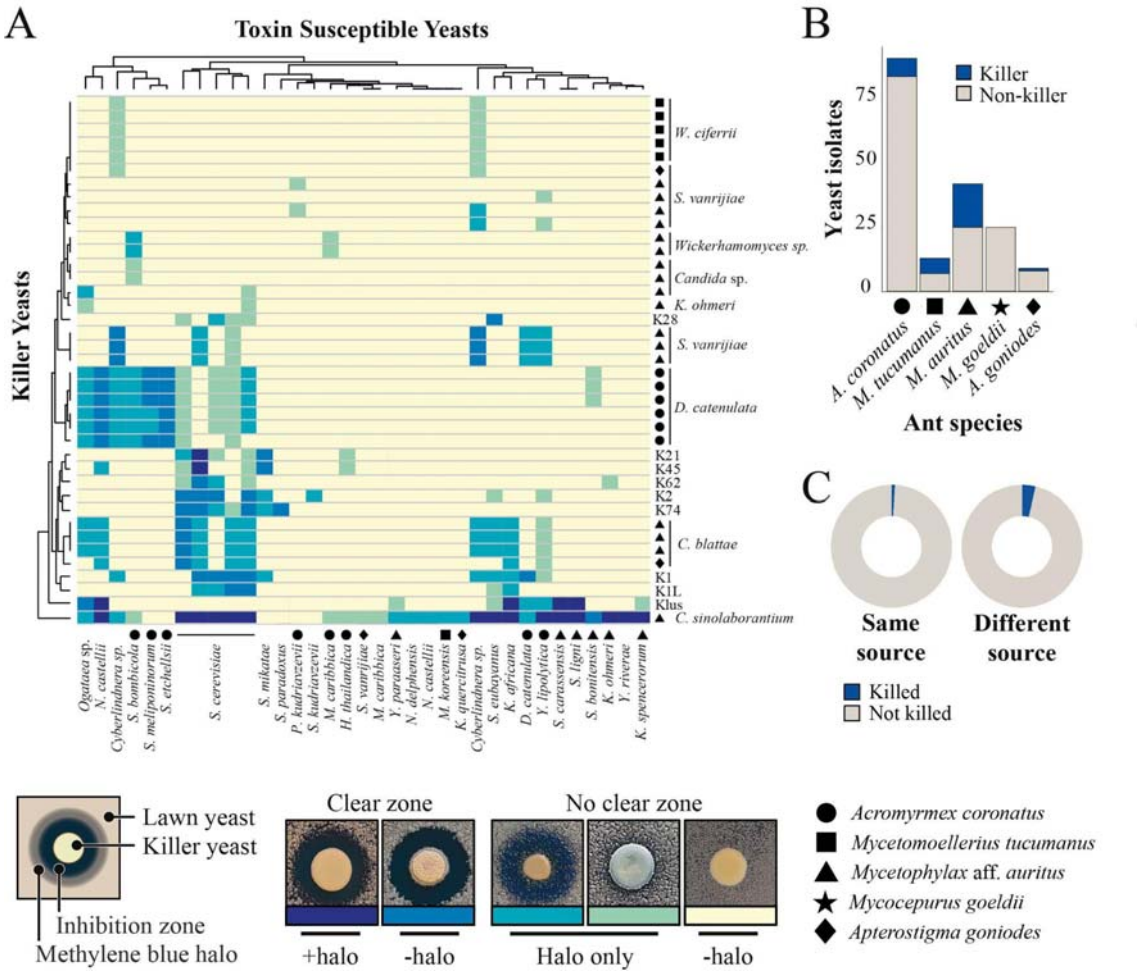

FIG 2. Killer yeasts from fungus gardens have unique spectrums of antifungal activity. A. Heatmap with the interactions between canonical *Saccharomyces* killer yeasts (K1, K1L, K2, Klus, K21, K28, K45, K62, K74), killer yeasts associated with ants, and killer toxin susceptible strains. Origins of the ant-associated killer yeasts; *Acromyrmex coronatus* (circle); *Mycetomoellerius tucumanus* (square); *Mycetophylax* aff. *auritus* (triangle), *Apterostigma goniodes* (diamond). Killer toxin activity was qualitatively assessed based on the presence and size of growth inhibition zones and/or methylene blue staining around killer yeasts as diagrammed. Darker colors on the heatmap represent a more prominent killer phenotype, with yellow indicating no observable killer phenotype. Clusters on the dendrograms connecting individual killers or susceptible yeasts indicate similar susceptibilities to killer toxins or antifungal activities. **B.** Number of killer yeasts and non-killers associated with the different attine ant fungicultures. **C**. Number of killer toxin-positive and negative interactions between yeast from attine ant environment and susceptible strains (Table S1.), growth inhibition by killer yeasts is different among the same or different fungicultures and locations.

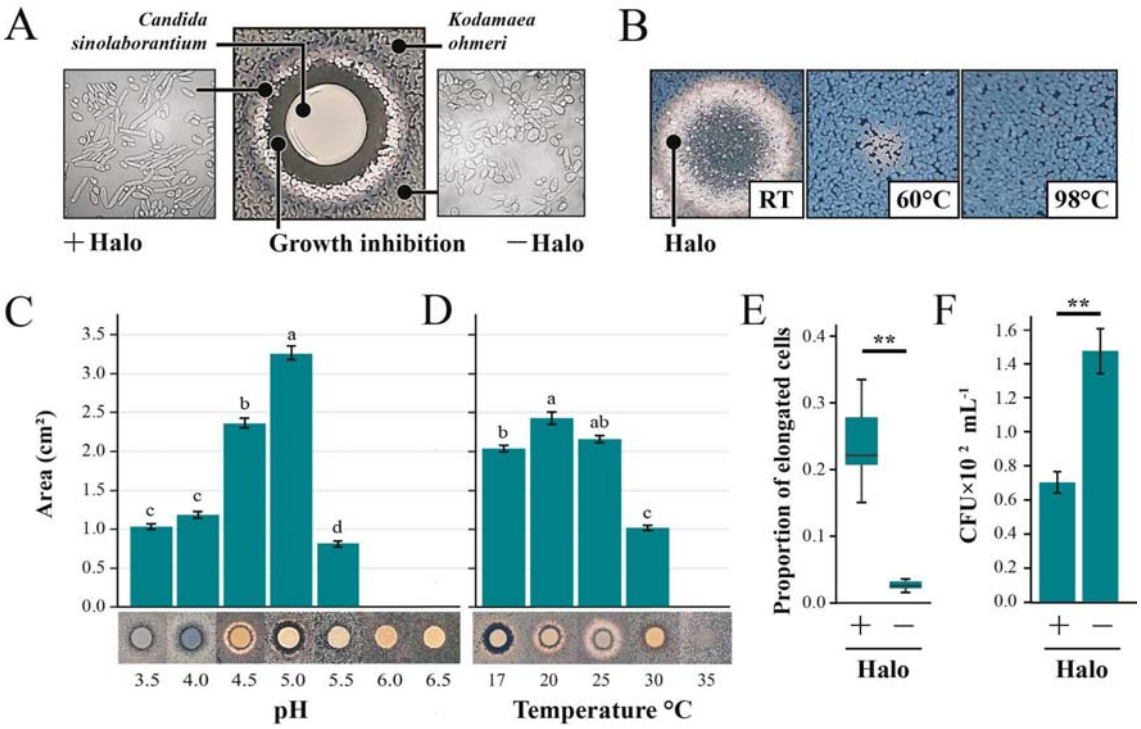

FIG 3. Properties of the killer toxin(s) produced by *Candida sinolaborantium*. **A**. Growth phenotypes associated with the co-culture of the killer yeast *C. sinolaborantium* with *K. ohmeri* at room temperature (RT) and pH 4.6. Cell morphology of *K. ohmeri* inside (+Halo) and outside (-Halo) the white halo around *C. sinolaborantium* was evaluated by microscopy. **B**. The antifungal activity of protein precipitates derived from the spent growth medium of *C. sinolaborantium* and the heat stability of these activities at 60°C and 98°C. Killer yeast activity under different **C**. pH and **D**. temperature conditions. Letters indicate different means for Kruskal-Wallis ($p < 0.01$), followed by the Wilcoxon rank sum test with Bonferroni correction as a *post hoc* analysis. **E.** Proportion of elongated to normal cells of *K. ohmeri* inside (+Halo) and outside (-Halo) the white halo around *C. sinolaborantium*, as depicted in Fig. 3A. **F.** The same growth areas as shown in **E.** but colony forming units (CFU) were measured to indicate *K. ohmeri* cell survival. Asterisks indicate different means for the Welch Two Sample t-test (p-value < 0.01).

The characterization of the killer yeast *Candida sinolaborantium*. *C. sinolaborantium* was identified as a killer yeast with a broad antifungal spectrum that could inhibit 39 of the 69 yeast strains tested (Fig. 2 and S1). In contrast, the next most potent killer yeasts could only inhibit 11 strains tested. *C. sinolaborantium* was also able to cause large zones of growth inhibition in many different species of yeasts that were resistant to other killer yeasts (Fig. 2A). After several days of incubation, we observed that *K. ohmeri* produced a striking white halo between a zone of growth inhibition and methylene blue staining when challenged by the killer yeast *C. sinolaborantium* (Fig. 3A). This phenotype was unique to the pairing of *C. sinolaborantium* and *K. ohmeri*, and was distinct from the growth inhibition caused by the killer toxin K62 (the only other known killer toxin capable of inhibiting *K. ohmeri*) (Fig. 2A). The white halo also appeared to be raised from the surface of the agar plate (Fig. S2). When

cells in this area were observed under a microscope, they appeared to be elongated compared to cells of *K. ohmeri* outside of the halo (Fig. 3A). The killer toxin (or toxins) secreted by *C. sinolaborantium* were precipitated by ethanol and remained active when incubated at room temperature, but were inactivated by heating to 60°C and 98°C (Fig. 3B). The killer inhibition of *K. ohmeri* by *C. sinolaborantium* was optimal at pH 5 (Fig. 3C, Table S3), with loss of killing at pH >5.5. The optimal temperature for killing *K. ohmeri* by *C. sinolaborantium* was 20°C and inactive at 35°C (Fig. 3D, Table S4). Further analysis of the white halo of *K. ohmeri* revealed an 8-fold increase in cell elongation in the white halos when compared to untreated cultures of *K. ohmeri* (Fig. 3E and Table S5). Cells of *K. ohmeri* from the white halo or untreated culture were seeded on agar to measure viability by colony-forming units. Cells isolated from the white halos showed a 2.1-fold reduction in colony-forming units compared to *K. ohmeri* isolated away from halos (Fig. 3F and Table S6). Ultrafiltration of culture media was used to determine the approximate molecular weight of the antifungal molecules produced by *C. sinolaborantium*. Antifungal activity was observed for fractions that enriched molecules >100 kDa and >30 kDa. Raw filtrates and concentrated ethanol-precipitated fractions were used to challenge a panel of yeasts previously shown to be susceptible to toxins produced by *C. sinolaborantium* (Fig. 2). The spent culture medium showed less antifungal activity compared to the precipitated medium, with the latter capable of inhibiting 21/29 susceptible yeasts that were inhibited in killer assays on agar (Fig. S3). Antifungal activities were similar before and after passage through a filter with a molecular weight cut-off (MWCO) of 100 kDa and were mostly retained in the MWCO 30 kDa filter. Only weak antifungal activity was detectable for the fraction that passed through the MWCO 30 kDa filter (Fig. S3). The appearance of white halos was observed using fractions captured by filters with MWCO 100 kDa and MWCO 30 kDa when tested against *K. ohmeri* but not with WCO 5 kDa. Together, these data show that *C. sinolaborantium* is a killer yeast with a broad spectrum of antifungal activities, with similar temperature and pH optima of other previously described yeast killer toxins, but with the ability to induce cell elongation in *K. ohmeri*. Fractions from ultrafiltration are consistent with the antifungal activities of *C. sinolaborantium*, suggesting either the production of multiple chromosomally encoded killer toxins with similar antifungal properties or perhaps large oligomers or complexes of a single >30 kDa killer toxin.

Ksino: a novel killer toxin produced by *C. sinolaborantium* with structural homology to the Klus killer toxin. To determine the gene or genes responsible for killer toxin production

by *C. sinolaborantium*, the genome sequence of the yeast was determined (Table S7). The resulting 11.21 Mb assembly resulted in a BUSCO completeness (Complete and single-copy BUSCOs) of around 98% using the saccharomycetes_odb10 dataset (Seppey et al., 2019), with GC content of 48.76%, an N50 of 155,979 bp, and a total of 5,951 protein-coding genes (Table S7). To identify genome-encoded killer toxins in the *C. sinolaborantium* proteome, BLASTp was performed using a database of known killer toxins from yeasts (Table S8). This approach identified 12 toxin-like candidates, all with a sequence alignment length greater than 100 amino acids and an identity of at least 23.5% compared to any known killer toxin (Table S9). One *C. sinolaborantium* protein had a 28% identity and 42% similarity over an alignment length of 151 amino acids with the *S. cerevisiae* killer toxin Klus (Table S9) (Rodríguez-Cousiño et al. 2011; Genbank Accession: ADG64740). Therefore, the putative killer toxin with homology to Klus from *C. sinolaborantium* was named Ksino.

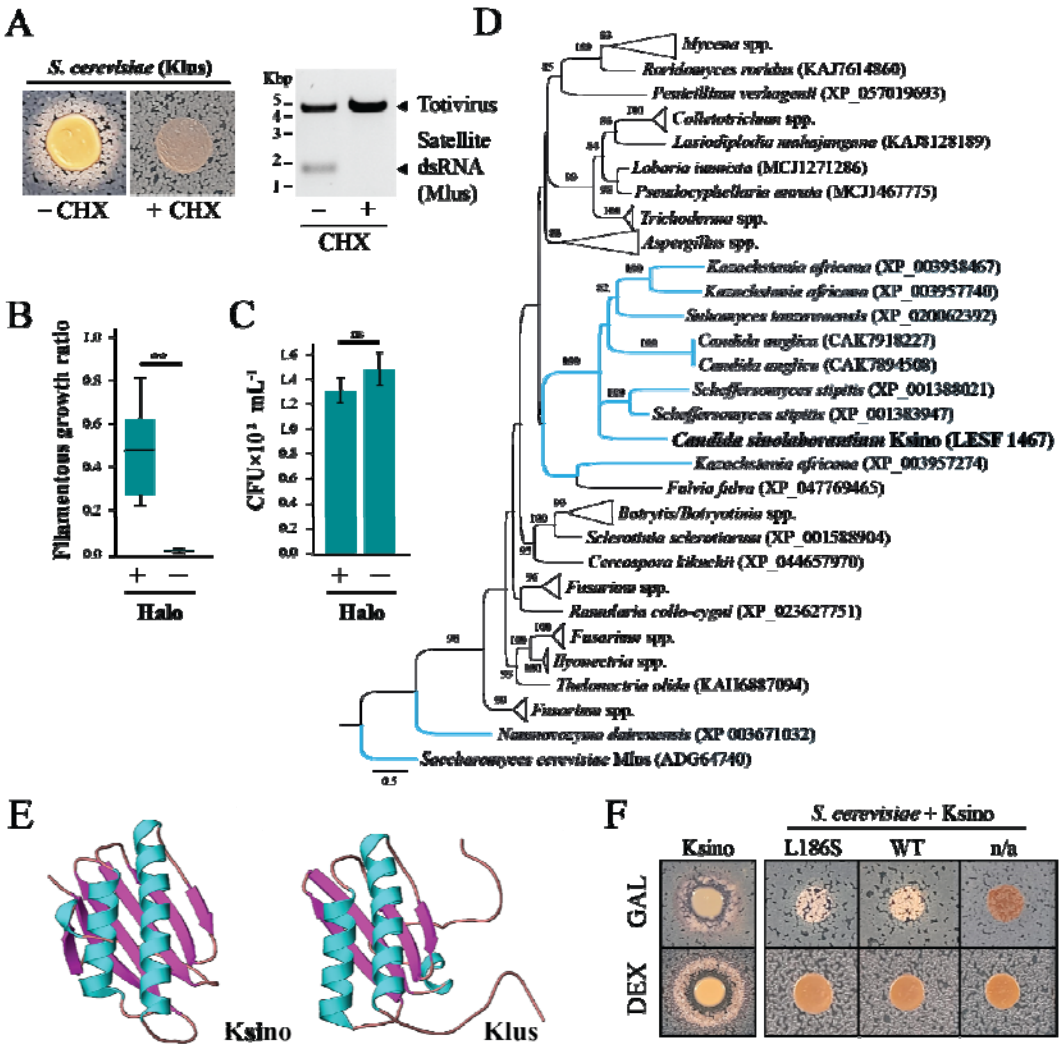

FIG 4. Ksino from *C. sinolaborantium* defines a novel family of killer toxins. **A.** The phenotypes associated with the co-culture of the Klus-encoding killer yeast *S. cerevisiae* strain DSM-70459 with *K. ohmeri* (+Mlus). Treatment with cyclohexamide (CHX) causes the loss of the Mlus satellite (-Mlus) and the loss of the white halo phenotype. The ratio of **B.** filamentous and **C.** viable *K. ohmeri* cells in the white halo around Klus-producing *S. cerevisiae* (+Halo) and in axenic culture (-Halo). Asterisks indicate different means for Welch Two Sample t-test (p-value <0.01), ns = not significant. **D.** A maximum likelihood phylogeny of Ksino homologs identified in diverse fungi. The Ksino from *C. sinolaborantium* is highlighted in bold, and all Saccharomycotina yeasts are highlighted in blue. The dsRNA-encoded killer toxin Klus is represented as an outgroup. Bootstrap values higher than 70 are shown. **E.** Predicted tertiary structures of Ksino and Klus using AlphaFold2. **F.** Recombinant expression of Ksino by *S. cerevisiae* using galactose induction with a lawn of *K. ohmeri*. Dextrose was used as a non-induced control. n/a indicates an empty vector negative expression control.

The Ksino open reading frame was determined to be 202 amino acids long, comparable to Klus at 242 amino acids. Linear representation of the secondary structure revealed a similar pattern of alpha helices and beta sheets (Fig. 4E; Fig. S5). There was also evidence of potential post-translational modification sites, including N-terminal signal sequence cleavage sites predicted by psipred (Buchan et al., 2013) and dibasic motifs in the

unstructured region before helix 1 (Fig. S5). Dibasic motifs in killer toxins are known to be proteolytically cleaved by the Golgi-specific protease Kex2 (Julius et al., 1984). As Ksino has no homology to a protein of known structure, AlphaFold2 was used to generate tertiary structure models of Ksino and Klus (Jumper et al., 2021). Ksino and Klus had global LDDT scores of 63.6 and 65.1, respectively, and per residue, LDDT was greater than 80 in regions of secondary structure for both proteins (Fig. 4E and S5). Molecular dynamics simulation improved the bond angles of the alphafold model to Ramachandran favored regions in models of Ksino (77.0% to 91.2%) and Klus (72.9% to 89.0%) (Table S10, Fig. S6). Ksino and Klus simulations reached a stable RMSD of around 1.6 nm after approximately 20 ns of simulation (Fig. S6). Molprobity scores, analogous to structure resolution, were determined to be 1.54 for Ksino and 1.86 for Klus (Studer et al., 2019). Overlay of the final energy-minimized structures of Ksino with Klus compared to the original AlphaFold2 models yielded an RMSD of 2.6 Å (Fig. 4E). The predicted organization of the Ksino structure consists of a discontinuous five-stranded antiparallel beta-sheet packed against a pair of antiparallel alpha helices (Fig. 4E, S5). The tertiary structure of Klus follows the same overall organization but with one less beta-turn. Ksino has eight cysteine residues, compared to the seven in Klus (Fig. S5). The predicted structures have three intramolecular disulfide bonds. In Ksino, C105-C127 is positioned to crosslink the C-terminus of helix 1 to the beta-sheet 2, similar to C141-C162 in Klus (Fig. S5). The remaining predicted disulfide bonds are unique to both structural models (Fig. S5). These simulations collectively suggest that the Klus and Ksino proteins share significant structural homology despite having low amino acid identity.

The sequence similarity between Ksino and Klus prompted a more detailed investigation into whether these killer toxins share similar antifungal properties. Although we had previously failed to detect growth inhibition of *K. ohmeri* by *S. cerevisiae* killer toxin Klus (Fig. 3), we noted the appearance of white halos instead of a zone of growth inhibition or methylene blue staining after prolonged co-culture (Fig. 4A). The appearance of white halos was similar to those produced by *C. sinolaborantium* and was dependent on the presence of the Mlus satellite dsRNA (Fig. 4A). Analysis of the cells within the white halo found a significant proportion of elongated cells, as previously observed upon exposure of *K. ohmeri* to Ksino (Fig. 4B). However, unlike the Ksino halos, Klus did not cause a significant loss of cell viability (Fig. 4C).

To determine whether the gene encoding Ksino was a killer toxin and solely responsible for the elongated cell phenotype of *K. ohmeri*, the Ksino gene was amplified by PCR and cloned into an *S. cerevisiae* expression vector under the control of a galactose-inducible promoter. *C. sinolaborantium* belongs to the Serinales order and uses the CUG codon to encode serine (Groenewald et al 2023; Krassowski et al., 2018). Ksino has one CUG codon that will introduce a leucine at position 186 when expressed by *S. cerevisiae*. This mutation is predicted to have a small destabilizing effect on folding compared to the wild type based on FoldX 5.0 and molecular dynamics simulation (estimated $\Delta\Delta G_{Folding}$ = 1.0 kcal/mol) (Fig. S7). Therefore, residue 186 was recoded for serine in *S. cerevisiae* (L186S). When the strains were grown on dextrose, no growth inhibition of *K. ohmeri* was observed during co-culture with a laboratory strain of *S. cerevisiae* transformed with the wild type or L186S Ksino expression vectors (Fig. 4F). However, growth of wild type or L186S on galactose triggered the white coloration of *K. ohmeri* on the plate only when co-cultured (Fig. 4F and S8). The altered coloration of *K. ohmeri* indicated that Ksino is likely exported from *S. cerevisiae* and produces a phenotype similar to that of the native expression of Ksino by *C. sinolaborantium*. These data support the hypothesis that Ksino is responsible for the observed growth effects on the yeast *K. ohmeri* and is a novel killer toxin.

To identify other possible Ksino-homologous proteins in different organisms, we performed a BLASTp search across the NCBI database, resulting in 84 protein sequences from various Ascomycota and Basidiomycota fungi. Ksino homologs were found in *Saccharomycetes*, *Pichiomycetes* yeasts, and other filamentous fungi with identity and alignment lengths higher than 30% and 109 amino acids, respectively (Fig. 4D and Table S11). Phylogenetic analysis of homologs, with Klus as an outgroup, indicates that proteins with the highest identity of Ksino (35-42% identity) were all uncharacterized genes of the Saccharomycotina yeasts from the lineages of *Debaryomycetaceae* and the *Saccharomycetaceae* (Fig. 4D). Saccharomycotina species with Ksino-like genes included *Candida anglica*, *Kazachstania africana*, *Scheffersomyces stipitis*, and *Suhomyces tanzawaensis*, with both *K. africana* and *S. stipitis* (Basionym: *Pichia stipitis*) being previously reported as killer yeasts (Antunes and Aguiar, 2012; Fredericks et al. 2021). Filamentous fungi encode the majority of Ksino homologs (75 out of 84), including species belonging to the genera *Fusarium*, *Mycena*, and *Aspergillus* (Fig. 4D and Table S11), known as plant and human pathogens (*Fusarium* spp.), saprophytic and biotrophic plant associated fungi (*Mycena* spp.), and fungi species that are ubiquitous in the environment (*Aspergillus*

spp.) (Summerell et al. 2010, Harder et al. 2023; Thoen et al. 2020; Houbraken et al. 2020; Jurjevic et al. 2012; Peterson et al. 2001).

3. Discussion

Identifying killer yeasts in fungicultures suggests they might play a role in attine ant fungus gardens by suppressing fungal competitors or allelopathy effects on complex dynamics of microbial interactions. Different studies have revealed that yeasts are abundant in attine ant environments that likely represent differences in the foraging composition and substrate preparation behaviors observed among the different fungicultures (Bizarria Jr. et al., 2022, de Fine Licht and Boomsma, 2010; Ronque et al., 2019). Yeasts from fungus gardens of the leaf-cutting ant *Atta texana* were observed to suppress the growth of fungal garden contaminants, especially *Escovopsis* and *Syncephalastrum* (Rodrigues et al. 2009). These antifungal properties were hypothesized to contribute to fungal garden "immunity," whereby the resident fungi within a fungiculture prevent invasion by other fungal species. This would require interplay between the cleaning behaviors of attine ants in their gardens to remove unwanted fungi and other microbial interactions within attine ant colonies, i.e., allelopathy. Our study indicates that fungus gardens of attine ants harbor killer yeasts with similar prevalence to other surveys (Phillisкirk and Young, 1975; Pieczynska et al., 2013; Starmer et al., 1987; Stumm et al., 1977; Trindade et al. 2002; Wojcik and Kordowska-Wiater, 2015; Abranches et al. 1997, Abranches et al. 1998). This expands the previous findings regarding the prevalence of killer yeasts in laboratory-reared attine ant colonies of *Atta sexdens* (Carreiro et al., 2002). Moreover, the prevalence of killer yeasts among the different ant species, such as *Mycetophylax* aff. *auritus* (42.86%, eight nests sampled) and *Mycetomoellerius tucumanus* (46.15%, four nests sampled) were considerably higher than in other surveyed fungicultures.

Killer yeasts from attine ant colonies were more likely to inhibit the growth of susceptible strains from different fungicultures. This supports previous observations of killer and non-killer yeast interactions whereby local selective pressure for killer toxin resistance allows the coexistence of killer and non-killer yeasts in a given niche (Starmer et al. 1987; Ganter and Starmer, 1992, Abranches et al. 1997, Trindade et al. 2002). The susceptibility of yeast populations that have never been exposed to a specific killer toxin would greatly depend on the standing genetic variation (perhaps in the cell wall and membrane toxin

receptors) among different lineages of yeasts dictated by the population's evolutionary history. Our findings support the hypothesis that yeast contributes to fungal garden "immunity" since killer yeasts are expected to prevent the invasion of other fungal species into the fungus garden. The coexistence of killer and non-killer yeast species could be an outcome of microhabitats in the spatially structured environment of the fungus garden, which may harbor different populations of yeasts and allow the colonization by killer yeasts (Giometto et al. 2021, Wloch-Salamon et al. 2008).

Saccharomycotina killer yeast species isolated in attine ant gardens have been previously found to secrete killer toxins. Among the yeast species, the ability to produce toxins was observed for *Diutina catenulata* (Basionym: *Candida catenulata*; Stopiglia et al., 2014; Fuentefria et al., 2007), *Kodamaea ohmeri* (Synonymy: *Pichia ohmeri*; Fuentefria et al., 2006, Fuentefria et al., 2008; Coelho et al., 2009), *Schwanniomyces vanrijiae* (Madbouly et al., 2020), and *Wickerhamomyces ciferrii* (Basionym: *Hansenula ciferrii*; Nomoto et al., 1984). The exception was *Kazachstania spencerorum*, which, to our knowledge, is the first report of a killer phenotype displayed by this species, although toxin production has been previously reported in the genus, specifically *K. africana*, *K. exigua* and *K. unispora* (Perez et al., 2016; Stopiglia et al., 2014; Fredericks et al., 2021). These yeast species have also been identified in substrates that are commonly foraged or associated with attine ants, including plants (*Schwanniomyces vanrijiae*, Madbouly et al., 2020; *Kodamaea ohmeri*, Fuentefria et al., 2006), insects and their environments (*Candida blattae*, Nguyen et al., 2007; *Candida sinolaborantium*, Suh et al., 2005; Guamán-Burneo et al., 2015; *Schwanniomyces vanrijiae*, Maksimova et al., 2016; *Kodamaea ohmeri*, Benda et al., 2008; Amos et al., 2019; Suh and Blackwell, 2005), and soil (*Kazachstania spencerorum* nom. inv., Basionym: *Saccharomyces spencerorum* nom. inv.; Vaughan-Martini et al., 1995; Kurtzman and Robnett, 2003).

Importantly, killer yeast species appear to be unique between colonies of the same ant species (Bizarria Jr. et al., 2023). This observed diversity could be due to the foraging behavior of ants, whereby sampling of the surrounding ecological niche would introduce different fungal species to the fungiculture of the same species of ants in different geographical locations (Bizarria Jr. et al., 2023). However, despite the potential role of killer yeasts in garden immunity, whether the occurrence of killer yeasts in a fungiculture is acquired by chance, inherited from the environment, or inherited during garden propagation remains unknown (Bizarria Jr. et al., 2022). Niche construction by the fungal cultivar species

could also play a role in yeast diversity in the fungus garden environment or by other features such as the pH of the fungus garden. Interestingly, the pH observed in the different fungus gardens (pH 5.1-5.4) is consistent with the optimal antifungal activities of both Ksino (~pH 5) and Klus (pH 4-4.7) and other known killer toxins (Bizarria Jr. et al., 2023). However, the association between killer yeasts and fungicultures still requires robust empirical evidence to reject the stochastic nature of killer yeast colonization. Future yeast isolation will provide new directions to clarify whether killer yeast occurrence is modulated by ant foraging choice or fungus garden features such as pH and fungal cultivar species.

Our survey of the encoding elements of killer toxins indicated that the 180 isolated strains of Saccharomycotina yeasts were devoid of cytoplasmic killer toxin-encoding elements such as dsRNA satellites and dsDNA linear plasmids. The frequency of dsRNA elements associated with *Saccharomyces* yeasts has been observed to range from 10% to 51% in wild and domesticated strains (Pieczynska et al., 2013; Crabtree et al., 2023). It is expected that more of these genetic elements will be found in other Saccharomycotina lineages, given their discovery in non-*Saccharomyces* yeasts and the frequency of genome-integrated molecular fossils of plasmid and virus sequences in different lineages (Frank and Wolfe, 2009; Liu et al., 2010; Satwika et al., 2012; Myers et al., 2020; Villan Larios, et al. 2023; Taylor and Bruenn, 2009, Lee et al., 2022). Most of the yeast isolated from fungicultures belong to the Serinales, where the CUG codon is translated into serine instead of leucine in the universal genetic code (Groenewald et al 2023). The rewiring of the fungal genetic code has been suggested to prevent the invasion of viruses and plasmids by stopping the faithful translation of viral proteins (Krassowski et al., 2018). Alternatively, RNAi might also contribute to limiting viral infections in these yeasts, even though, in some cases, yeast lineages maintain viruses that suppress RNAi (Drinnenberg et al., 2009; Drinnenberg et al., 2011; Lee et al., 2022; Segers et al., 2006; Segers et al., 2007; Rodriguez Coy et al., 2022). RNAi and genome recoding could be possible reasons for the absence of cytoplasmic elements in the yeasts associated with attine ant fungiculture. However, this still requires a more in-depth investigation to exclude the stochastic nature of virus acquisition by fungi and sampling biases.

The lack of extrachromosomal elements in killer yeasts associated with attine ant fungiculture suggests that killer toxin genes are genome-encoded. Our survey indicates that the killer yeasts from different Saccharomycotina lineages associated with fungus gardens

differ in their spectrum of antifungal activity from canonical *Saccharomyces* killer toxins (K1, K2, K28, etc.). In particular, toxins secreted by *Candida sinolaborantium* had the broadest activity, including toward infectious human pathogens (e.g., *Candida albicans, C. glabrata,* and *C. auris*). The broad antifungal spectrum of *C. sinolaborantium* and the ability to fractionate antifungal activities by ultrafiltration indicates the likely presence of multiple unidentified chromosomally encoded toxins. After determining the genomic sequence of *C. sinolaborantium*, the new killer toxin Ksino was discovered due to its sequence homology to the canonical *Saccharomyces* killer toxin Klus. However, the killer activity of *C. sinolaborantium* was not fully reproduced when Ksino was heterologously expressed by *S. cerevisiae*. This potentially supports the expression of multiple killer toxins by *C. sinolaborantium* or that ectopic heterologous expression by *S. cerevisiae* is inadequate due to potential deficiencies in extracellular export, maturation, or Ksino's innate toxicity. However, in all cases, it was observed that natural and heterologous expression of Ksino and Klus stimulated the production of elongated/filamentous cells by *K. ohmeri*, a unique phenotype observed in our screens for killer yeasts. Usually, this dimorphism in yeasts has been demonstrated to be triggered by nitrogen starvation (Gimeno et al., 1992), different carbon sources, and temperature (Rupert and Rusche, 2022). However, to our knowledge, this is the first case of this phenotype associated with exposure to killer toxins.

Many proteins from different Ascomycete and Basidiomycete fungi lineages were identified in our search for Ksino-like proteins, including filamentous fungi and yeast (from Saccharomycetes and Pichiomycetes). The Ksino-like proteins from yeasts of the Saccharomycotina subphylum (*Candida anglica*, *Kazachstania africana*, *Scheffersomyces stipitis*, and *Suhomyces tanzawaensis*) share a closer evolutionary origin to Ksino and therefore might represent bonafide killer toxins. Despite our approach to identifying killer toxins being limited by primary sequence similarity to known toxins, it has successfully identified Ksino. This combination of genome sequencing, sequence homology searches, and structural modeling could be used more widely on the many killer yeasts that are devoid of cytoplasmic extrachromosomal elements to identify new killer toxins (Boynton, 2019; Crabtree et al. 2023).

In summary, this study demonstrates that (i) Fungus gardens of attine ants can harbor killer yeasts, an underappreciated environment for killer yeasts. (ii) DsRNA and dsDNA extrachromosomal elements are lacking from yeasts associated with attine ant fungicultures.

(iii) Genome mining can discover new chromosomally encoded killer toxins, specifically Ksino secreted by *Candida sinolaborantium*. (iv) Ksino has sequence and structural homology to the *Saccharomyces* killer toxin Klus and is a member of a putative new family of killer toxins in Ascomycete and Basidiomycete fungi.

Funding sources

This work was supported by Fundação de Amparo à Pesquisa do Estado de São Paulo (FAPESP) [scholarships No. 2019/24412–2 and 2021/09980-4] to RBJ and [grant No. 2019/03746–0] to AR. The authors also thank the Conselho Nacional de Desenvolvimento Científico e Tecnológico (CNPq) for a research fellowship [grant No. 305269/2018–6] to AR and a scholarship [No. 142396/2019–2] to RBJ. This work was supported by the Institute for Modeling Collaboration and Innovation at the University of Idaho (National Institutes of Health grant P20GM104420), Idaho Institutional Development Awards Network of Biomedical Research Excellence (INBRE) Program Core Technology Access Grant (NIH Grant Nos. P20GM103408), and National Science Foundation Grant No. 2143405. The content is solely the responsibility of the authors and does not necessarily represent the official views of these funding agencies.

Data Availability

Data supporting the results in the paper are available in the Supplementary Material. The GenBank accession number for the Open reading frames of the Ksino killer toxin of *Candida sinolaborantium* LESF 1467 is PP790515. The sequenced genome of *Candida sinolaborantium* can be accessed through BioProject PRJNA916362, BioSample SAMN32422847, Assembly JAQRFW000000000. The raw sequence reads are also available through the NCBI Sequence Read Archive (SRR23081998). Gene prediction and annotation are provided in https://figshare.com/s/1f31cd262fc9de969d38 (10.6084/m9.figshare.25895278).

Acknowledgments

We would like to thank Conselho de Gestão do Patrimônio Genético (CGEn) for providing permits for access to genetic heritage: #AE012D8, #A877F11 and #AA39A6D. We also thank Amanda Viana and Luciana Simão Carneiro for preparing and preserving yeast cultures. We also would like to thank the ARS Culture Collection (NRRL), Westerdijk Fungal Biodiversity Institute (WI-KNAW), and Dr. Roland Klassen for providing yeast cultures used in this study. We also thank Dr. Primrose Boynton for the critical reading of this manuscript. Photos of ants in Fig. 1 were accessed from "www.antweb.org": CASENT0173791 *Acromyrmex coronatus* (Photographer: April Nobile); CASENT0909391 *Mycetomoellerius tucumanus* (Photographer: Will Ericson); CASENT0901666 *Mycetophylax auritus* (Photographer: Ryan Perry); CASENT0173988 *Mycocepurus goeldii* (Photographer: April Nobile); CASENT0922040 *Apterostigma goniodes* (Photographer: Michele Esposito).

Authors' contributions

RB wrote the manuscript supervised by PAR and with inputs from AR, JWC, and MY; RB conducted cross-interaction killer assays and dsRNA extractions. JWC performed protein structure predictions and analysis. TJB conducted cross-interactions with pathogenic yeasts. RACS performed genome assemblage and annotation. SAC performed killer assays for Ksino characterization. SAC performed microscopic evaluations and killer assays. RB and RTT performed dsDNA extractions. NF and MJD performed genome sequencing. PAR and AR supervised and obtained funding for the project. AR is responsible for permit applications. All authors discussed and reviewed the manuscript and approved the final version.

Supplementary figures

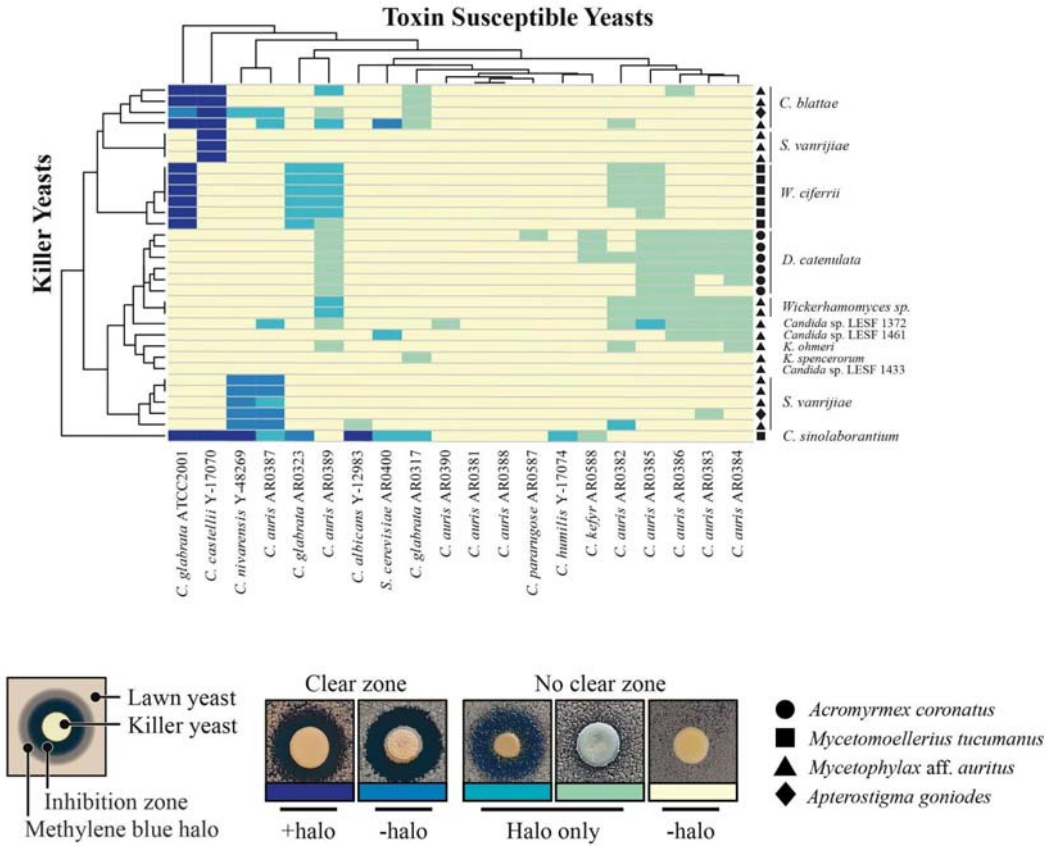

FIG S1. Killer yeasts from attine ant gardens can inhibit the growth of opportunistic human pathogens. A heatmap showing interactions between killer yeasts associated with attine ants and opportunistic human pathogens. Origins of the ant-associated killer yeasts; *Acromyrmex coronatus* (circle); *Mycetomoellerius tucumanus* (square); *Mycetophylax* aff. *auritus* (triangle), *Apterostigma goniodes* (diamond). Killer toxin activity was qualitatively assessed based on the presence and size of growth inhibition zones and/or methylene blue staining around killer yeasts as diagrammed. Darker colors on the heatmap represent a more prominent killer phenotype, with yellow indicating no observable killer phenotype. Clusters on the dendrograms connecting individual killers or susceptible yeasts indicate similar susceptibilities to killer toxins or antifungal activities. Darker colors on the cluster diagram represent a more prominent killer phenotype, with yellow indicating no observable killer phenotype.

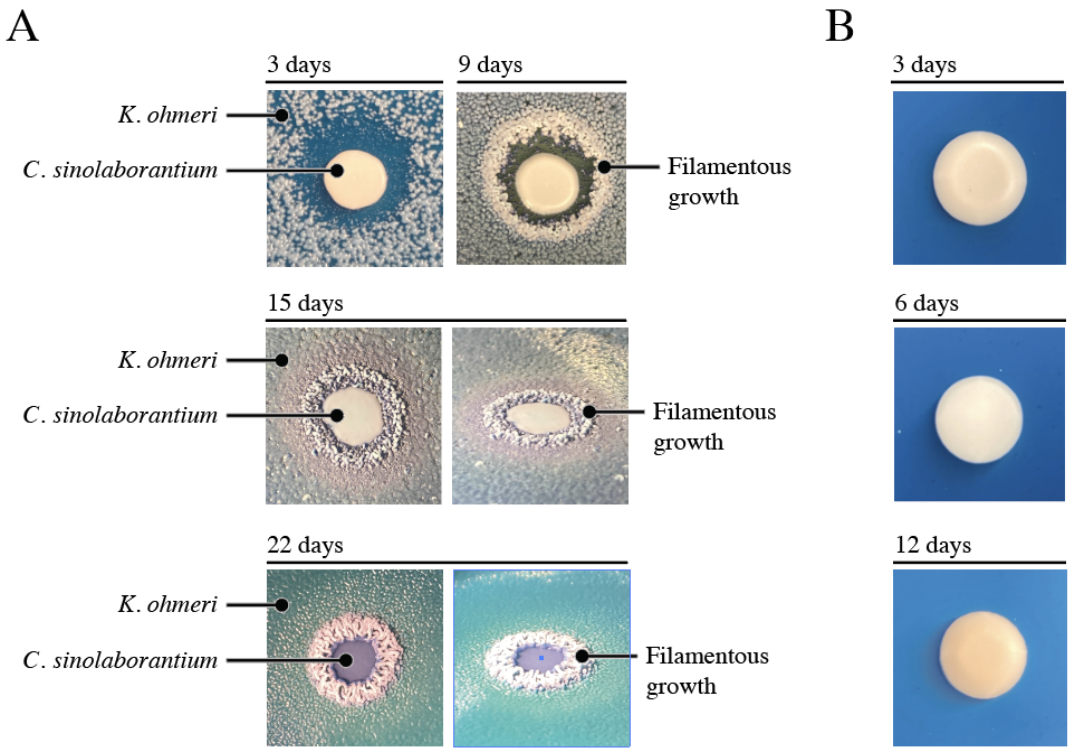

FIG S2. Filamentous growth of *K. ohmeri* after coculture with the killer yeast *C. sinolaborantium*. A. Representative images showing the interaction between *K. ohmeri* and the killer yeast *C. sinolaborantium* on YPD agar. After extended incubation times at ~22°C (15 - 22 days), vertical growth from the surface of the agar was observed. B. Filamentous growth phenotypes are not observed when *C. sinolaborantium* is grown in isolation on agar.

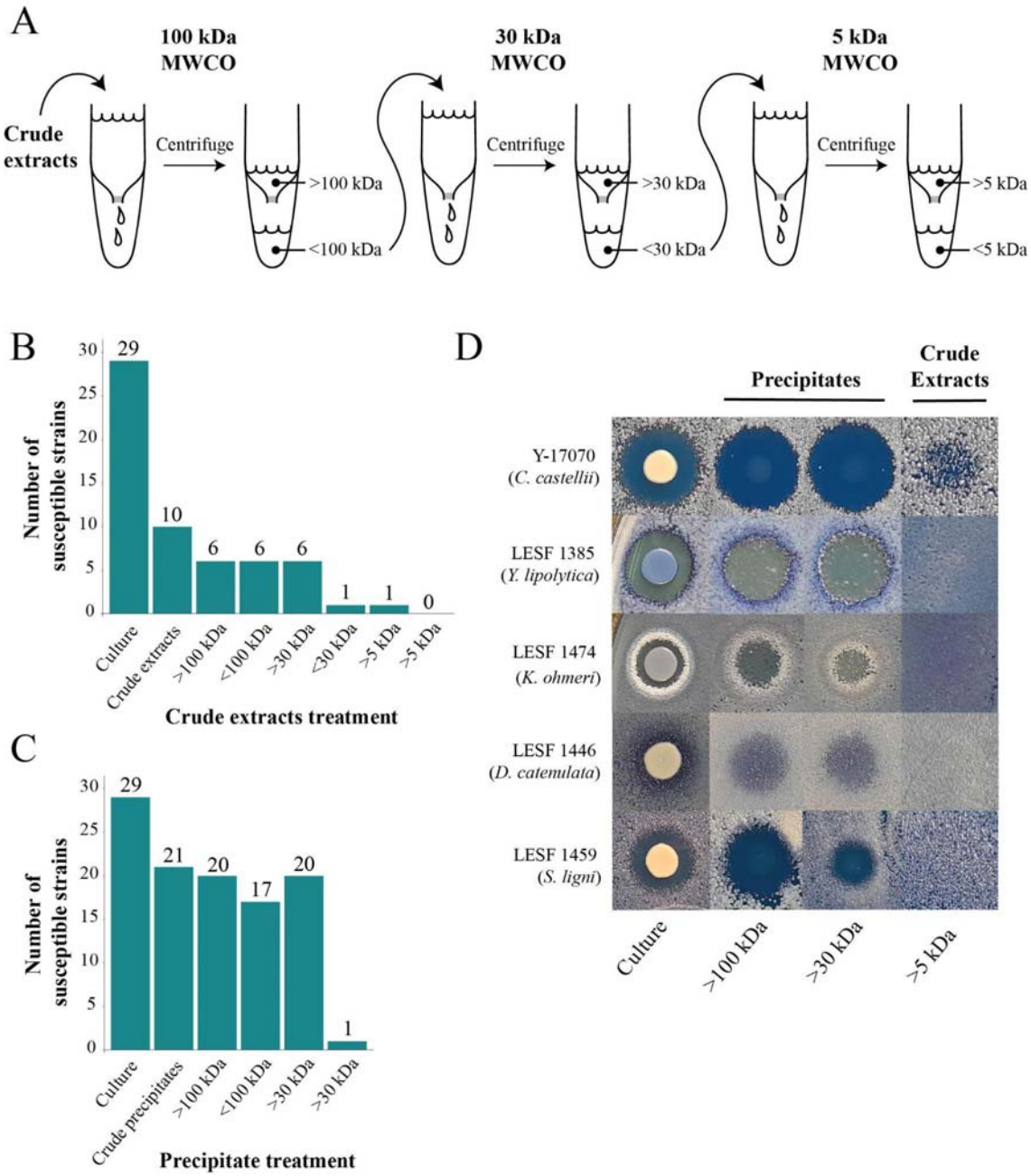

FIG S3. Antifungal activities exhibited by fractionated media after growth of *Candida sinolaborantium*. A. The workflow demonstrates the ultrafiltration of YPD-spent growth media to obtain fractions of antifungal molecules. Crude extracts were processed by ultrafiltration with molecular weight cut-off (MWCO) filters of 100 kDa, 30 kDa, and 5 kDa. The resulting protein preparations were used to challenge susceptible yeasts before (>) and after (<) ultrafiltration. Fractions were used **B.** before or **C.** after ethanol-precipitation **D.** Phenotypic examples of antifungal activity detectable in different fractions against representative susceptible yeast species.

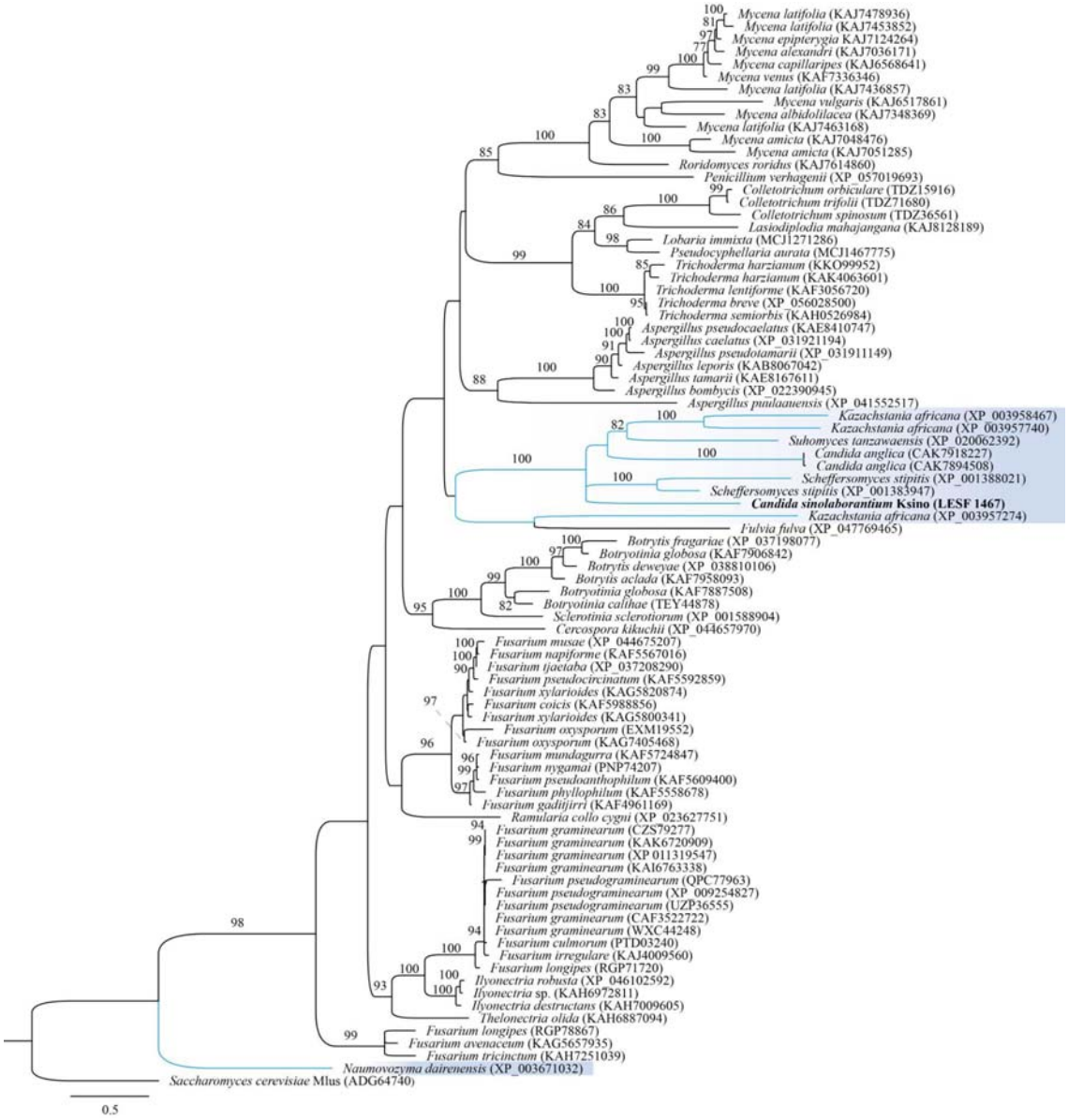

FIG S4. Phylogeny of Ksino homologs identified in diverse fungi. The Ksino-encoding yeast *C. sinolaborantium* is highlighted in bold, and Saccharomycotina in blue. The tree was inferred with maximum likelihood criteria, and numbers on branches are ultrafast bootstrap support values (only values higher than 70 are shown). The dsRNA-encoded killer toxin Klus is represented as an outgroup.

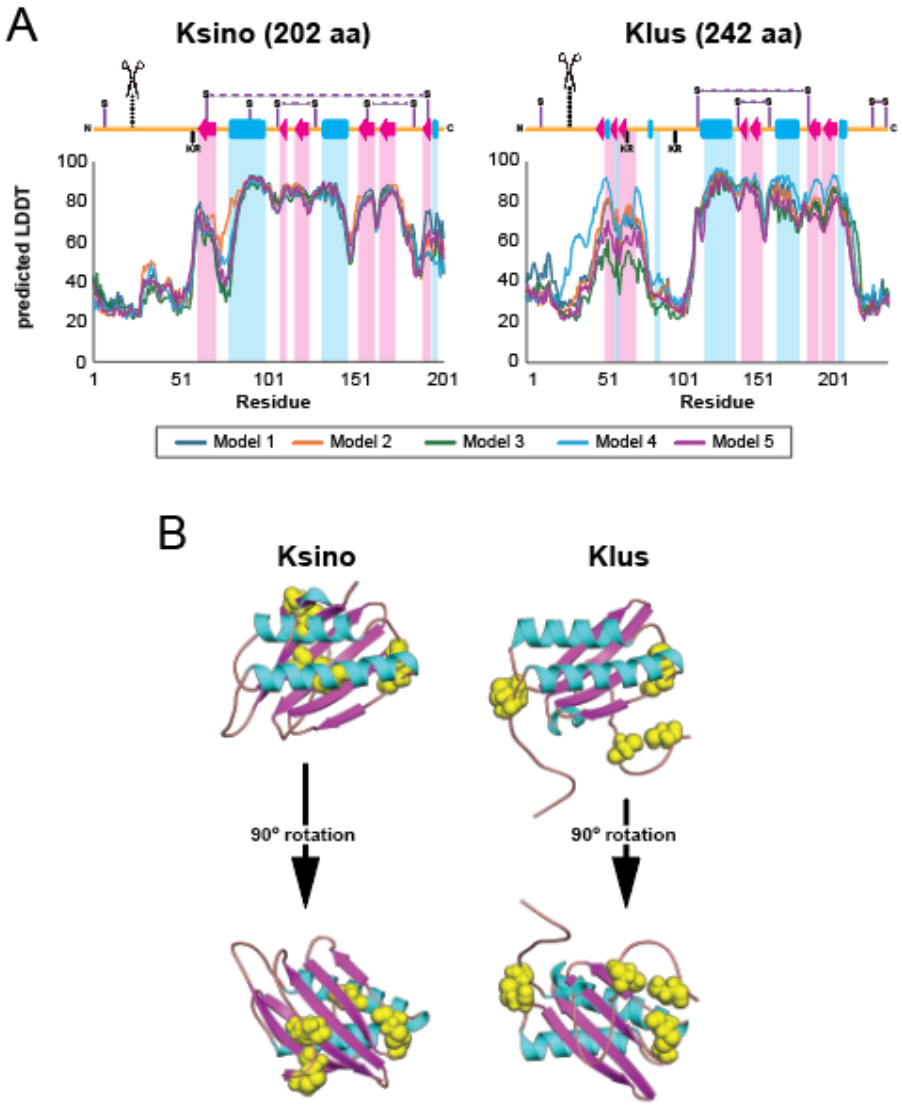

FIG S5. pLDDT confidence per residue and predicted disulfide bond arrangement of AlphaFold2 models of Ksino and Klus. A. Secondary structure representations aligned with per-residue pLDDT (predicted local distance difference test) scores from AlphaFold2. Alpha helices are represented as blue rectangles, beta sheets as red arrows, and unstructured regions as orange lines. Predicted disulfide linkages are indicated as horizontal dashed lines. Scissors with vertical dashed lines represent predicted signal sequence cleavage sites. **B.** Ksino and Klus AlphaFold2 models with cysteine residues highlighted as yellow spheres to illustrate predicted disulfide linkage arrangement. The cartoon helices and beta sheets are colored to match panel A.

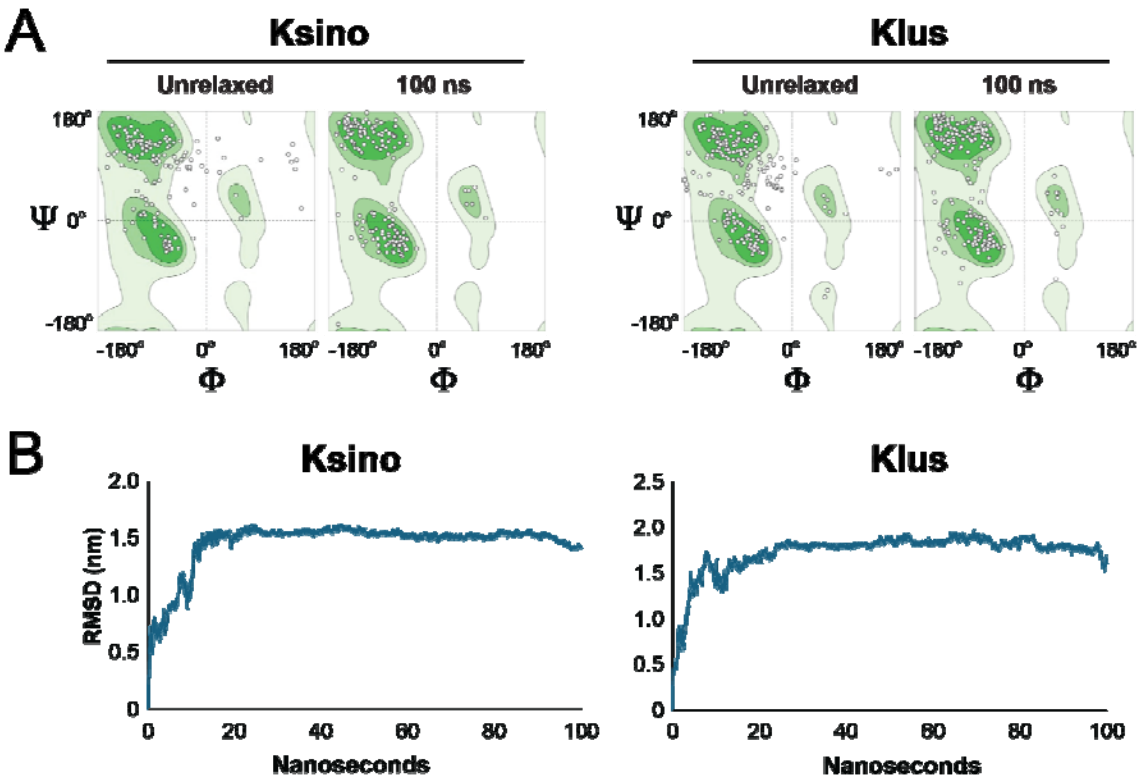

FIG S6. Molecular dynamics simulations of AlphaFold2 models of Ksino and Klus. A. Ramachandran plots of general residues (non-proline/glycine) generated by SWISS structure assessment tool demonstrating improved Ramachandran favored after performing 100 ns simulation. The unrelaxed structure represents AlphaFold2's raw output (Ramachandran et al., 1963). **B.** Full protein RMSD over 100 ns molecular dynamics simulation. GROMACS was used to generate alignments of each snapshot back to the structure at 0 ns.

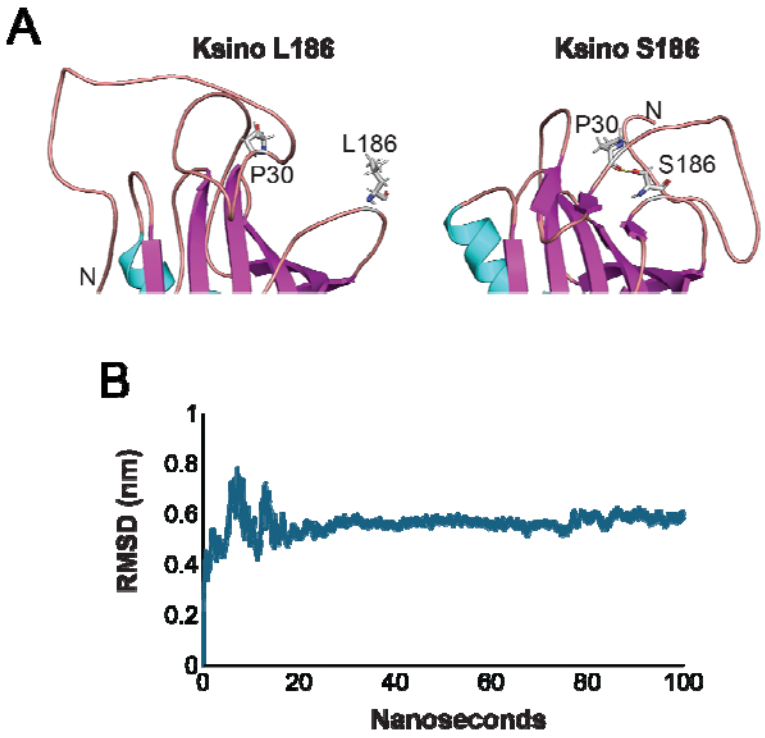

FIG S7. Computational predictions of protein stability with leucine and serine at position 186 in Ksino. A. AlphaFold2 models of Ksino wild type S186 and mutant L186 after 100 ns of molecular dynamics simulation. Residues 186 and P30 are shown as sticks. P30 forms a hydrogen bond (1.6 □) with the hydroxyl of S186 but is too distant to create this bond in L186. FoldX 5.0 analysis revealed a $\Delta\Delta G_{Folding}$ of 1.0 kcal/mol for L186S. **B.** 100 ns MD simulation of Ksino L186 AlphaFold2 model. Unlike wild type and Klus, the RMSD stabilizes around 0.55 nm.

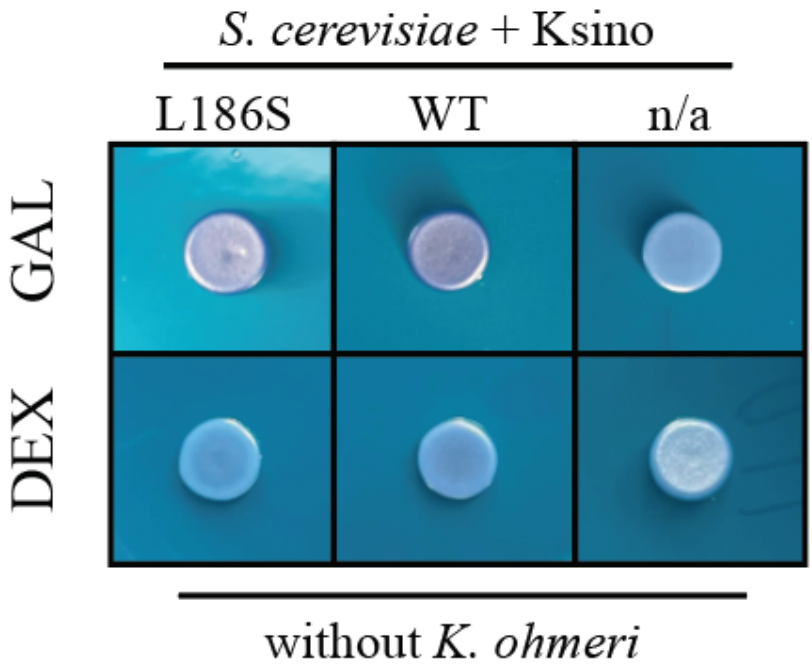

FIG S8. Recombinant expression of Ksino does not cause a white coloration of *S. cerevisiae*. Recombinant expression of Ksino by *S. cerevisiae* using galactose induction without a lawn of *K. ohmeri*. Dextrose was used as a non-induced control. n/a indicates an empty vector negative expression control.

Supplementary Tables

Table S1. Strains and species of yeasts used in the current study.

Table S2. The effect of isolation source on killer yeasts activity.

Table S3. The effect of pH on the growth inhibition of *Kodamaea ohmeri* LESF 1474 by *Candida sinolaborantium* LESF 1467

Table S4. The effect of temperature on the growth inhibition of *Kodamaea ohmeri* LESF 1474 by *Candida sinolaborantium* LESF 1467.

Table S5. The ratio between elongated and yeast morphology of *Kodamaea ohmeri* LESF 1474 cells challenged with killer toxins.

Table S6. Cell survival of *Kodamaea ohmeri* LESF 1474 cells against killer toxins.

Table S7. Statistics of the assembly, prediction, and annotation of the *Candida sinolaborantium* LESF1467 genome.

Table S8. Killer toxins were used as queries for the BLASTp search of the *Candida sinolaborantium* LESF1467 genome.

Table S9. Blastp hits of killer toxins towards *Candida sinolaborantium* LESF1467 genome.

Table S10. SWISS-MODEL structure assessment scores of Ksino top unrelaxed model and Klus top unrelaxed model compared to models after 100 ns of molecular dynamics simulation. Global pLDDT score is also included in the last row.

Table S11. Statistics of Blastp hits of Ksino homologs.

Table S12. Nucleotide sequences used in phylogenetic analysis of yeast species delimitation.

Table S13. Yeasts used in killer assays as susceptible or killer positive standards.

Supplementary files

File S1 - All killer assay data.

4. Materials and Methods

4.1. Yeast source and phylogenetic analysis

To investigate the prevalence of killer yeast in the fungus garden of attine ants, a representative collection of 180 yeasts previously characterized by Bizarria Jr. et al. (2023) was examined (Table S1). Briefly, yeasts were obtained by fungus garden suspension in saline solution (0.85% NaCl) supplemented with 0.05% Tween 80. Suspensions were ten-fold diluted and surface spread on nutrient media (Yeast-malt agar and Sabouraud dextrose agar, supplemented with 150 µg mL^{-1} chloramphenicol, and pH adjusted to 4.5; details in Bizarria Jr. et al. 2023). Yeast characterization involved microsatellite amplification analysis (MSP-PCR; Meyer et al. 1993) and sequencing of the D1/D2 region of the large subunit (LSU) ribosomal RNA gene (Kurtzman and Robnett, 1998). Our selection of the 180 *Saccharomycotina* yeasts spanned from fungus gardens of the leaf-cutting ant *Acromyrmex coronatus* (n = 91), the non-leaf-cutting ant *Mycetomoellerius tucumanus* (n = 13), the lower

attines *Mycetophylax* aff. *auritus* (n = 42), and *Mycocepurus goeldii* (n = 25), which cultivate *Agaricaceae* fungi; and *Apterostigma goniodes* (n = 9), which cultivates *Pterulaceae* fungi.

To assess the phylogenetic relationship between the yeast strains, we performed a phylogenetic analysis with representative species and their closest relatives (the accession number of sequences used in phylogenetic analysis is listed in Table S12). Sequences were aligned with MAFFT v.7. (Katoh et al. 2019), and nucleotide substitution models were generated using the Bayesian information criterion (BIC) by the standard model generation in IQ-TREE2. SYM+FQ+I+G4 was selected as the nucleotide substitution model. Maximum likelihood (ML) phylogenetic trees were reconstructed with ultrafast bootstrap in IQTREE2 (Nguyen et al. 2015), with 10,000 replicates for ultrafast bootstrap (tree completed after 262 iterations, LogL: -14973.244). The final trees were edited in FigTree v.1.4.3 (Rambaut, 2016).

4.2. Killer yeast assays

Killer assays were performed to confirm killer toxin production by yeasts, as described in Crabtree et al. (2019). The 180 yeast strains were seeded onto YPD 4.6 dextrose "killer assay" agar plates (yeast extract 10 g l^{-1}, peptone 20 g l^{-1}, dextrose 20 g l^{-1}, sodium citrate 29.9 g l^{-1}, supplemented with 0.003% w/v methylene blue, and pH adjusted to 4.6 with HCl), seeded 10^5 cells mL^{-1} with one of the 49 selected yeast susceptible strains (i.e. from fungus gardens and sources not related to attine ant environment, Table S13). Nine *Saccharomyces* spp. strains that encode known toxins were used as positive controls, including K1, K1L, K21, K2, K28, K45, K62, K74, and Klus (Table S13). Yeasts were also evaluated using 20 pathogenic yeasts as susceptible strains (Table S13). Toxin production was recorded after five days of incubation at room temperature, either by an inhibition zone or a methylene blue stain of susceptible strains. Killer activity severity was scored following Fredericks et al. (2021) by zone of inhibition with or without methylene blue halo or by strong or weak methylene blue halo without inhibition. To evaluate the effect of the yeast sources (i.e., same or different fungicultures or sites) on killer toxin activity (i.e., killed or non-killed). We selected 9,000 interactions (toward 50 strains that showed susceptibility to killer toxins) and analyzed them with Pearson's Chi-squared test.

4.3. Extraction of dsRNA encoding elements

To determine if the yeast strains host dsRNA elements, we extracted the dsRNA elements from all yeast strains following Okada et al. (2015), with modifications as stipulated in Crabtree et al. (2019). Specifically, yeast cultures were grown in yeast-peptone-dextrose broth (YPD: yeast extract 10 g l^{-1}, peptone 20 g l^{-1}, dextrose 20 g l^{-1}), centrifuged at 3000 × g for 5 min, and the broth was removed by aspiration. Cells were resuspended in water, centrifuged at 8,000 × g, and aspirated. A total of 450 µL of 2× sodium chloride-Tris-EDTA buffer (STE: 200 mM NaCl; 20 mM Tris-HCl, pH 8.0; 30 mM EDTA) and 0.5 µL β-mercaptoethanol were added, and cells were disrupted in a cell disruptor (Digital Disruptor Genie, Scientific Industries) for 3 min at 3000 rpm. Then, 50 µL of 10 % (w/v) sodium dodecyl sulfate (SDS) solution and 350 µL phenol–chloroform–isoamyl alcohol (25:24:1) were added to crude extracts, which were homogenized and centrifuged at 10,000 × g for 5 min. Then, 500 µL of supernatant was mixed with absolute ethanol (5:1), and the final volume of 600 µL was transferred to cellulose columns (i.e., 0.05 g cellulose D in a 0.6 mL tube bottom punctured and placed in collecting tubes).

Column tubes were centrifuged at 10,000 × g for 30 seconds, and the flow-through was discarded. Then, 350 µL of wash buffer (1× STE containing 16% v/v EtOH) was added to the column, and the tubes were centrifuged at 10,000 × g for 30 seconds, followed by the flow-through discard. Columns were transferred to a collecting tube, adding 350 µL of 1× STE, and tubes were centrifuged at 10,000 × g for 30 seconds. The eluted fraction was recovered, and 1 mL of absolute ethanol with 40 µL of 3 M aqueous sodium acetate (pH 5.2) was added. Tubes were inverted ten times and centrifuged at 20,000 × g for 15 min. The ethanol mix was aspirated without disturbing the precipitated pellet, which was then air-dried and dissolved in 15 µL of molecular-grade water. The presence of dsRNAs was examined (loading 5 µL of each sample) by 0.8% TAE agarose gel electrophoresis, stained with ethidium bromide, at 130 v for 30 min in 1% TAE buffer. As a molecular weight reference, a 1 kb DNA ladder was used. The *Saccharomyces cerevisiae* strain YJM1307, known to host dsRNA totivirus and satellites, was used as positive control.

4.4. Extraction of dsDNA linear plasmid

To determine if dsDNA linear plasmids encode the killer toxins, we extracted the dsDNA elements from positive killer yeast, *Kluyveromyces lactis* AWJ137 with the linear

DNA plasmids pGKL2 (13.5 kb) and pGKL1 (8.9 kb) and *Pichia acaciae* NRRL Y-18665 with the linear plasmids pPac1-1 (12.6 kb) and pPac1-2 (6.8 kb) (Worsham and Bolen, 1990; Gietz et al., 1995). Cultures were grown in YPD overnight, 200 µL were centrifuged at 3000 × g for 5 min, and the broth was removed by aspiration. Yeast cells were resuspended in 10 µL Zymolase solution (5% of 50 mM Tris-HCl, pH 8; 10% of 5 m M EDTA, and 85% water) and 7.2 µL of 10 mg mL^{-1} of Zymolase (United States Biological Life Sciences, Swampscott, MA), and the suspension was incubated at 30°C for one h. After incubation, 1 µL of 10% SDS and 3 µL of proteinase K (New England Biolabs, Ipswich, MA) were added to the suspension, followed by an incubation of 1 h at 65°C. After incubation, 5 µL of loading dye was added, and the suspension was centrifuged at 3000 × g for 5 min. The presence of dsDNA plasmids was examined (loading 10 µL of each sample) by 0.6% TAE agarose gel electrophoresis, stained with ethidium bromide, at 130 v for 1 h in 1% TAE buffer.

4.5. Toxin precipitation and stability

To investigate the stability of the toxins produced by *C. sinolaborantium* LESF 1467, the isolate extracts on YPD medium (pH 4.6) were filtered, mixed with 1:1 absolute ethanol, centrifuged at 20,000 × g for 20 min, followed by supernatant aspiration and suspension in 10 µL of YPD (pH 4.6). To confirm the killer activity of the precipitates, 4 µL of the suspended proteins were used in killer assays against *Kodamaea ohmeri* LESF 1474. To evaluate the thermostability, the precipitated toxins were screened in killer assays incubating at room temperature or heat-inactivated at 60°C and 98°C for 2 min. The killer activity was also evaluated for stability at different pHs, adjusting the pH to 3.5, 4, 4.5, 5, 5.5, and 6 with HCl 12N, and in various temperatures, incubating at 17, 20, 25, 30, and 35°C. The area of activity on killer assays (i.e., zone of inhibition and cell differentiation of the lawn strain) was measured in cm^2 after four days with ImageJ 1.53t (Schneider et al., 2012). Since the area data do not satisfy the assumptions of parametric tests, we analyzed variance with Kruskal-Wallis followed by the Wilcoxon rank sum test with Bonferroni correction as a post-hoc for pairwise multiple comparisons. Analyses were performed using the software RStudio v. 2023.12.0.369 (POSIT TEAM, 2023), and R v. 4.3.2 (R CORE TEAM, 2023). Figures were prepared using ggplot2 (Wickham, 2016).

4.6. Production of elongated cells by *Kodamaea ohmeri* against killer toxins

We observed that the yeast *K. ohmeri* LESF 1474 produces elongated cells in the presence of *C. sinolaborantium* toxins and their precipitates. We suspended the cells in the white and raised zones of killer assays and on axenic cultures in 1× PBS. Cell morphology was checked under a microscope (Zeiss Primo Star iLED) by counting budding (2 to 17 × 10^6 cells mL^{-1}) and elongated cells (2 to 15 × 10^5 cells mL^{-1}) with a Neubauer chamber. Cell survival was evaluated by adjusting the suspensions to 10^3 cells mL^{-1} and seeding 100 µL in YPD. Colony-forming units (CFU) were counted after three days of incubation at room temperature. A similar elongated cell phenotype was observed in the presence of *S. cerevisiae* DSM-70459, which secretes the known killer toxin Klus (encoded by dsRNA elements). Microscopic and survival evaluations were also conducted in the presence of *S. cerevisiae* DSM-70459, as described above. To confirm that the elongated cell phenotype is related to the presence of the dsRNA satellites, dsRNA satellites were cured from *S. cerevisiae* by growing on a YPD medium supplemented with 5.0 µM cyclohexamide. Loss of killer toxin production and the loss of dsRNAs were assayed as described above. The ratio between normal and elongated cells was compared between *K. ohmeri* in the white halo around *C. sinolaborantium* and *S. cerevisiae* DSM-70459 with axenic cultures surrounding the halo, with ten independent replicates. The data was checked for the assumption of parametric tests (performing Shapiro-Wilk and Bartlett tests, respectively, for normality and homogeneity of variances). The ratio data in both treatments, towards *C. sinolaborantium* and *S. cerevisiae* DSM-70459, were found not to satisfy the assumptions of equal variance (Bartlett test, df = 1, p-value = 0.00), so we conducted the Welch Two Sample t-test to compare means between treatments. The same procedure was performed for cell survival data towards *C. sinolaborantium*, which also did not satisfy the assumptions of equal variance (Bartlett's K-squared = 4.16, df = 1, p-value = 0.04). Cell survival data towards *S. cerevisiae* DSM-70459 satisfied the assumptions for parametric tests (Bartlett's K-squared = 0.52, df = 1, p-value = 0.47; Shapiro-Wilk p-value > 0.05), so we conducted the Two Sample t-test to compare means between treatments.

4.7. Genomic DNA extraction, sequencing, and annotation

To extract genomic DNA from *C. sinolaborantium*, the yeast was grown in YPD broth; cells were recovered by centrifugation (3000 × g for 5 min), washed, and suspended in 500 µL TE buffer (10 mM Tris-Cl; 0.1 mM EDTA, pH 8). Recovered cells were transferred to a microtube, centrifugation as previously described, and the supernatant was removed. The

pellet was disrupted by vortexing. Cells were suspended in a lysis buffer (2% Triton X-100, 1% SDS, 100 mM NaCl, 10 mM Tris-HCl, pH 8, 1 mM EDTA pH 8) with approximately 300 µL of glass beads. A volume of 200 µL of phenol-chloroform-isoamyl alcohol solution was added, and the sample was vortex for 3 min at 3000 rpm (Disruptor Genie), followed by the addition of 200 µL of TE buffer and centrifugation for 5 min at 21000 × g. The upper layer was transferred to a new microtube and mixed by inversion with 1 mL of absolute ethanol. The tube was centrifuged for 3 min at 21000 × g, the supernatant removed, and the pellet suspended in 400 µL of TE buffer. Then, 30 µL of DNAse-free RNAse A was added, and the solution was mixed and incubated for 5 min at 37°C. The DNA was precipitated by adding 10 µL of 4 M ammonium acetate and 1 mL of absolute ethanol, mixing by inversion, and centrifuging for 3 min at 21000 × g. The supernatant was discarded and the pellet was dried for approximately 20 min at room temperature. Genomic DNA was suspended in 100 µL of TE buffer and stored at -20°C.

The genome was sequenced by Illumina NextSeq 550 using the paired-end method. Libraries were created with the Illumina DNA Prep kit for WGS (https://www.illumina.com/products/by-type/sequencing-kits/library-prep-kits/nextera-dna-flex.html). The initial quality analysis and cleaning steps were performed with fastp v. 0.20.1 (CHEN et al., 2018). The genome was assembled with SPAdes v. 3.15.5 (GUREVICH et al., 2013) with multiple k-mers (21, 31, 41, 51, 61, 71, and 81). The blobtools v. 3.5.2 software (LAETSCH; BLAXTER, 2017) was used to check contaminants. Briefly, Blastn 2.13.0+ (ALTSCHUL et al., 1990) was used to search for structures across the entire NCBI nt database; minimap2 v. 2.24-r1122 (LI, 2018) and samtools v.1.13 (LI et al., 2009) were used to obtain sequencing coverage. The blobtools visualization was used to ascertain the results. The rDNA and ITS regions were annotated with ITSx v. 1.3 (BENGTSSON-PALME et al., 2013), which was compared to an amplicon previously submitted to NCBI for this isolate (accession: ON493969) as part of the contamination verification steps. Final assembly statistics were obtained with QUAST v. 5.2.0 (BANKEVICH et al., 2012). Completeness was checked using BUSCO v. 5.4.4 (SEPPEY et al., 2019) with the saccharomycetes_odb10 dataset (2,137 BUSCOs). The genetic prediction was performed using Braker v. 2.1.6 (BRŮNA et al., 2021) [which includes Augustus v. 3.4.0 (STANKE; MORGENSTERN, 2005), ProtHint v. 2.6.0 and GeneMark-ES v. 4.71 (LOMSADZE et al. 2005)] with OrthoDB v. 10 methods (KRIVENTSEVA et al., 2019). InterProScan v. 5.60 (Jones et al., 2014) was used for functional annotation of predicted proteins.

4.8. Genome mining for toxin-encoding regions

To identify toxin-encoding chromosomal regions, a search using proteins predicted from whole genome sequencing was performed with BLASTP 2.9.0, using a protein sequence database of known killer toxins. Results with query/hit alignments greater than 100 were selected. An open reading frame similar to the Klus toxin (28% identity, with 151 aa alignment length and an e-value of $1.56E^{-05}$) was found and selected for further analysis. Polymerase chain reactions (PCR) were performed to amplify the region of interest using primers designed with Primer3 software. 4.1.0 (https://primer3.ut.ee/). The primers were designed to target Ksino untranslated regions (961F: 5'-TTAACGACTTTCGTCTTCGCTATCC-3' and 961R: 5'-ATTGAGATCAGGTGGCCTGTGTAGC-3') followed by nested-PCR to amplify the open reading frame using the previous PCR product as the template (961NF: 5'-CGATCACCTAGCCCAAAATGC-3' and 961NR: 5'-AAAGTGTTGGCCAAGGACACG-3'). Both of the amplification reactions used Phusion high fidelity master mix (New England Biolabs, Ipswich, MA) with the amplification conditions of 98°C for 3 min, 30 cycles at 98°C for 30 s, 63°C for 30 s, 72°C for 30 s, and a final extension step at 72°C for 5 min. Amplicons were sequenced to confirm the identity of the region of interest.

4.9. Prediction of tertiary structure and comparative analysis of proteins

After confirming the genomic coding region of Ksino was the correct size using PCR, the sequence was used to predict protein structure via the AlphaFold2 software (Jumper et al., 2021) with default parameters. The B factor columns of each unrelaxed structure were used to create per residue pLDDT graphs. Secondary structure was assigned using PyMol to create a linear representation of the protein and aligned to per residue graphs. The top-scoring relaxed model from AlphaFold2 was used for molecular dynamics simulation using the GROMACS package (Spoel et al., 2005). Briefly, the system was set up using the AMBER99SB-ILDN force field with TIP3P water, a dodecahedral box with 1.0 nm padding, and 0.15 M NaCl. The system was then subjected to energy minimization by steepest descent, followed by NVT and NPT equilibration with a pressure of 1.0 atm and temperature of 300 K. Pressure and temperature were maintained constant using arrinello-Rahman with isotropic coupling and V-rescale with Protein Non-protein as the coupling groups, respectively. This setup was chosen to match standard cellular conditions closely: 26.85°C,

0.15 M NaCl, pH 7, and 1 atm. Simulations were run for 100 ns with a 2.0 fs timestep, and snapshots were saved every 2 fs. The RMSD was calculated as a function of time using the resulting trajectories. In addition, the final snapshot of each trajectory was saved as a PDB structure file and compared to relaxed and unrelaxed AlphaFold2 models using the SWISS structure assessment tool (Studer et al., 2019).

FoldX was used to predict the $\Delta\Delta G_{Folding}$ of L186S (Delgado et al., 2019). Amber relaxed Ksino L186 was used as the starting structure, and FoldX PDBrepair was carried out six times to optimize the structure. Then, L186 in the optimized structure was mutated to every other residue using PositionScan. $\Delta\Delta G_{Folding}$ was taken from the output file.

4.10. Bioinformatic discovery of Ksino homologs in fungi

A search for similar sequences in NCBI (https://www.ncbi.nlm.nih.gov/) was also carried out with Blastp, with the results filtered by alignment length (above 109), identity (above 30%), and e-value (less than 0.03). The protein sequences were aligned with MUSCLE (https://www.ebi.ac.uk/jdispatcher/msa/muscle), with the alignment consisting of 86 sequences and 426 positions. Amino acid substitution models were generated according to the Bayesian information criterion (BIC), with WAG+R4 being the chosen model. Maximum likelihood (ML) phylogenetic trees were reconstructed in IQTREE2 (Nguyen et al., 2015), with 10,000 ultrafast bootstrap replicates (tree completed after 163 iterations, LogL: -18525.485). The final trees were edited in FigTree v.1.4.3 (RAMBAUT, 2016).

4.11. Cloning and transformation in *Escherichia coli*

To study the coding region, a "TA" terminal was added to the amplicon in a reaction that included 1 µL Taq polymerase, 19 µL of PCR product, 1 µL of 10 µM dNTPs, 5 µL of 10× buffer, and 24 µL of sterile ultrapure water. The reaction was incubated at 72°C for 20 min. For cloning, the pCR™8/GW/TOPO™ TA Cloning kit (Invitrogen, Waltham, MA) was used, adding 1 µL of amplicons with TA terminals, 0.25 µL of saline solution from the kit, and 0.25 µL of the pCR™8/GW/TOPO™ vector. The reaction was incubated at room temperature for 2 h, followed by adding 25 µL of competent *E. coli* cells (One-Shot TOP10 Competent Cells, Invitrogen, Waltham, MA). The reaction was kept on ice for 30 min, followed by heat shock at 42°C for 30 s and then ice bath for 2 min. Subsequently, 250 µL of Super Optimal broth (SOC: 20 g L^{-1} Tryptone, 5 g L^{-1} Yeast extract, 0.58 g L^{-1} NaCl, 0.19 g

L^{-1} KCl, 2, 03 g L^{-1} $MgCl_2$, 1.20 g L^{-1} $MgSO_4$, and 3.6 g L^{-1} dextrose) preheated to 37°C was added, and incubated at 37°C for 1 h. Then, 250 µL were plated on Luria bertani medium (LB: 10 g L^{-1} of tryptone, 5 g L^{-1} of yeast extract, 10 g L^{-1} of NaCl, and 15 g L^{-1} of agar) supplemented with 100 µg mL-1 of spectinomycin. Plasmids were extracted using the High-Speed Mini Plasmid kit (IBI Scientific, Dubuque, IA), following manufacturer recommendations.

Due to the transcriptional diversity of CUG-Leu codons in some yeasts (Krassowski et al., 2018), the vectors containing the region of interest were subjected to targeted mutations (SDM: Site-Directed Mutagenesis) in a CUG codon starting at position 556 of the DNA sequence (position 186 in the protein sequence). Thus, the mutants consist of the alternatives identified for CUG in other yeasts, being called L186A and L186S, with L being the original amino acid, 186 the position, and "S" the mutation for Ser. To obtain the mutants, we design primers targeting position 186 as follows: 961GCG: 5'-CAGCTGTGGCGCGAACCATAGCGGG-3', 961TCG: 5'-CAGCTGTGGCTCGAACCATAGCGGG-3' (forward), and 961SNM: 5'-AGTCCCGCAGGCCAATCC-3' (reverse). Amplification reactions included 12.5 µL of Phusion High Fidelity Master Mix, 1 µL 10 µM forward primer, 1 µL 10 µM reverse primer, 9.5 µL sterile ultrapure water, 1 µL 1:9 diluted DNA (i.e., pCR™8 plasmid with the region of interest). Amplification conditions were as follows: 98°C for 30 min, 25 cycles at 98°C for 5 s, 67°C for 10 s, 72°C for 50 s, and a final extension step at 72°C for 5 min. To remove the template DNA from the reaction, a Dpnl treatment was performed by mixing 22 µL of PCR product, 2 µL Dpnl, 3 µL CutSmart buffer, and 3 µL sterile ultrapure water. The reaction was incubated at 37°C for 1 day. For the addition of 5'-P and 3'-OH, we performed a PNK treatment: 30 µL of the treated product, 5 µL PNK buffer, 1 µL PNK, 5 µL 10 mM ATP, 1 µL 0.1 M DTT, 8 µL of sterile ultrapure water. The reactions were incubated for 30 min at 37°C and inactivated at 65°C for 10 min. The product was purified using the Monarch DNA & PCR Cleanup kit (New England Biolabs, Ipswich, MA), following the manufacturer's protocols. To re-ligate the plasmids, the following reaction was performed: 2 µL of purified product, 1 µL T4 DNA ligase, 2 µL 10× binding buffer, 15 µL sterile ultrapure water. The reaction was incubated for 2 h at room temperature, and then 25 µL of competent *E. coli* cells (One-Shot TOP10 Competent Cells, Invitrogen, Waltham, MA) were added. Transformed cultures were selected in LB supplemented with 100 µg mL^{-1} spectinomycin, plasmids extracted with the High-Speed Mini Plasmid kit (IBI Scientific, Dubuque, IA), and mutations checked by sequencing (ELIM Biopharmaceuticals, Hayward, CA).

The vectors were subjected to a Gateway™ recombination from the vectors in pCR8 to pAG306-GAL-ccdB. For recombination, the reaction was conducted with 0.5 μL of the source vector, 0.5 μL of the destination vector, 1 μL of sterile ultrapure water, and 0.5 μL of LR Clonase II (New England Biolabs, Ipswich, MA). The reaction was incubated for 4 h at room temperature, followed by adding 0.25 μL of Proteinase K (New England Biolabs, Ipswich, MA) and incubating at 37°C for 10 min. Finally, the *E. coli* transformation was performed as previously described, and cultures were selected in LB supplemented with 100 μg mL^{-1} of chloramphenicol and ampicillin.

4.12. Transformation and heterologous expression in *Saccharomyces cerevisiae*

For yeast transformation, the vector containing the region of interest was linearized with the NcoI enzyme by cutting at the *URA3* locus, followed by inactivation of the enzyme at 65°C for 30 min. The product was purified using the Monarch DNA & PCR Cleanup kit (New England Biolabs, Ipswich, MA), following the manufacturer's recommendations. *Saccharomyces cerevisiae* cry1 cells were grown in YPD until an optical density of 1.3 was obtained, then the cells were washed with sterile water and suspended in 10 mL of TE buffer supplemented with 100 mM LiAc, and incubated at 30°C for 30 min under 130 rpm agitation. Cells were recovered by centrifugation at 1500 × g for 5 min at 4°C and suspended in 5 mL of ice-cold 1M sorbitol, followed by centrifugation and suspended in 550 μL of ice-cold 1M sorbitol. For transformation, 80 μL of the suspended cells were added to 5 to 10 μg of the linearized plasmids and transferred to electroporation cuvettes. The cuvettes were incubated on ice for 10 min and pulsed with GenePulser (200 Ω, 1.5 kV, and 25 μF). To recover the transformed cultures, the cells were grown at 30°C for 2 days in CM medium without uracil (complete media: 2.5 g L^{-1} of the drop-out mix without uracil, 1.7 g L^{-1} of yeast nitrogen base YNB, 5 g L^{-1} ammonium sulfate, 20 g L^{-1} dextrose). For expression of the region of interest, the killer phenotype was performed in YPGal (yeast extract 10 g L^{-1}, peptone 20 g L^{-1}, galactose 20 g L^{-1}, citrate-phosphate 29.9 g L^{-1}, supplemented with 0.003% w/v methylene blue, with 1M NaCl, and pH adjusted to 4.6 with HCl and 15 g L^{-1} agar). *C. sinolaborantium* and *S. cerevisiae* CRY1 were used as positive and negative controls for killer activity, respectively.

References

Abranches, J., Mendonça-Hagler, L. C., Hagler, A. N., Morais, P. B., Rosa, C. A. (1997). The incidence of killer activity and extracellular proteases in tropical yeast communities. **Canadian Journal of Microbiology**, 43(4), 328-336. doi: 10.1139/m97-046

Abranches, J., Valente, P., Nóbrega, H. N., Fernandez, F. A., Mendonça-Hagler, L. C., Hagler, A. N. (1998). Yeast diversity and killer activity dispersed in fecal pellets from marsupials and rodents in a Brazilian tropical habitat mosaic. **FEMS Microbiology Ecology**, 26(1), 27-33. doi: 10.1111/j.1574-6941.1998.tb01558.x

Altschul, S. F., Gish, W., Miller, W., Myers, E. W., Lipman, D. J. (1990). Basic local alignment search tool. **Journal of molecular biology**, 215(3), 403-410. doi: 10.1016/S0022-2836(05)80360-2

Amos, B. A., Hayes, R. A., Leemon, D. M., Furlong, M. J. (2019). Small hive beetle (Coleoptera: Nitidulidae) and the yeast, *Kodamaea ohmeri*: a facultative relationship under laboratory conditions. **Journal of Economic Entomology**, 112(2), 515-524. doi: 10.1093/jee/toy378

Antunes, J., Aguiar, C. (2012). Search for killer phenotypes with potential for biological control. **Annals of microbiology**, 62, 427-433. doi: 10.1007/s13213-011-0256-z

Arcuri, S. L., Pagnocca, F. C., da Paixão Melo, W. G., Nagamoto, N. S., Komura, D. L., Rodrigues, A. (2014). Yeasts found on an ephemeral reproductive caste of the leaf-cutting ant *Atta sexdens rubropilosa*. **Antonie Van Leeuwenhoek**, 106(3), 475–487. doi: 10.1007/s10482-014-0216-2

Bankevich, A., et al. (2012). SPAdes: a new genome assembly algorithm and its applications to single-cell sequencing. **Journal of computational biology**, 19(5), 455-477. doi: 10.1089/cmb.2012.0021

Belda, I., Ruiz, J., Alonso, A., Marquina, D., Santos, A. (2017). The biology of *Pichia membranifaciens* killer toxins. **Toxins**, 9(4), 112. doi: 10.3390/toxins9040112

Benda, N. D., Boucias, D., Torto, B., Teal, P. (2008). Detection and characterization of *Kodamaea ohmeri* associated with small hive beetle *Aethina tumida* infesting honey bee hives. **Journal of Apicultural Research**, 47(3), 194-201. doi: 10.1080/00218839.2008.11101459

Bengtsson-Palme, J., et al. (2013). Improved software detection and extraction of ITS1 and ITS 2 from ribosomal ITS sequences of fungi and other eukaryotes for analysis of environmental sequencing data. **Methods in Ecology and Evolution**, 4(10), 914-919. doi: 10.1111/2041-210X.12073

Bevan, E. A., Herring, A. J., Mitchell, D. J. (1973). Preliminary characterization of two species of dsRNA in yeast and their relationship to the “killer” character. **Nature**, 245(5420), 81-86. doi: 10.1038/245081b0

Bizarria Jr, R., de Castro Pietrobon, T., Rodrigues, A. (2023). Uncovering the Yeast Communities in Fungus-Growing Ant Colonies. **Microbial Ecology**, 86(1), 624-635. doi: 10.1007/s00248-022-02099-1

Bizarria Jr, R., Pagnocca, F. C., Rodrigues, A. (2022). Yeasts in the attine ant–fungus mutualism: Diversity, functional roles, and putative biotechnological applications. **Yeast**, 39(1-2), 25-39. doi: 10.1002/yea.3667

Boynton, P. J. (2019). The ecology of killer yeasts: Interference competition in natural habitats. **Yeast**, 36(8), 473–485. doi: 10.1002/yea.3398

Branstetter, M. G., Ješovnik, A., Sosa-Calvo, J., Lloyd, M. W., Faircloth, B. C., Brady, S. G., and Schultz, T. R. (2017). Dry habitats were crucibles of domestication in the evolution of agriculture in ants. **Proceedings of the Royal Society B: Biological Sciences**, 284(1852), 20170095. doi: 10.1098/rspb.2017.0095

Brown, D. W. (2011). The KP4 killer protein gene family. **Current genetics**, 57, 51-62. doi: 10.1007/s00294-010-0326-y

Brůna, T., Hoff, K. J., Lomsadze, A., Stanke, M., Borodovsky, M. (2021). BRAKER2: automatic eukaryotic genome annotation with GeneMark-EP+ and AUGUSTUS supported by a protein database. **NAR genomics and bioinformatics**, 3(1), lqaa108. doi: 10.1093/nargab/lqaa108

Buchan DWA, Minneci F, Nugent TCO, Bryson K, Jones DT (2013). Scalable web services for the PSIPRED Protein Analysis Workbench. **Nucleic Acids Res.** 41(W1): W349–W357. doi: 10.1093/nar/gkt381.

Buser, C. C., Jokela, J., Martin, O. Y. (2021). Scent of a killer: How could killer yeast boost its dispersal?. **Ecology and Evolution**, 11(11), 5809-5814. doi: 10.1002/ece3.7534

Bussey, H., Vernet, T., Sdicu, A. M. (1988). Mutual antagonism among killer yeasts: Competition between Kl and K2 killers and a novel cDNA-based K1-K2 killer strain of *Saccharomyces cerevisiae*. **Canadian journal of microbiology**, 34(1), 38-44. doi: 10.1139/m88-007

Buzzini, P., Martini, A. (2001). Discrimination between *Candida albicans* and other pathogenic species of the genus *Candida* by their differential sensitivities to toxins of a panel of killer yeasts. **Journal of clinical microbiology**, 39(9), 3362-3364. doi:10.1128/jcm.39.9.3362-3364.2001

Carreiro, S. C., Pagnocca, F. C., Bacci, M., Bueno, O. C., Hebling, M. J. A., Middelhoven, W. J. (2002). Occurrence of killer yeasts in leaf-cutting ant nests. **Folia Microbiologica**, 47(3), 259–262. doi: 10.1007/BF02817648

Castillo, A., Cifuentes, V. (1994). Presence of double-stranded RNA and virus-like particles in *Phaffia rhodozyma*. **Current genetics**, 26, 364-368. doi: 10.1007/BF00310502

Chen, S., Zhou, Y., Chen, Y., Gu, J. (2018). fastp: an ultra-fast all-in-one FASTQ preprocessor. **Bioinformatics**, 34(17), i884-i890. doi: 10.1093/bioinformatics/bty560

Chessa, R., et al. (2017). Biotechnological exploitation of *Tetrapisispora phaffii* killer toxin: heterologous production in *Komagataella phaffii* (*Pichia pastoris*). **Applied microbiology and biotechnology**, 101(7), 2931-2942. doi: 10.1007/s00253-016-8050-2

Coelho, A. R., Tachi, M., Pagnocca, F. C., Nobrega, G. M. A., Hoffmann, F. L., Harada, K. I., Hirooka, E. Y. (2009). Purification of *Candida guilliermondii* and *Pichia ohmeri* killer toxin as an active agent against *Penicillium expansum*. **Food Additives and Contaminants**, 26(1), 73-81. doi: 10.1080/02652030802227227

Corrêa, M. M., Silva, P. S., Wirth, R., Tabarelli, M., Leal, I. R. (2010). How leaf-cutting ants impact forests: drastic nest effects on light environment and plant assemblages. **Oecologia**, 162, 103-115. doi: 10.1007/s00442-009-1436-4

Crabtree, A. M., Kizer, E. A., Hunter, S. S., Van Leuven, J. T., New, D. D., Fagnan, M. W., Rowley, P. A. (2019). A rapid method for sequencing double-stranded RNAs purified from yeasts and the identification of a potent K1 killer toxin isolated from *Saccharomyces cerevisiae*. **Viruses**, 11(1), 70. doi: 10.3390/v11010070

Crabtree, A. M., Taggart, N. T., Lee, M. D., Boyer, J. M., Rowley, P. A. (2023). The prevalence of killer yeasts and double-stranded RNAs in the budding yeast *Saccharomyces cerevisiae*. **FEMS Yeast Research**, 23, foad046. doi: 10.1093/femsyr/foad046

Craven, S. E., Dix, M. W., Michaels, G. E. (1970). Attine fungus gardens contain yeasts. **Science**, 169(3941), 184–186. doi: 10.1126/science.169.3941.184

Crucitti, D., Chiapello, M., Oliva, D., Forgia, M., Turina, M., Carimi, F., La Bella, F., Pacifico, D. (2021). Identification and molecular characterization of novel mycoviruses in *Saccharomyces* and non-*Saccharomyces* yeasts of oenological interest. **Viruses**, 14(1), 52. doi: 10.3390/v14010052

De Fine Licht, H. H., Boomsma, J. J. (2010). Forage collection, substrate preparation, and diet composition in fungus□growing ants. **Ecological Entomology**, 35(3), 259-269. doi: 10.1111/j.1365-2311.2010.01193.x

Delgado J, Radusky LG, Cianferoni D, Serrano L (2019). FoldX 5.0: Working with RNA, small molecules and a new graphical interface. **Bioinformatics**. 35(20): btz184. doi: 10.1093/bioinformatics/btz184.

Drinnenberg, I. A., Fink, G. R., Bartel, D. P. (2011). Compatibility with killer explains the rise of RNAi-deficient fungi. **Science**, 333(6049), 1592-1592. doi: 10.1126/science.1209575

Drinnenberg, I. A., Weinberg, D. E., Xie, K. T., Mower, J. P., Wolfe, K. H., Fink, G. R., Bartel, D. P. (2009). RNAi in budding yeast. **Science**, 326(5952), 544-550. doi: 10.1126/science.1176945

Farji□brener, A. G., Werenkraut, V. (2015). A meta□analysis of leaf□cutting ant nest effects on soil fertility and plant performance. **Ecological Entomology**, 40(2), 150-158. doi: 10.1111/een.12169

Fisher, P. J., Stradling, D. J., Sutton, B. C., Petrini, L. E. (1996). Microfungi in the fungus gardens of the leaf-cutting ant *Atta cephalotes*: a preliminary study. **Mycological Research**, 100(5), 541–546. doi: 10.1016/S0953-7562(96)80006-2

Frank, A. C., Wolfe, K. H. (2009). Evolutionary capture of viral and plasmid DNA by yeast nuclear chromosomes. **Eukaryotic Cell**, 8(10), 1521-1531. doi: 10.1128/ec.00110-09

Fredericks, L. R., et al. (2021). The species-specific acquisition and diversification of a K1-like family of killer toxins in budding yeasts of the *Saccharomycotina*. **PLoS genetics**, 17(2), e1009341. doi: 10.1371/journal.pgen.1009341

Fuentefria, A. M., Faganello, J., Pazzini, F., Schrank, A., Valente, P., Vainstein, M. (2007). Typing and patterns of cellular morphological alterations in *Cryptococcus neoformans* and *Cryptococcus gattii* isolates exposed to a panel of killer yeasts. **Medical mycology**, 45(6), 503-512. doi: 10.1080/13693780701416580

Fuentefria, A. M., Franskoviaki, I. M., Mercado, L. W., Ramos, J. P., Vainstein, M. H., Valente, P. (2006). Inhibition of clinical and environmental *Cryptococcus neoformans* isolates by two Brasilian killer yeasts. **Journal of basic microbiology**, 46(2), 87-93. doi: 10.1002/jobm.200510018

Fuentefria, A. M., Perez, L. R., Alves d'Azevedo, P., Pazzini, F., Schrank, A., Vainstein, M. H., Valente, P. (2008). Typing of *Staphylococcus epidermidis* clinical strains by a selected panel of Brasilian killer yeasts. **Journal of basic microbiology**, 48(1), 25-30. doi: 10.1002/jobm.200700143

Ganter, P. F., Starmer, W. T. (1992). Killer Factor as a Mechanism of Interference Competition in Yeasts Associated with Cacti: Ecological Archives. **Ecology**, 73(1), 54-67. doi: 10.2307/1938720

Gietz, R. D., Schiestl, R. H., Willems, A. R., Woods, R. A. (1995). Studies on the transformation of intact yeast cells by the LiAc/SS□DNA/PEG procedure. **Yeast**, 11(4), 355-360. doi: 10.1002/yea.320110408

Gimeno, C. J., Ljungdahl, P. O., Styles, C. A., Fink, G. R. (1992). Unipolar cell divisions in the yeast *S. cerevisiae* lead to filamentous growth: regulation by starvation and RAS. **Cell**, 68(6), 1077-1090. doi: 10.1016/0092-8674(92)90079-R

Giometto, A., Nelson, D. R., Murray, A. W. (2021). Antagonism between killer yeast strains as an experimental model for biological nucleation dynamics. **Elife**, 10, e62932. doi: 10.7554/eLife.62932

Giovati, L., et al. (2018). Candidacidal activity of a novel killer toxin from *Wickerhamomyces anomalus* against fluconazole-susceptible and-resistant strains. **Toxins**, 10(2), 68. doi: 10.3390/toxins10020068

Golubev, W. I. (1998). Mycocins (killer toxins). In **The Yeasts** (pp. 55-62). Elsevier. doi: 10.1016/B978-044481312-1/50011-3

Golubev, W. I. (2006). Antagonistic interactions among yeasts. In: Péter, G., Rosa, C. (eds) Biodiversity and Ecophysiology of Yeasts. **The Yeast Handbook**. Springer, Berlin, Heidelberg. doi: 10.1007/3-540-30985-3_10

Golubev, W. I., Pfeiffer, I., Golubeva, E. (2002). Mycocin production in *Trichosporon pullulans* populations colonizing tree exudates in the spring. **FEMS microbiology ecology**, 40(2), 151-157. doi: 10.1111/j.1574-6941.2002.tb00947.x

Goto, K., Iwatuki, Y., Kitano, K., Obata, T., Hara, S. (1990). Cloning and nucleotide sequence of the KHR killer gene of *Saccharomyces cerevisiae*. **Agricultural and biological chemistry**, 54(4), 979-984. doi: 10.1080/00021369.1990.10870081

Goto, K., Fukuda, H., Kichise, K., Kitano, K., Hara, S. (1991). Cloning and nucleotide sequence of the KHS killer gene of *Saccharomyces cerevisiae*. **Agricultural and biological chemistry**, 55(8), 1953-1958. doi: 10.1080/00021369.1991.10870924

Greig, D., Travisano, M. (2008). Density-dependent effects on allelopathic interactions in yeast. **Evolution**, 62(3), 521-527. doi: 10.1111/j.1558-5646.2007.00292.x

Groenewald, M., et al. (2023). A genome-informed higher rank classification of the biotechnologically important fungal subphylum Saccharomycotina. **Studies in Mycology**, 105, 1–22. doi: 10.3114/sim.2023.105.01

Guamán-Burneo, M. C., et al. (2015). Xylitol production by yeasts isolated from rotting wood in the Galápagos Islands, Ecuador, and description of *Cyberlindnera galapagoensis* fa, sp. nov. **Antonie Van Leeuwenhoek**, 108, 919-931. doi: 10.1007/s10482-015-0546-8

Gurevich, A., Saveliev, V., Vyahhi, N., Tesler, G. (2013). QUAST: quality assessment tool for genome assemblies. **Bioinformatics**, 29(8), 1072-1075. doi: 10.1093/bioinformatics/btt086

Harder, C. B. et al. (2023). *Mycena* species can be opportunist□generalist plant root invaders. **Environmental Microbiology**, 25(10), 1875-1893. doi: 10.1111/1462-2920.16398

Hidalgo, P., Flores, M. (1994). Occurrence of the killer character in yeasts associated with Spanish wine production. **Food microbiology**, 11(2), 161-167. doi: 10.1006/fmic.1994.1019

Hodgson, V. J., Button, D., Walker, G. M. (1995). Anti-*Candida* activity of a novel killer toxin from the yeast *Williopsis mrakii*. **Microbiology**, 141(8), 2003-2012. doi:10.1099/13500872-141-8-2003

Houbraken, J. et al. (2020). Classification of *Aspergillus*, *Penicillium*, *Talaromyces* and related genera (Eurotiales): An overview of families, genera, subgenera, sections, series and species. **Studies in mycology**, 95, 5-169. doi: 10.1016/j.simyco.2020.05.002

Ivannikova, Y. V., Naumova, E. S., Naumov, G. I. (2006). Detection of viral dsRNA in the yeast *Saccharomyces bayanus*. **Doklady Biological Sciences**. Vol. 406. New York: Consultants Bureau, c1965-1992. doi: 10.1134/S0012496606010297

Ivannikova, Y. V., Naumova, E. S., Naumov, G. I. (2007). Viral dsRNA in the wine yeast *Saccharomyces bayanus* var. *uvarum*. **Research in microbiology**, 158(8-9), 638-643. doi: 10.1016/j.resmic.2007.07.008

Jones, P., et al. (2014). InterProScan 5: genome-scale protein function classification. **Bioinformatics**, 30(9), 1236-1240. doi: 10.1093/bioinformatics/btu031

Julius D, Brake A, Blair L, Kunisawa R, Thorner J (1984). Isolation of the putative structural gene for the lysine-arginine-cleaving endopeptidase required for processing of yeast prepro-α-factor. **Cell**. 37(3): 1075–1089. doi: 10.1016/0092-8674(84)90442-2.

Jumper, J., et al. (2021). Highly accurate protein structure prediction with AlphaFold. **Nature**, 596(7873), 583-589. doi: 10.1038/s41586-021-03819-2

Jurjevic, Z., Peterson, S. W., Horn, B. W. (2012). *Aspergillus* section *Versicolores*: nine new species and multilocus DNA sequence based phylogeny. **IMA fungus**, 3(1), 59-79. doi:10.5598/imafungus.2012.03.01.07

Károlyi, G., Neufeld, Z., Scheuring, I. (2005). Rock-scissors-paper game in a chaotic flow: The effect of dispersion on the cyclic competition of microorganisms. **Journal of theoretical biology**, 236(1), 12-20. doi: 10.1016/j.jtbi.2005.02.012

Katoh, K., Rozewicki, J., Yamada, K. D. (2019). MAFFT online service: multiple sequence alignment, interactive sequence choice and visualization. **Briefings in Bioinformatics**, 20(4), 1160-1166. doi: 10.1093/bib/bbx108

Kerr, B., Riley, M. A., Feldman, M. W., & Bohannan, B. J. (2002). Local dispersal promotes biodiversity in a real-life game of rock–paper–scissors. **Nature**, 418(6894), 171-174. doi: 10.1038/nature00823

Klassen, R., Meinhardt, F. (2007). Linear protein-primed replicating plasmids in eukaryotic microbes. **Microbial Linear Plasmids**. Berlin, Heidelberg: Springer Berlin Heidelberg, 187-226. doi: 10.1007/7171_2007_095

Klassen, R., Schaffrath, R., Buzzini, P., Ganter, P. F. (2017). Antagonistic interactions and killer yeasts. **Yeasts in natural ecosystems: ecology**, 229-275. doi: 10.1007/978-3-319-61575-2_9

Koltin, Y., Day, P. R. (1976). Suppression of the killer phenotype in *Ustilago maydis*. **Genetics**, 82(4), 629-637. doi: 10.1093/genetics/82.4.629

Krassowski, T., et al. (2018). Evolutionary instability of CUG-Leu in the genetic code of budding yeasts. **Nature communications**, 9(1), 1887. doi: 10.1038/s41467-018-04374-7

Kriventseva, E. V., Kuznetsov, D., Tegenfeldt, F., Manni, M., Dias, R., Simão, F. A., Zdobnov, E. M. (2019). OrthoDB v10: sampling the diversity of animal, plant, fungal, protist, bacterial and viral genomes for evolutionary and functional annotations of orthologs. **Nucleic acids research**, 47(D1), D807-D811. doi: 10.1093/nar/gky1053

Kurtzman C. P., Robnett, C. J. (1998) Identification and phylogeny of ascomycetous yeasts from analysis of nuclear large subunit (26S) ribosomal DNA partial sequences. **Antonie Van Leeuwenhoek,** 73(4):331–371. doi: 10.1023/a:1001761008817.

Kurtzman, C. P., Robnett, C. J. (2003). Phylogenetic relationships among yeasts of the '*Saccharomyces* complex' determined from multigene sequence analyses. **FEMS yeast research**, 3(4), 417-432. doi: 10.1016/S1567-1356(03)00012-6

Laetsch, D. R., Blaxter, M. L. (2017). BlobTools: Interrogation of genome assemblies. **F1000Research**, 6(1287), 1287. doi: 10.12688/f1000research.12232.1

Leal, I. R., Oliveira, P. S. (1998). Interactions between Fungus□Growing Ants (Attini), Fruits and Seeds in Cerrado Vegetation in Southeast Brasil. **Biotropica**, 30(2), 170-178. doi: 10.1111/j.1744-7429.1998.tb00052.x

Lee, M. D., Creagh, J. W., Fredericks, L. R., Crabtree, A. M., Patel, J. S., Rowley, P. A. (2022). The Characterization of a Novel Virus Discovered in the Yeast *Pichia membranifaciens*. **Viruses**, 14(3), 594. doi: 10.3390/v14030594

Li, H. (2018). Minimap2: pairwise alignment for nucleotide sequences. **Bioinformatics**, 34(18), 3094-3100. doi: 10.1093/bioinformatics/bty191

Li, H., et al. (2009). The sequence alignment/map format and SAMtools. **Bioinformatics**, 25(16), 2078-2079. doi: 10.1093/bioinformatics/btp352

Libberton, B., Horsburgh, M. J., Brockhurst, M. A. (2015). The effects of spatial structure, frequency dependence and resistance evolution on the dynamics of toxin□mediated microbial invasions. **Evolutionary applications**, 8(7), 738-750. doi: 10.1111/eva.12284

Liu, H., Fu, Y., Jiang, D., Li, G., Xie, J., Cheng, J., Peng, Y., Ghabrial, S. A. Yi, X. (2010). Widespread horizontal gene transfer from double-stranded RNA viruses to eukaryotic nuclear genomes. **Journal of virology**, 84(22), 11876-11887. doi: 10.1128/jvi.00955-10

Lomsadze, A., Ter-Hovhannisyan, V., Chernoff, Y. O., Borodovsky, M. (2005). Gene identification in novel eukaryotic genomes by self-training algorithm. **Nucleic acids research**, 33(20), 6494-6506. doi: 10.1093/nar/gki937

Lu, S., Faris, J. D. (2019). *Fusarium graminearum* KP4-like proteins possess root growth-inhibiting activity against wheat and potentially contribute to fungal virulence in seedling rot. **Fungal genetics and biology**, 123, 1-13. doi: 10.1016/j.fgb.2018.11.002

Madbouly, A. K., Elyousr, K. A. A., Ismail, I. M. (2020). Biocontrol of *Monilinia fructigena*, causal agent of brown rot of apple fruit, by using endophytic yeasts. **Biological control**, 144, 104239. doi: 10.1016/j.biocontrol.2020.104239

Magliani, W., Conti, S., Gerloni, M., Bertolotti, D., Polonelli, L. (1997). Yeast killer systems. **Clinical microbiology reviews**, 10(3), 369-400. doi: 10.1128/cmr.10.3.369

Makower, M., Bevan, E. A. (1963). The inheritance of a killer character in yeast (*Saccharomyces cerevisiae*). **Genetics today. Proceedings of the XI International Congress of Genetics**, v. 1, 202.

Maksimova, I. A., Glushakova, A. M., Kachalkin, A. V., Chernov, I. Y., Panteleeva, S. N., Reznikova, Z. I. (2016). Yeast communities of Formica aquilonia colonies. **Microbiology**, 85, 124-129. doi: 10.1134/S0026261716010045

Marquina, D., Santos, A., Peinado, J. (2002). Biology of killer yeasts. **International Microbiology**, 5, 65-71. doi: 10.1007/s10123-002-0066-z

McBride, R., Greig, D., Travisano, M. (2008). Fungal viral mutualism moderated by ploidy. **Evolution**, 62(9), 2372-2380. doi: 10.1111/j.1558-5646.2008.00443.x

Meyer, W., Mitchell, T.G., Freedman, E.Z., Vilgalys, R. (1993) Hybridization probes for conventional DNA fingerprinting used as single primers in the polymerase chain reaction to distinguish strains of *Cryptococcus neoformans*. **Journal of Clinical Microbiology**, 31(9):2274–2280. doi: 10.1128/jcm.31.9.2274-2280.1993.

Meyer, S. T., Leal, I. R., Tabarelli, M., Wirth, R. (2011). Ecosystem engineering by leaf-cutting ants: nests of *Atta cephalotes* drastically alter forest structure and microclimate. **Ecological entomology**, 36(1), 14-24. doi: 10.1111/j.1365-2311.2010.01241.x

Middelbeek, E. J., Hermans, J. M., Stumm, C., Muytjens, H. L. (1980). High incidence of sensitivity to yeast killer toxins among *Candida* and *Torulopsis* isolates of human origin. **Antimicrobial Agents and Chemotherapy**, 17(3), 350-354. doi: 10.1128/aac.17.3.350

Möller, A. (1893). **Die Pilzgärten einiger südamerikanischer Ameisen** (No. 6). G. Fischer.

Myers, J. M., et al. (2020). Survey of early-diverging lineages of fungi reveals abundant and diverse mycoviruses. **mBio** 11: e02027-20. doi: 10.1128/mbio.02027-20

Naumov, G. I., Ivannikova, Y. V., Chernov, I. Y., Naumova, E. S. (2009). Natural polymorphism of the plasmid double-stranded RNA of the *Saccharomyces* yeasts. **Microbiology**, 78, 208-213. doi: 10.1134/S0026261709020118

Nguyen, L. T., Schmidt, H. A., Von Haeseler, A., Minh, B. Q. (2015). IQ-TREE: a fast and effective stochastic algorithm for estimating maximum-likelihood phylogenies. **Molecular Biology and Evolution**, 32(1), 268-274. doi: 10.1093/molbev/msu300

Nguyen, N. H., Suh, S. O., Blackwell, M. (2007). Five novel *Candida* species in insect-associated yeast clades isolated from Neuroptera and other insects. **Mycologia**, 99(6), 842–858. doi: 10.1080/15572536.2007.11832516

Nomoto, H., Kitano, K., Shimazaki, T., Kodama, K., Hara, S. (1984). Distribution of killer yeasts in the genus *Hansenula*. **Agricultural and biological chemistry**, 48(3), 807-809. doi: 10.1271/bbb1961.48.807

Nygaard, S., et al. (2016). Reciprocal genomic evolution in the ant–fungus agricultural symbiosis. **Nature Communications**, 7(1), 12233. doi: 10.1038/ncomms12233

Okada, R., Kiyota, E., Moriyama, H., Fukuhara, T., Natsuaki, T. (2015). A simple and rapid method to purify viral dsRNA from plant and fungal tissue. **Journal of General Plant Pathology**, 81, 103-107. doi: 10.1007/s10327-014-0575-6

Pagnocca, F. C., Carreiro, S. C., Bueno, O. C., Hebling, M. J., Da Silva, O. A. (1996). Microbiological changes in the nests of leaf□cutting ants fed on sesame leaves. **Journal of Applied Entomology**, 120(1□5), 317–320. doi: 10.1111/j.1439-0418.1996.tb01612.x

Pagnocca, F. C., Rodrigues, A., Nagamoto, N. S., Bacci, M. (2008). Yeasts and filamentous fungi carried by the gynes of leaf-cutting ants. **Antonie van Leeuwenhoek**, 94(4), 517–526. doi: 10.1007/s10482-008-9268-5

Perez, M. F., Contreras, L., Garnica, N. M., Fernández-Zenoff, M. V., Farías, M. E., Sepulveda, M., Ramallo, J., Dib, J. R. (2016). Native killer yeasts as biocontrol agents of postharvest fungal diseases in lemons. **PloS One**, 11(10), e0165590. doi: 10.1371/journal.pone.0165590

Peterson, S. W., Ito, Y., Horn, B. W., Goto, T. (2001). *Aspergillus bombycis*, a new aflatoxigenic species and genetic variation in its sibling species, *A. nomius*. **Mycologia**, 93(4), 689-703. doi: 10.1080/00275514.2001.12063200

Pfeiffer, I., Golubev, W. I., Farkas, Z., Kucsera, J., Golubev, N. (2004). Mycocin production in *Cryptococcus aquaticus*. **Antonie Van Leeuwenhoek**, 86, 369-375. doi: 10.1007/s10482-004-0888-0

Philliskirk, G., Young, T. W. (1975). The occurrence of killer character in yeasts of various genera. **Antonie van Leeuwenhoek**, 41, 147-151. doi: 10.1007/BF02565046

Pieczynska, M. D., de Visser, J. A. G., Korona, R. (2013). Incidence of symbiotic dsRNA 'killer' viruses in wild and domesticated yeast. **FEMS Yeast Research**, 13(8), 856–859. doi: 10.1111/1567-1364.12086

Pieczynska, M. D., Wloch-Salamon, D., Korona, R., de Visser, J. A. G. (2016). Rapid multiple-level coevolution in experimental populations of yeast killer and nonkiller strains. **Evolution**, 70(6), 1342-1353. doi: 10.1111/evo.12945

Pintar, J., Starmer, W. T. (2003). The costs and benefits of killer toxin production by the yeast Pichia kluyveri. **Antonie van Leeuwenhoek**, 83, 89-97. doi: 10.1023/A:0000000089097

Posit team (2023). RStudio: Integrated Development Environment for R. Posit Software, PBC, Boston, MA. URL http://www.posit.co/.

R Core Team. (2023). R: A Language and Environment for Statistical Computing.; **R Foundation for Statistical Computing: Vienna, Austria**; Available online: https://www.R-project.org/

Ramachandran GN, Ramakrishnan C, Sasisekharan V (1963). Stereochemistry of polypeptide chain configurations. **J Mol Biol**. 7(1): 95–99. doi: 10.1016/s0022-2836(63)80023-6.

Rambaut, A., 2016. **Figtree v. 1.4.3**. http://tree.bio.ed.ac.uk/software/figtree/2016.

Ramírez, M., Velázquez, R., Maqueda, M., López-Piñeiro, A., Ribas, J. C. (2015). A new wine *Torulaspora delbrueckii* killer strain with broad antifungal activity and its toxin-encoding double-stranded RNA virus. **Frontiers in microbiology**, 6, 983. doi: 10.3389/fmicb.2015.00983

Robledo-Leal, E., Elisondo-Zatuche, M., Treviño-Rangel, R. J., González, G. M., Hernández-Luna, C. (2016). Isolation of killer yeasts from ants of the genus *Atta* and their effect on the red tomato's fungal pathogen *Geotrichum candidum*. **Mexican Journal of Phytopathology**, 34, 258–269. doi: 10.18781/r.mex.fit.1605-3

Rodrigues, A., Bacci Jr, M., Mueller, U. G., Ortiz, A., Pagnocca, F. C. (2008). Microfungal "weeds" in the leafcutter ant symbiosis. **Microbial Ecology**, 56, 604-614. doi: 10.1007/s00248-008-9380-0

Rodrigues, A., Cable, R. N., Mueller, U. G., Bacci, M., Pagnocca, F. C. (2009). Antagonistic interactions between garden yeasts and microfungal garden pathogens of leaf-cutting ants. **Antonie Van Leeuwenhoek**, 96, 331-342. doi: 10.1007/s10482-009-9350-7

Rodríguez-Cousiño, N., Gómez, P., Esteban, R. (2017). Variation and distribution of LA helper totiviruses in *Saccharomyces* sensu stricto yeasts producing different killer toxins. Toxins, 9(10), 313. doi: doi.org/10.3390/toxins9100313

Rodríguez-Cousiño, N., Maqueda, M., Ambrona, J., Zamora, E., Esteban, R., Ramírez, M. (2011). A new wine *Saccharomyces cerevisiae* killer toxin (Klus), encoded by a double-stranded RNA virus, with broad antifungal activity is evolutionarily related to a chromosomal host gene. **Applied and environmental microbiology**, 77(5), 1822-1832. doi: 10.1128/AEM.02501-10

Rodriguez Coy, L., Plummer, K. M., Khalifa, M. E., MacDiarmid, R. M. (2022). Mycovirus-encoded suppressors of RNA silencing: Possible allies or enemies in the use of RNAi to control fungal disease in crops. **Frontiers in Fungal Biology**, 3, 965781. doi: 10.3389/ffunb.2022.965781

Ronque, M. U., Feitosa, R. M., Oliveira, P. S. (2019). Natural history and ecology of fungus-farming ants: a field study in Atlantic rainforest. **Insectes Sociaux**, 66(3), 375-387. doi: 10.1007/s00040-019-00695-y

Rowley, P. A. (2017). The frenemies within: viruses, retrotransposons and plasmids that naturally infect *Saccharomyces* yeasts. **Yeast**, 34(7), 279-292. doi: 10.1002/yea.3234

Rupert, C. B., Rusche, L. N. (2022). The Pathogenic Yeast *Candida parapsilosis* Forms Pseudohyphae through Different Signaling Pathways Depending on the Available Carbon Source. **Msphere**, 7(3), e00029-22. doi: 10.1128/msphere.00029-22

Satwika, D., Klassen, R., Meinhardt, F. (2012). Repeated capture of a cytoplasmic linear plasmid by the host nucleus in *Debaryomyces hansenii*. **Yeast**, 29(3-4), 145-154. doi: 10.1002/yea.2893

Schaffrath, R., Meinhardt, F., Klassen, R. (2018). Yeast killer toxins: Fundamentals and applications. **Physiology and Genetics: Selected Basic and Applied Aspects**, 87-118. doi: 10.1007/978-3-319-71740-1_3

Schmitt, M. J., Neuhausen, F. (1994). Killer toxin-secreting double-stranded RNA mycoviruses in the yeasts *Hanseniaspora uvarum* and *Zygosaccharomyces bailii*. **Journal of virology**, 68(3), 1765-1772. doi: 10.1128/jvi.68.3.1765-1772.1994

Schneider, C. A., Rasband, W. S., Eliceiri, K. W. (2012). NIH Image to ImageJ: 25 years of image analysis. **Nature methods**, 9(7), 671-675. doi: 10.1038/nmeth.2089

Schultz, T. R., Brady, S. G. (2008). Major evolutionary transitions in ant agriculture. **Proceedings of the National Academy of Sciences**, 105(14), 5435–5440. doi: 10.1073/pnas.0711024105

Schultz, T. R., Sosa-Calvo, J., Brady, S. G., Lopes, C. T., Mueller, U. G., Bacci Jr, M., Vasconcelos, H. L. (2015). The most relictual fungus-farming ant species cultivates the most recently evolved and highly domesticated fungal symbiont species. **The American Naturalist**, 185(5), 693–703. doi: 10.1086/680501

Segers, G. C., van Wezel, R., Zhang, X., Hong, Y., Nuss, D. L. (2006). Hypovirus papain-like protease p29 suppresses RNA silencing in the natural fungal host and in a heterologous plant system. **Eukaryotic Cell**, 5(6), 896-904. doi: 10.1128/EC.00373-05

Segers, G. C., Zhang, X., Deng, F., Sun, Q., Nuss, D. L. (2007). Evidence that RNA silencing functions as an antiviral defense mechanism in fungi. **Proceedings of the National Academy of Sciences**, 104(31), 12902-12906. doi: 10.1073/pnas.070250010

Seppey, M., Manni, M., Zdobnov, E.M. (2019). BUSCO: Assessing Genome Assembly and Annotation Completeness. In: Kollmar, M. (eds) Gene Prediction. **Methods in Molecular Biology**, vol 1962. Humana, New York, NY. doi: 10.1007/978-1-4939-9173-0_14

Silva, A., Bacci Jr, M., de Siqueira, C. G., Bueno, O. C., Pagnocca, F. C., Hebling, M. J. A. (2003). Survival of *Atta sexdens* workers on different food sources. **Journal of Insect Physiology**, 49(4), 307-313. doi: 10.1016/S0022-1910(03)00004-0

Silva, A., Bacci Jr, M., Pagnocca, F. C., Bueno, O. C., Hebling, M. J. A. (2006). Starch metabolism in *Leucoagaricus gongylophorus*, the symbiotic fungus of leaf-cutting ants. **Microbiological research**, 161(4), 299-303. doi: 10.1016/j.micres.2005.11.001

Somers, J. M., Bevan, E. A. (1969). The inheritance of the killer character in yeast. **Genetics Research**, 13(1), 71-83. doi: 10.1017/S0016672300002743

Spoel D. V. D., Lindahl E, Hess B, Groenhof G, Mark AE, Berendsen HJC (2005). GROMACS: Fast, flexible, and free. **J Comput Chem**. 26(16): 1701–1718. doi: 10.1002/jcc.20291.

Stanke, M., Morgenstern, B. (2005). AUGUSTUS: a web server for gene prediction in eukaryotes that allows user-defined constraints. **Nucleic acids research**, 33(suppl_2), W465-W467. doi: 10.1093/nar/gki458

Starmer, W. T., Ganter, P. F., Aberdeen, V., Lachance, M. A., Phaff, H. J. (1987). The ecological role of killer yeasts in natural communities of yeasts. **Canadian journal of microbiology**, 33(9), 783-796. doi: 10.1139/m87-134

Sternberg, L. D. S., Pinzon, M. C., Moreira, M. Z., Moutinho, P., Rojas, E. I., Herre, E. A. (2007). Plants use macronutrients accumulated in leaf-cutting ant nests. **Proceedings of the Royal Society B: Biological Sciences**, 274(1608), 315-321. doi: 10.1098/rspb.2006.3746

Stopiglia, C. D. O., Heidrich, D., Sorrentino, J. M., Vieira, F. J., Landell, M. F., Valente, P., Scroferneker, M. L. (2014). Susceptibility of species within the *Sporothrix schenckii* complex to a panel of killer yeasts. **Journal of Basic Microbiology**, 54(6), 578-584. doi: 10.1002/jobm.201200516

Studer G, Rempfer C, Waterhouse AM, Gumienny R, Haas J, Schwede T (2019). QMEANDisCo – Distance Constraints Applied on Model Quality Estimation. **Bioinformatics**. 36(6): 1765–1771. doi: 10.1093/bioinformatics/btz828.

Stumm, C., Hermans, J. M. H., Middelbeek, E. J., Croes, A. F., De Vries, G. J. M. L. (1977). Killer-sensitive relationships in yeasts from natural habitats. **Antonie van Leeuwenhoek**, 43, 125-128. doi: 10.1007/BF00395667

Suh, S. O., Blackwell, M. (2005). Four new yeasts in the *Candida mesenterica* clade associated with basidiocarp-feeding beetles. **Mycologia**, 97(1), 167-177. doi: 10.1080/15572536.2006.11832850

Suh, S. O., McHugh, J. V., Pollock, D. D., Backwell, M. (2005). The beetle gut: a hyperdiverse source of novel yeasts. **Mycological Research**, 109(3), 261–265. doi: 10.1017/S0953756205002388

Summerell, B. A., Laurence, M. H., Liew, E. C., Leslie, J. F. (2010). Biogeography and phylogeography of *Fusarium*: a review. **Fungal Diversity**, 44(1), 3-13. doi: 10.1007/s13225-010-0060-2

Suzuki, C., Nikkuni, S. (1994). The primary and subunit structure of a novel type killer toxin produced by a halotolerant yeast, *Pichia farinosa*. **Journal of Biological Chemistry**, 269(4), 3041-3046. doi: 10.1016/S0021-9258(17)42044-8

Taylor, D. J., Ballinger, M. J., Bowman, S. M., Bruenn, J. A. (2013). Virus-host co-evolution under a modified nuclear genetic code. **PeerJ**, 1, e50. doi: 10.7717/peerj.50

Taylor, D. J., Bruenn, J. (2009). The evolution of novel fungal genes from non-retroviral RNA viruses. **BMC biology**, 7, 1-11. doi: 10.1186/1741-7007-7-88

Thoen, E., et al. (2020). In vitro evidence of root colonization suggests ecological versatility in the genus *Mycena*. **New Phytologist**, 227(2), 601-612. doi: 10.1111/nph.16545

Travers-Cook, T. J., Jokela, J., Buser, C. C. (2023). The evolutionary ecology of fungal killer phenotypes. **Proceedings of the Royal Society B**, 290, 20231108. doi: 10.1098/rspb.2023.1108

Trindade, R. C., Resende, M. A., Silva, C. M., Rosa, C. A. (2002). Yeasts associated with fresh and frozen pulps of Brasilian tropical fruits. **Systematic and Applied Microbiology**, 25(2), 294-300. doi: 10.1078/0723-2020-00089

Vadasz, A. S., Vadasz, P., Gupthar, A. S., Abashar, M. E. (2003). Theoretical and experimental evidence of extinction and coexistence of killer and sensitive strains of yeast grown as a mixed culture in water. **International journal of food microbiology**, 84(2), 157-174. doi: 10.1016/S0168-1605(02)00417-8

Vaughan-Martini, A. (1995). *Saccharomyces barnetti* and *Saccharomyces spencerorum*: two new species of *Saccharomyces* sensu lato (van der Walt). **Antonie van Leeuwenhoek**, 68, 111-118. doi: 10.1007/BF00873098

Vijayraghavan, S., Kozmin, S. G., Strope, P. K., Skelly, D. A., Magwene, P. M., Dietrich, F. S., McCusker, J. H. (2023). RNA viruses, M satellites, chromosomal killer genes, and killer/nonkiller phenotypes in the 100-genomes *S. cerevisiae* strains. **G3: Genes, Genomes, Genetics**, 13(10), jkad167. doi: 10.1093/g3journal/jkad167

Villan Larios, et al. (2023). Exploring the Mycovirus Universe: Identification, Diversity, and Biotechnological Applications. **Journal of Fungi**, 9(3), 361. doi: 10.3390/jof9030361

Walker, G. M., Mcleod, A. H., Hodgson, V. J. (1995). Interactions between killer yeasts and pathogenic fungi. **FEMS microbiology letters**, 127(3), 213-222. doi: 10.1111/j.1574-6968.1995.tb07476.x

Weber, N. A. (1972). The fungus-culturing behavior of ants. **American Zoologist**, 12(3), 577–587. doi: 10.1093/icb/12.3.577

Wickham H (2016). ggplot2: Elegant Graphics for Data Analysis. Springer-Verlag New York. ISBN 978-3-319-24277-4, https://ggplot2.tidyverse.org.

Wloch-Salamon, D. M., Gerla, D., Hoekstra, R. F., de Visser, J. A. G. (2008). Effect of dispersal and nutrient availability on the competitive ability of toxin-producing yeast. **Proceedings of the Royal Society B: Biological Sciences**, 275(1634), 535-541. doi: 10.1098/rspb.2007.1461

Wójcik, M., Kordowska-Wiater, M. (2015). The occurrence of killer activity in yeasts isolated from natural habitats. **Acta Biochimica Polonica**, 62(4). doi: 10.18388/abp.2015_1141

Woods, D. R., Bevan, E. A. (1968). Studies on the nature of the killer factor produced by *Saccharomyces cerevisiae*. **Microbiology**, 51(1), 115–126. doi: 10.1099/00221287-51-1-115

Worsham, P. L., Bolen, P. L. (1990). Killer toxin production in *Pichia acaciae* is associated with linear DNA plasmids. **Current genetics**, 18, 77-80. doi: 10.1007/BF00321119

Zorg, J., Kilian, S., Radler, F. (1988). Killer toxin producing strains of the yeasts *Hanseniaspora uvarum* and *Pichia kluyveri*. **Archives of microbiology**, 149, 261-267. doi: 10.1007/BF00422015

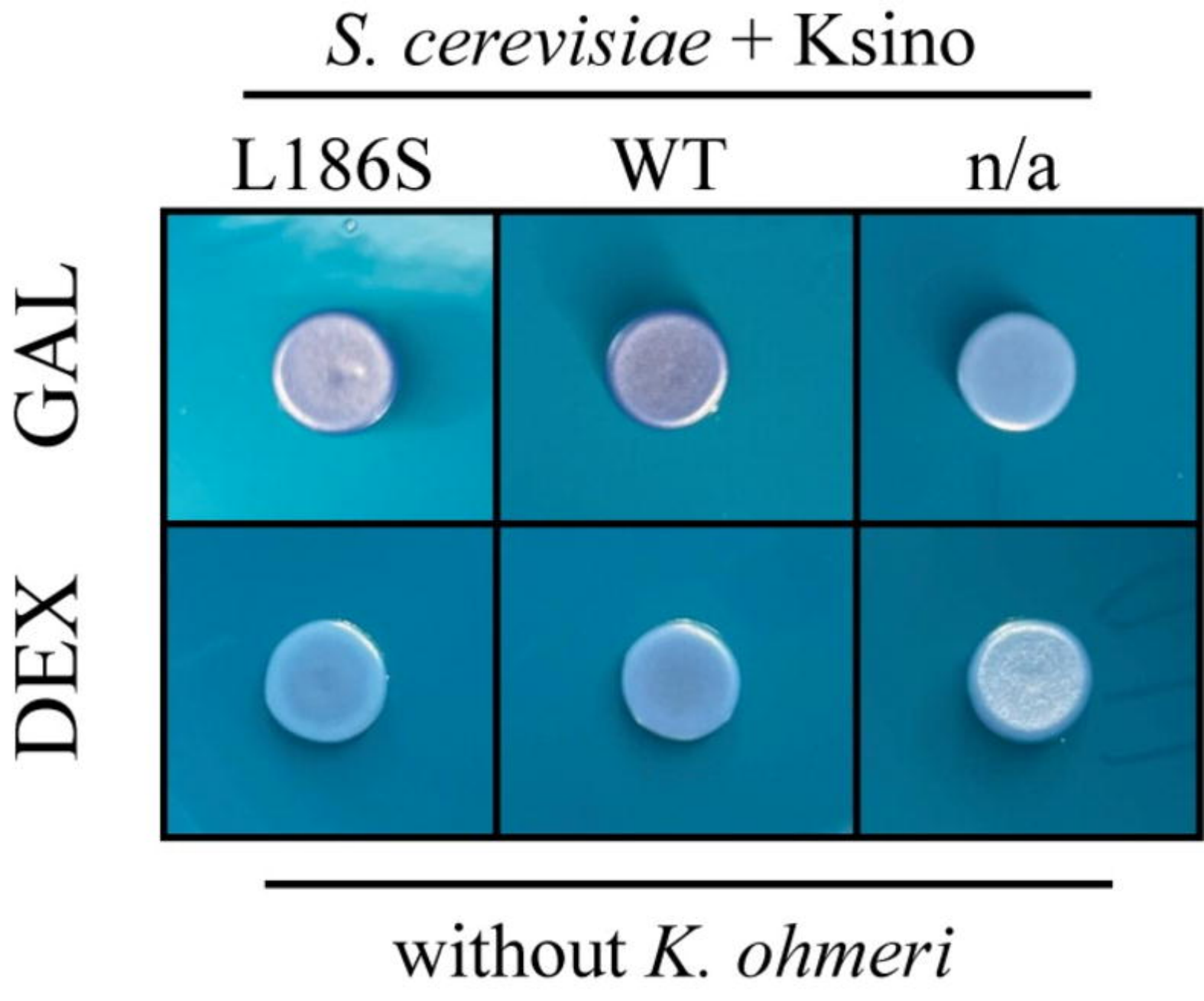
S. cerevisiae + Ksino
L186S
WT
n/a
GAL
DEX
without K. ohmeri

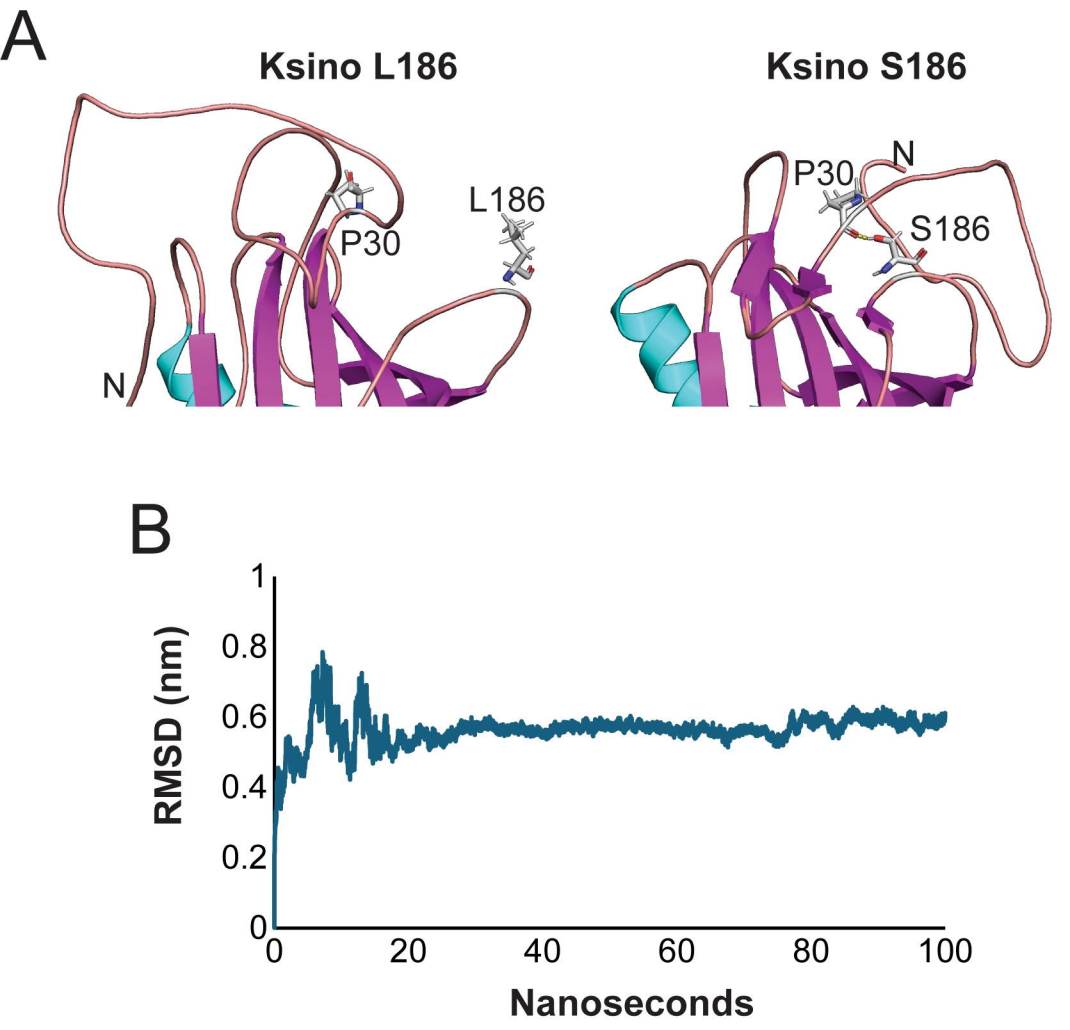
A
Ksino L186
Ksino S186
L186
P30
N
P30
N
S186
B
RMSD (nm)
1
0.8
0.6
0.4
0.2
0
0
20
40
60
80
100
Nanoseconds

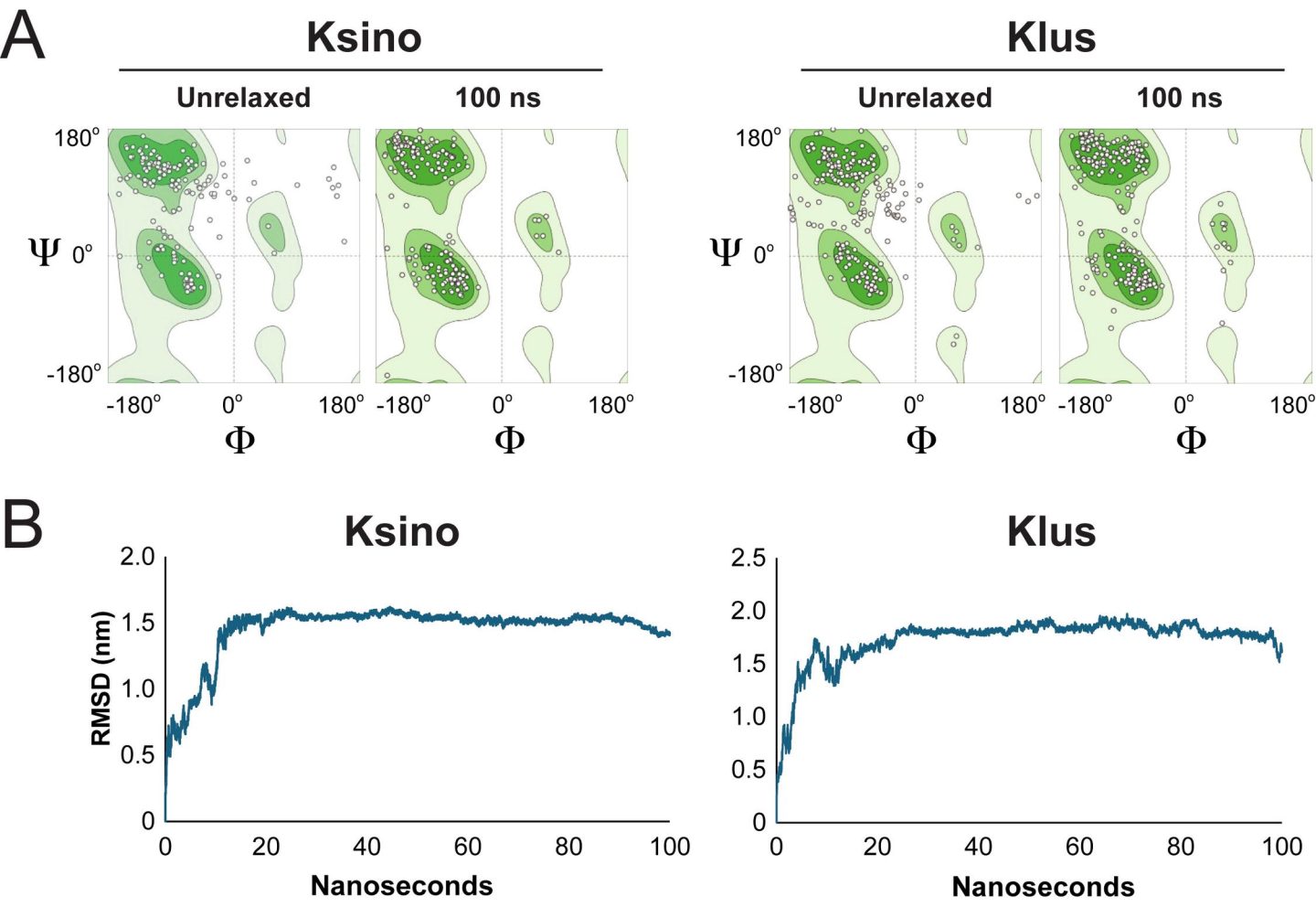
A
Ksino
Unrelaxed
100 ns
Klus
Unrelaxed
100 ns
180°
Ψ 0°
-180°
-180°
0°
180°
Φ
B
Ksino
Klus
RMSD (nm)
2.0
1.5
1.0
0.5
0
2.5
0
20
40
60
80
100
Nanoseconds

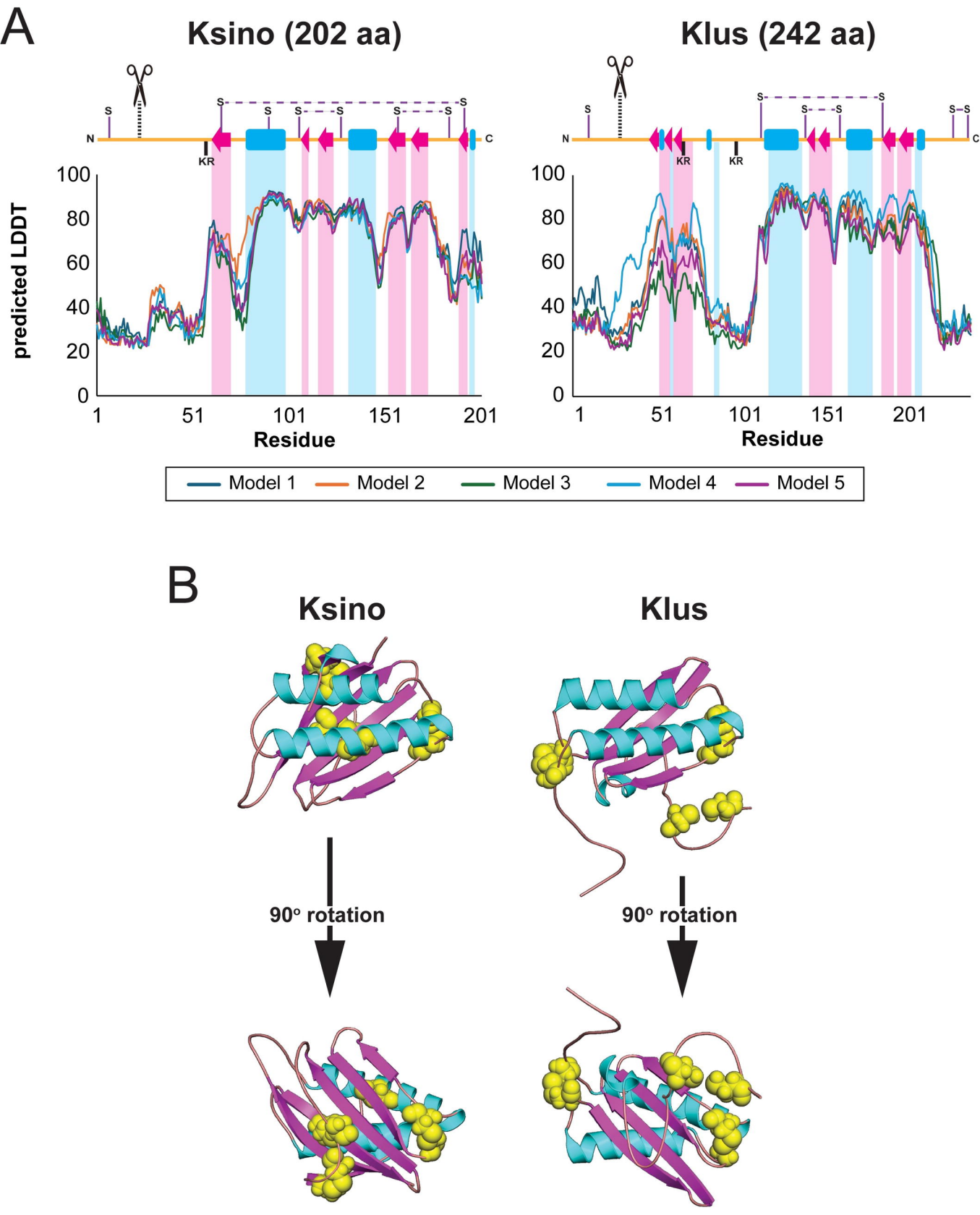
A
Ksino (202 aa)
Klus (242 aa)
predicted LDDT
Residue
Model 1
Model 2
Model 3
Model 4
Model 5
B
Ksino
Klus
90° rotation
90° rotation

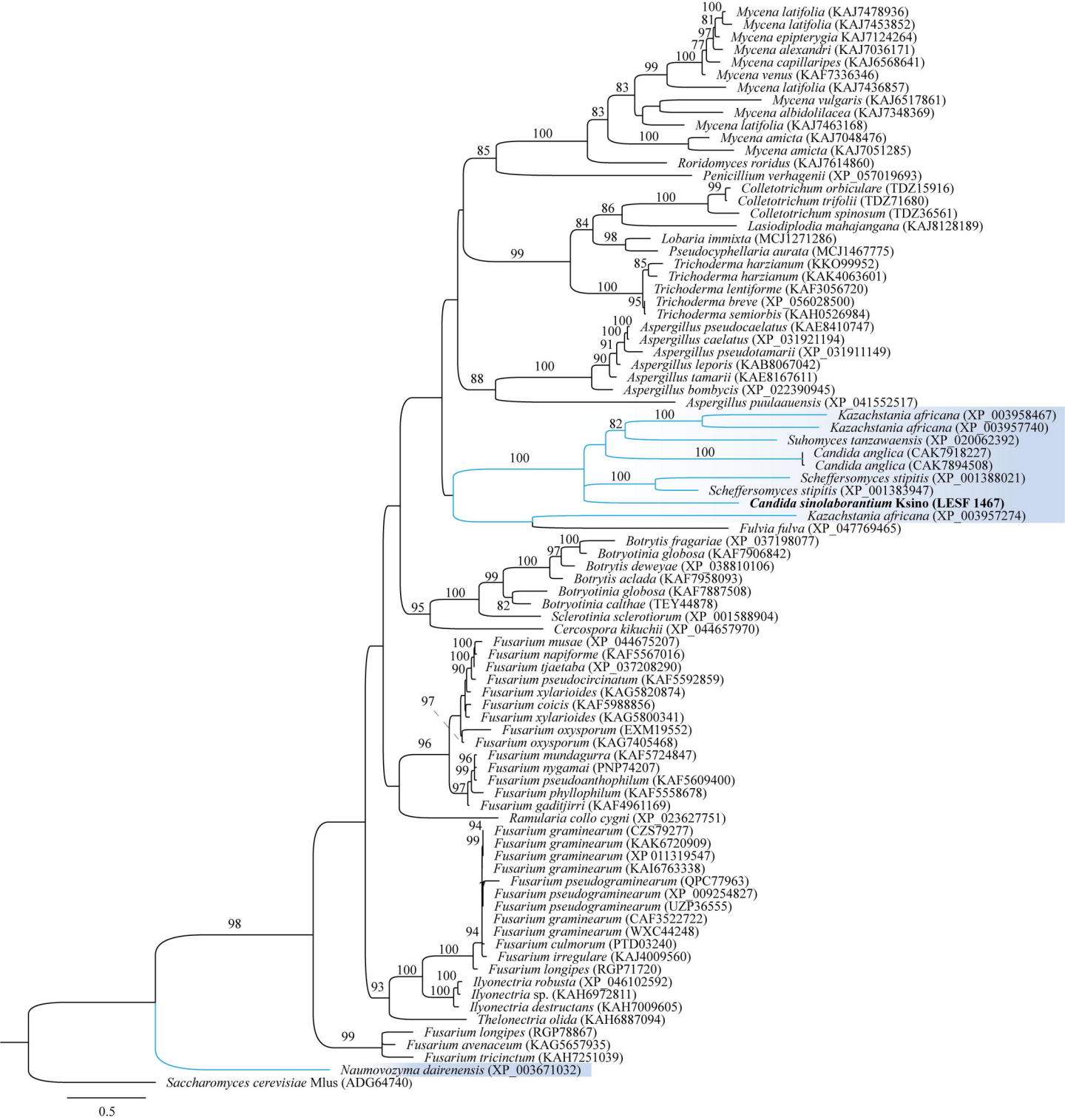
Mycena latifolia (KAJ7478936)
Mycena latifolia (KAJ7453852)
Mycena epipterygia KAJ7124264)
Mycena alexandri (KAJ7036171)
Mycena capillaripes (KAJ6568641)
Mycena venus (KAF7336346)
Mycena latifolia (KAJ7436857)
Mycena vulgaris (KAJ6517861)
Mycena albidolilacea (KAJ7348369)
Mycena latifolia (KAJ7463168)
Mycena amicta (KAJ7048476)
Mycena amicta (KAJ7051285)
Roridomyces roridus (KAJ7614860)
Penicillium verhagenii (XP_057019693)
Colletotrichum orbiculare (TDZ15916)
Colletotrichum trifolii (TDZ71680)
Colletotrichum spinosum (TDZ36561)
Lasiodiplodia mahajangana (KAJ8128189)
Lobaria immixta (MCJ1271286)
Pseudocyphellaria aurata (MCJ1467775)
Trichoderma harzianum (KKO99952)
Trichoderma harzianum (KAK4063601)
Trichoderma lentiforme (KAF3056720)
Trichoderma breve (XP_056028500)
Trichoderma semiorbis (KAH0526984)
Aspergillus pseudocaelatus (KAE8410747)
Aspergillus caelatus (XP_031921194)
Aspergillus pseudotamarii (XP_031911149)
Aspergillus leporis (KAB8067042)
Aspergillus tamarii (KAE8167611)
Aspergillus bombycis (XP_022390945)
Aspergillus puulaauensis (XP_041552517)
Kazachstania africana (XP_003958467)
Kazachstania africana (XP_003957740)
Suhomyces tanzawaensis (XP_020062392)
Candida anglica (CAK7918227)
Candida anglica (CAK7894508)
Scheffersomyces stipitis (XP_001388021)
Scheffersomyces stipitis (XP_001383947)
Candida sinolaborantium Ksino (LESF 1467)
Kazachstania africana (XP_003957274)
Fulvia fulva (XP_047769465)
Botrytis fragariae (XP_037198077)
Botryotinia globosa (KAF7906842)
Botrytis deweyae (XP_038810106)
Botrytis aclada (KAF7958093)
Botryotinia globosa (KAF7887508)
Botryotinia calthae (TEY44878)
Sclerotinia sclerotiorum (XP_001588904)
Cercospora kikuchii (XP_044657970)
Fusarium musae (XP_044675207)
Fusarium napiforme (KAF5567016)
Fusarium tjaetaba (XP_037208290)
Fusarium pseudocircinatum (KAF5592859)
Fusarium xylarioides (KAG5820874)
Fusarium coicis (KAF5988856)
Fusarium xylarioides (KAG5800341)
Fusarium oxysporum (EXM19552)
Fusarium oxysporum (KAG7405468)
Fusarium mundagurra (KAF5724847)
Fusarium nygamai (PNP74207)
Fusarium pseudoanthophilum (KAF5609400)
Fusarium phyllophilum (KAF5558678)
Fusarium gaditjirri (KAF4961169)
Ramularia collo cygni (XP_023627751)
Fusarium graminearum (CZS79277)
Fusarium graminearum (KAK6720909)
Fusarium graminearum (XP 011319547)
Fusarium graminearum (KAI6763338)
Fusarium pseudograminearum (QPC77963)
Fusarium pseudograminearum (XP_009254827)
Fusarium pseudograminearum (UZP36555)
Fusarium graminearum (CAF3522722)
Fusarium graminearum (WXC44248)
Fusarium culmorum (PTD03240)
Fusarium irregulare (KAJ4009560)
Fusarium longipes (RGP71720)
Ilyonectria robusta (XP_046102592)
Ilyonectria sp. (KAH6972811)
Ilyonectria destructans (KAH7009605)
Thelonectria olida (KAH6887094)
Fusarium longipes (RGP78867)
Fusarium avenaceum (KAG5657935)
Fusarium tricinctum (KAH7251039)
Naumovozyma dairenensis (XP_003671032)
Saccharomyces cerevisiae Mlus (ADG64740)
0.5

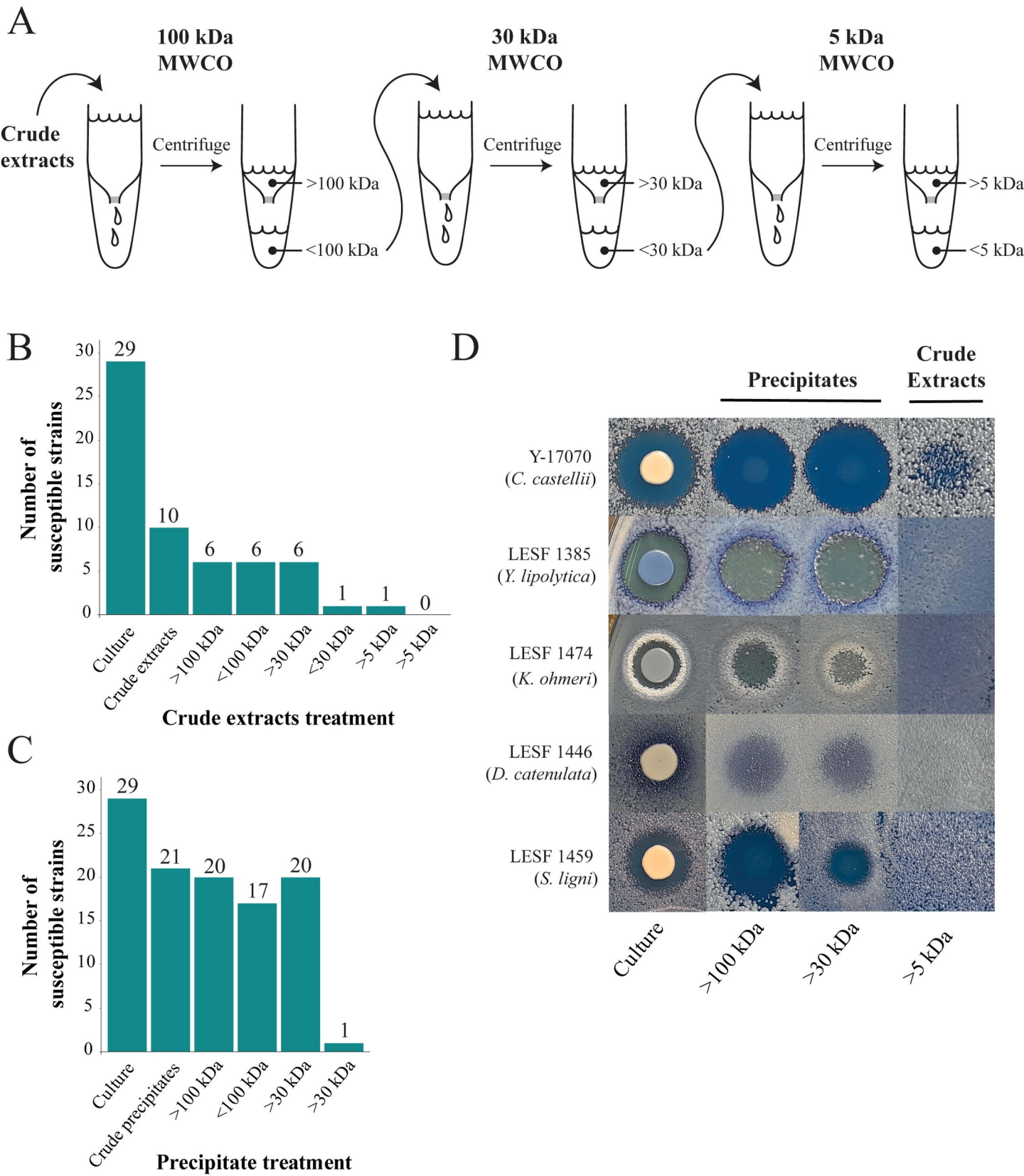
A
100 kDa MWCO
30 kDa MWCO
5 kDa MWCO
Crude extracts
Centrifuge
>100 kDa
<100 kDa
Centrifuge
>30 kDa
<30 kDa
Centrifuge
>5 kDa
<5 kDa
B
Number of susceptible strains
30
25
20
15
10
5
0
29
10
6
6
6
1
1
0
Culture
Crude extracts
>100 kDa
<100 kDa
>30 kDa
<30 kDa
>5 kDa
<5 kDa
Crude extracts treatment
C
Number of susceptible strains
30
25
20
15
10
5
0
29
21
20
17
20
1
Culture
Crude precipitates
>100 kDa
<100 kDa
>30 kDa
>30 kDa
Precipitate treatment
D
Precipitates
Crude Extracts
Y-17070 (C. castellii)
LESF 1385 (Y. lipolytica)
LESF 1474 (K. ohmeri)
LESF 1446 (D. catenulata)
LESF 1459 (S. ligni)
Culture
>100 kDa
>30 kDa
>5 kDa

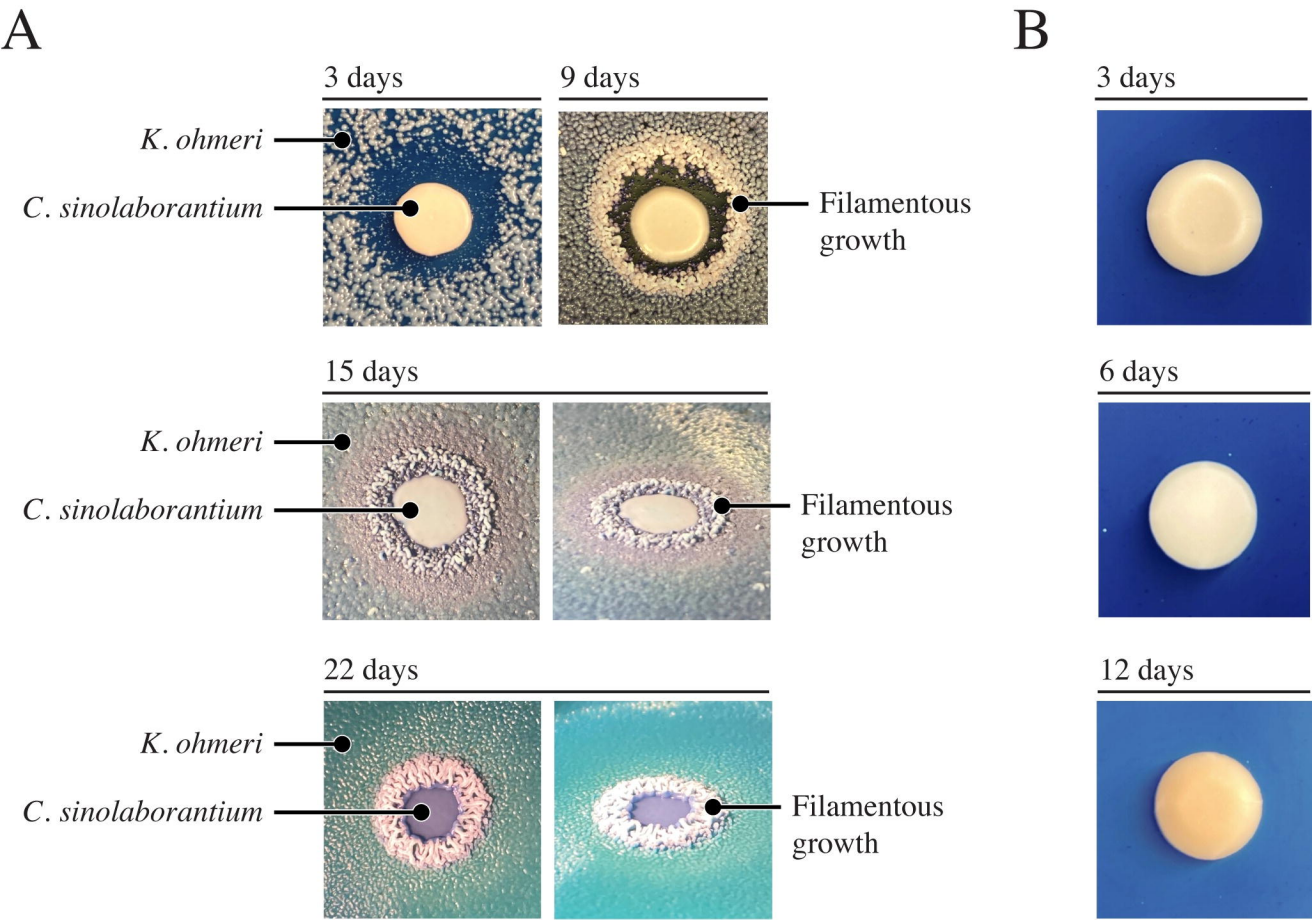
A
3 days
9 days
K. ohmeri
C. sinolaborantium
Filamentous growth
15 days
K. ohmeri
C. sinolaborantium
Filamentous growth
22 days
K. ohmeri
C. sinolaborantium
Filamentous growth
B
3 days
6 days
12 days

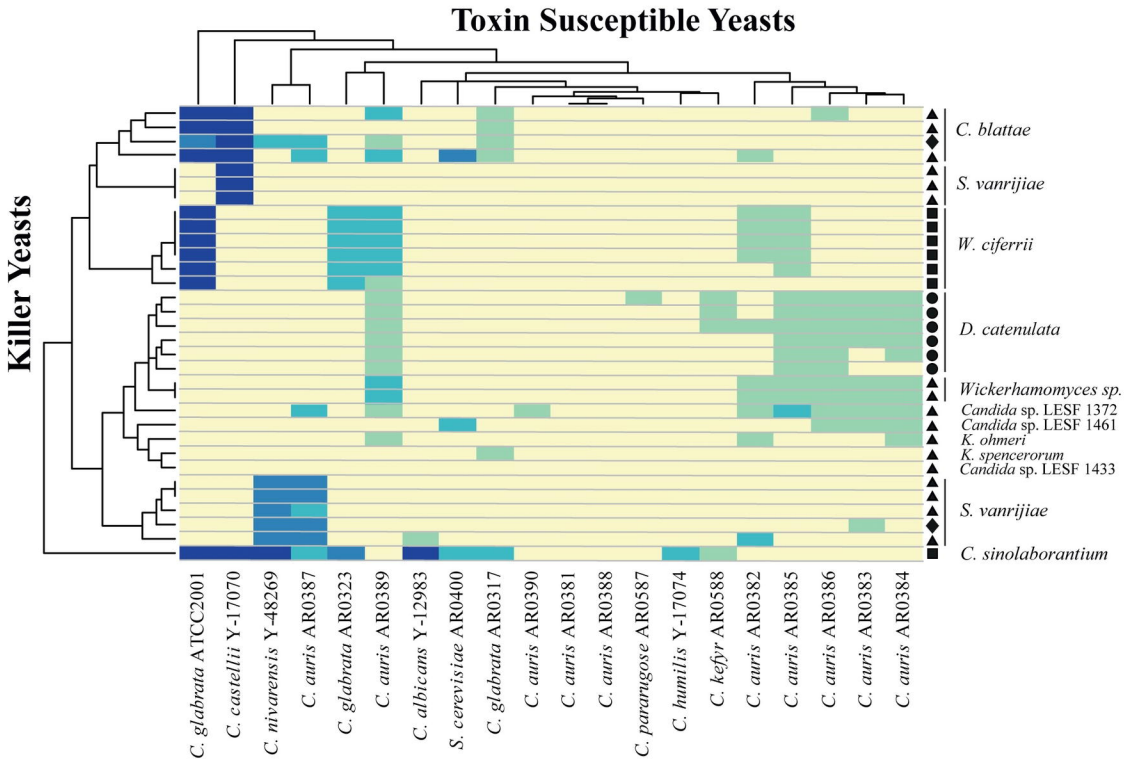
Toxin Susceptible Yeasts
Killer Yeasts
C. blattae
S. vanrijiae
W. ciferrii
D. catenulata
Wickerhamomyces sp.
Candida sp. LESF 1372
Candida sp. LESF 1461
K. ohmeri
K. spencerorum
Candida sp. LESF 1433
S. vanrijiae
C. sinolaborantium
C. glabrata ATCC2001
C. castellii Y-17070
C. nivarensis Y-48269
C. auris AR0387
C. glabrata AR0323
C. auris AR0389
C. albicans Y-12983
S. cerevisiae AR0400
C. glabrata AR0317
C. auris AR0390
C. auris AR0381
C. auris AR0388
C. parapsilosis AR0587
C. humilis Y-17074
C. kefyr AR0588
C. auris AR0382
C. auris AR0385
C. auris AR0386
C. auris AR0383
C. auris AR0384

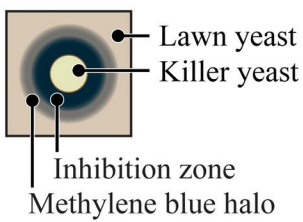
Lawn yeast
Killer yeast
Inhibition zone
Methylene blue halo

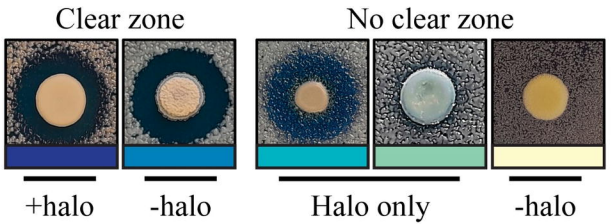
Clear zone
No clear zone
+halo
-halo
Halo only
-halo

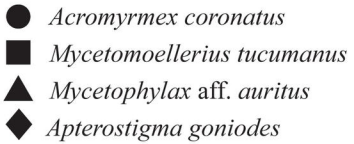
Acromyrmex coronatus
Mycetomoellerius tucumanus
Mycetophylax aff. auritus
Apterostigma goniodes

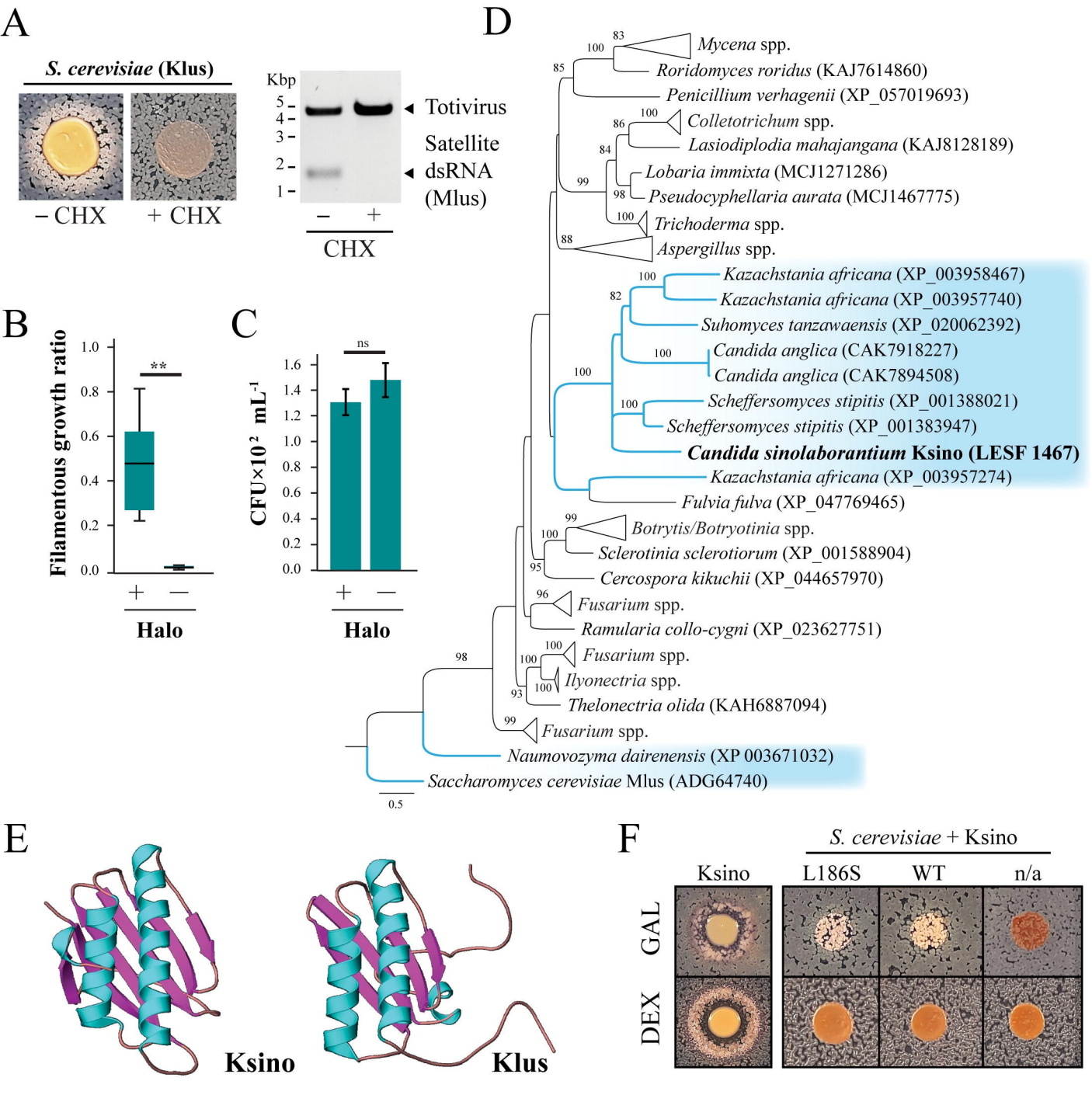
A
S. cerevisiae (Klus)
− CHX
+ CHX
Kbp
5
4
3
2
1
Totivirus
Satellite dsRNA (Mlus)
−
+
CHX
B
Filamentous growth ratio
1.0
0.8
0.6
0.4
0.2
0.0
**
+
−
Halo
C
CFU×10² mL⁻¹
1.6
1.4
1.2
1.0
0.8
0.6
0.4
0.2
0.0
ns
+
−
Halo
D
Mycena spp.
Roridomyces roridus (KAJ7614860)
Penicillium verhagenii (XP_057019693)
Colletotrichum spp.
Lasiodiplodia mahajangana (KAJ8128189)
Lobaria immixta (MCJ1271286)
Pseudocyphellaria aurata (MCJ1467775)
Trichoderma spp.
Aspergillus spp.
Kazachstania africana (XP_003958467)
Kazachstania africana (XP_003957740)
Suhomyces tanzawaensis (XP_020062392)
Candida anglica (CAK7918227)
Candida anglica (CAK7894508)
Scheffersomyces stipitis (XP_001388021)
Scheffersomyces stipitis (XP_001383947)
Candida sinolaborantium Ksino (LESF 1467)
Kazachstania africana (XP_003957274)
Fulvia fulva (XP_047769465)
Botrytis/Botryotinia spp.
Sclerotinia sclerotiorum (XP_001588904)
Cercospora kikuchii (XP_044657970)
Fusarium spp.
Ramularia collo-cygni (XP_023627751)
Fusarium spp.
Ilyonectria spp.
Thelonectria olida (KAH6887094)
Fusarium spp.
Naumovozyma dairenensis (XP 003671032)
Saccharomyces cerevisiae Mlus (ADG64740)
0.5
E
Ksino
Klus
F
S. cerevisiae + Ksino
Ksino
L186S
WT
n/a
GAL
DEX

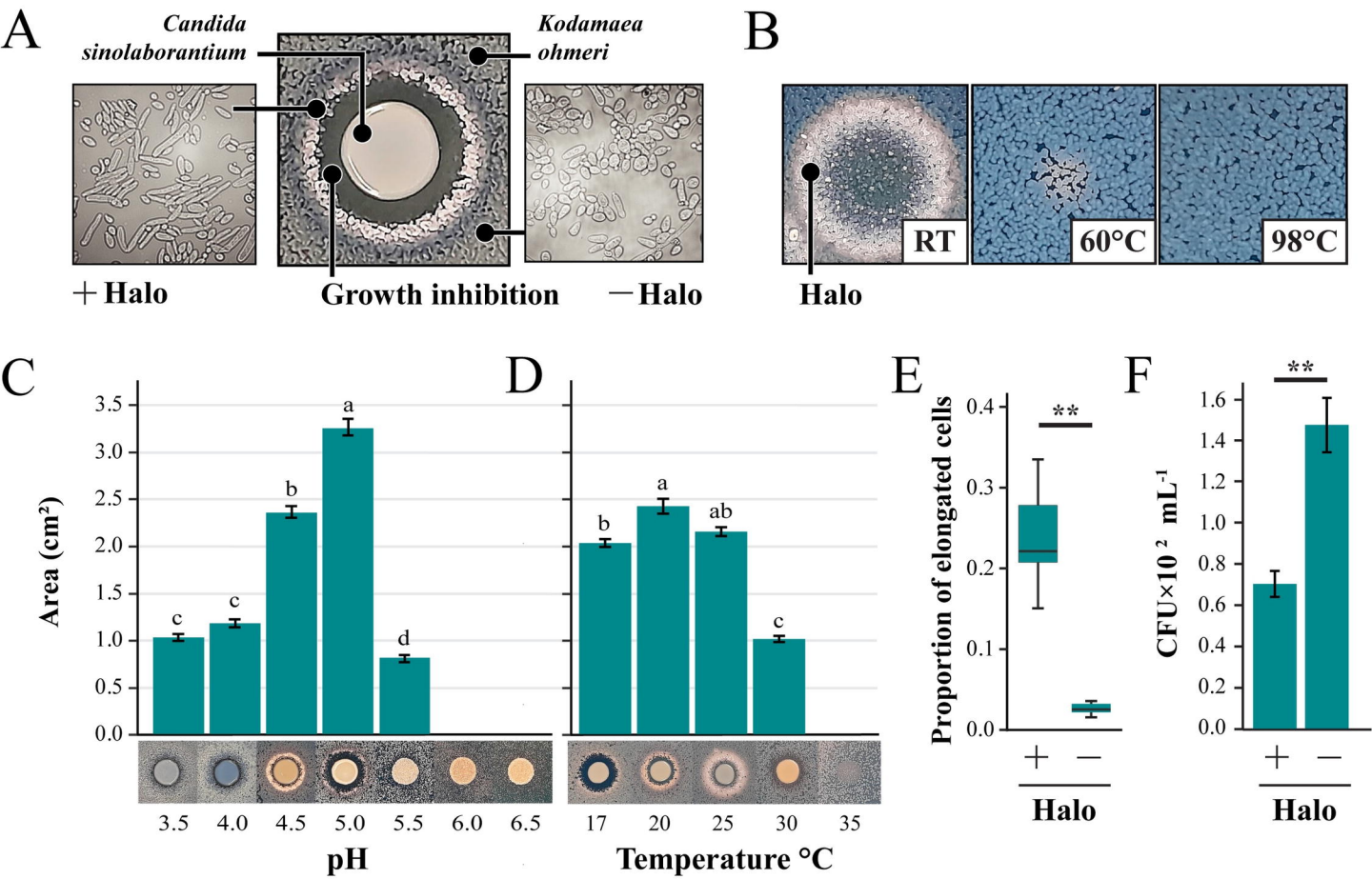
A
Candida sinolaborantium
Kodamaea ohmeri
+ Halo
Growth inhibition
− Halo
B
RT
60°C
98°C
Halo
C
Area (cm²)
3.5
3.0
2.5
2.0
1.5
1.0
0.5
0.0
c
c
b
a
d
3.5
4.0
4.5
5.0
5.5
6.0
6.5
pH
D
b
a
ab
c
17
20
25
30
35
Temperature °C
E
Proportion of elongated cells
0.4
0.3
0.2
0.1
0.0
**
+
−
Halo
F
CFU×10 ² mL⁻¹
1.6
1.4
1.2
1.0
0.8
0.6
0.4
0.2
0.0
**
+
−
Halo

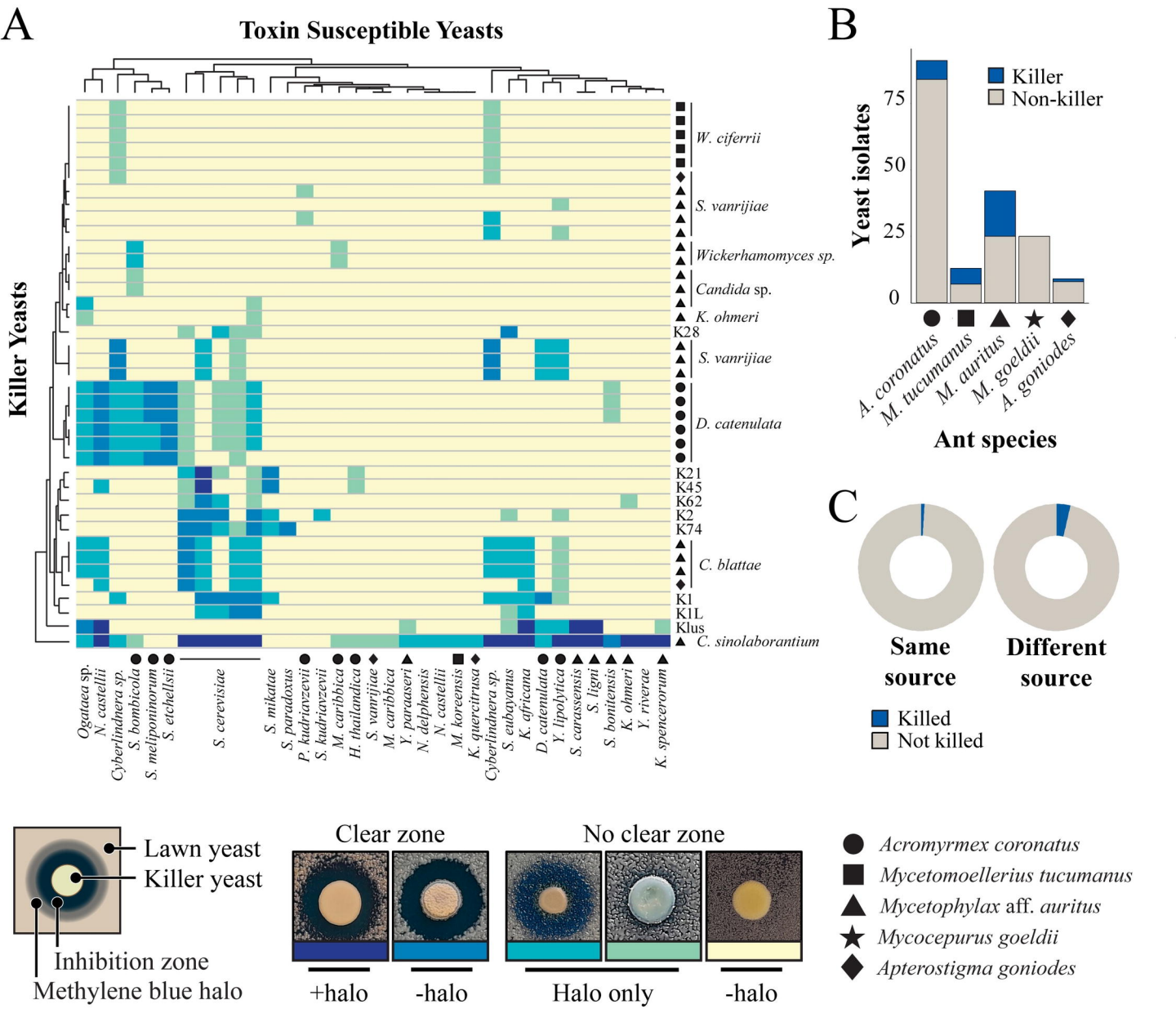
A
Toxin Susceptible Yeasts
Killer Yeasts
W. ciferrii
S. vanrijiae
Wickerhamomyces sp.
Candida sp.
K. ohmeri
K28
S. vanrijiae
D. catenulata
K21
K45
K62
K2
K74
C. blattae
K1
K1L
Klus
C. sinolaborantium
Ogataea sp.
N. castellii
Cyberlindnera sp.
S. bombicola
S. meliponinorum
S. etchellsii
S. cerevisiae
S. mikatae
S. paradoxus
P. kudriavzevii
S. kudriavzevii
M. caribbica
H. thailandica
S. vanrijiae
M. caribbica
Y. paraaseri
N. delphensis
N. castellii
M. koreensis
K. quercitrusa
Cyberlindnera sp.
S. eubayanus
K. africana
D. catenulata
Y. lipolytica
S. carassensis
S. ligni
S. bonitensis
K. ohmeri
Y. riverae
K. spencerorum
B
Killer
Non-killer
Yeast isolates
75
50
25
0
A. coronatus
M. tucumanus
M. auritus
M. goeldii
A. goniodes
Ant species
C
Same source
Different source
Killed
Not killed
Lawn yeast
Killer yeast
Inhibition zone
Methylene blue halo
Clear zone
No clear zone
+halo
-halo
Halo only
-halo
Acromyrmex coronatus
Mycetomoellerius tucumanus
Mycetophylax aff. auritus
Mycocepurus goeldii
Apterostigma goniodes

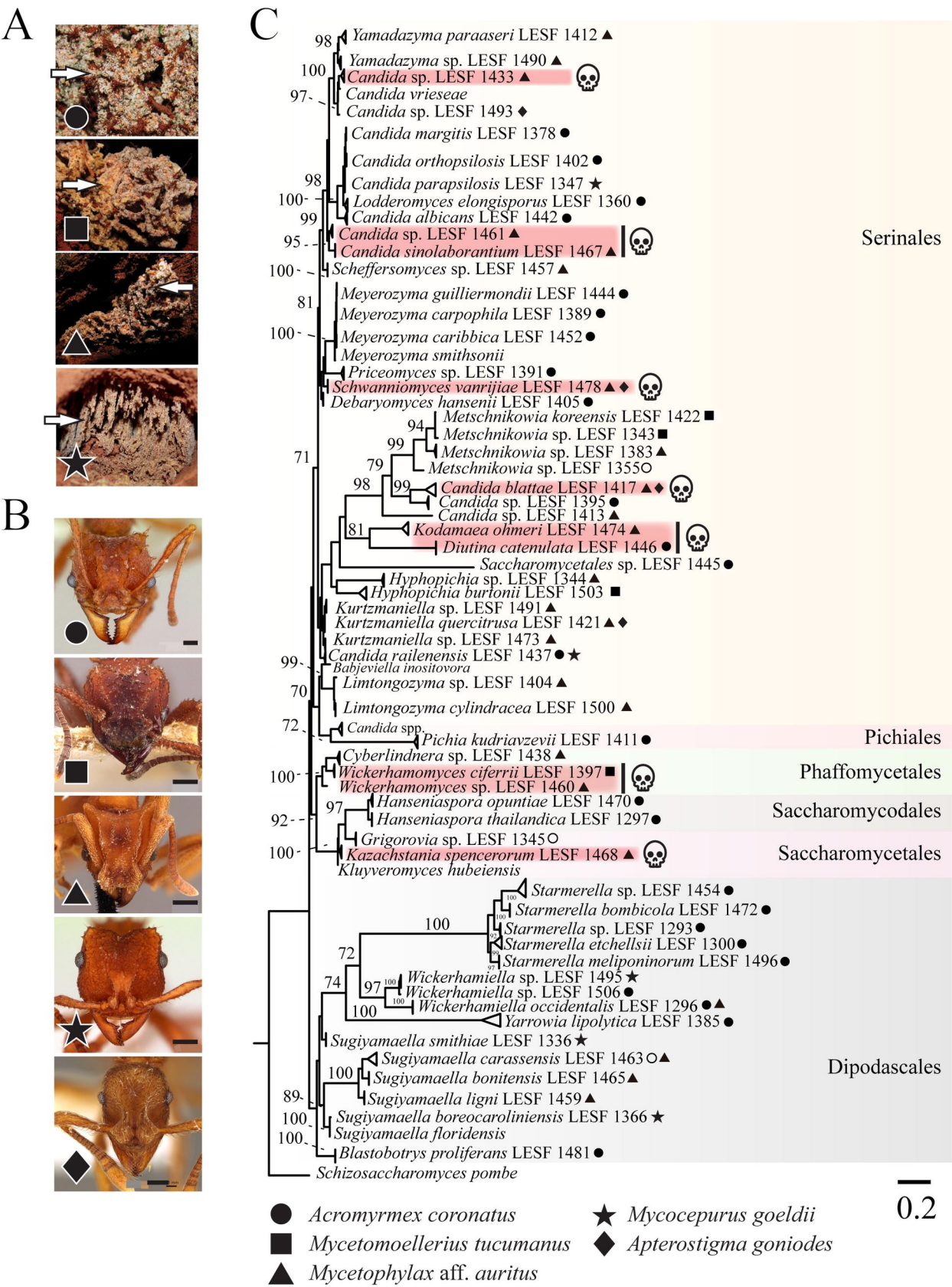
A
B
C
Yamadazyma paraaseri LESF 1412
Yamadazyma sp. LESF 1490
Candida sp. LESF 1433
Candida vrieseae
Candida sp. LESF 1493
Candida margitis LESF 1378
Candida orthopsilosis LESF 1402
Candida parapsilosis LESF 1347
Lodderomyces elongisporus LESF 1360
Candida albicans LESF 1442
Candida sp. LESF 1461
Candida sinolaborantium LESF 1467
Scheffersomyces sp. LESF 1457
Meyerozyma guilliermondii LESF 1444
Meyerozyma carpophila LESF 1389
Meyerozyma caribbica LESF 1452
Meyerozyma smithsonii
Priceomyces sp. LESF 1391
Schwanniomyces vanrijiae LESF 1478
Debaryomyces hansenii LESF 1405
Metschnikowia koreensis LESF 1422
Metschnikowia sp. LESF 1343
Metschnikowia sp. LESF 1383
Metschnikowia sp. LESF 1355
Candida blattae LESF 1417
Candida sp. LESF 1395
Candida sp. LESF 1413
Kodamaea ohmeri LESF 1474
Diutina catenulata LESF 1446
Saccharomycetales sp. LESF 1445
Hyphopichia sp. LESF 1344
Hyphopichia burtonii LESF 1503
Kurtzmaniella sp. LESF 1491
Kurtzmaniella quercitrusa LESF 1421
Kurtzmaniella sp. LESF 1473
Candida railenensis LESF 1437
Babjeviella inositovora
Limtongozyma sp. LESF 1404
Limtongozyma cylindracea LESF 1500
Candida spp.
Pichia kudriavzevii LESF 1411
Cyberlindnera sp. LESF 1438
Wickerhamomyces ciferrii LESF 1397
Wickerhamomyces sp. LESF 1460
Hanseniaspora opuntiae LESF 1470
Hanseniaspora thailandica LESF 1297
Grigorovia sp. LESF 1345
Kazachstania spencerorum LESF 1468
Kluyveromyces hubeiensis
Starmerella sp. LESF 1454
Starmerella bombicola LESF 1472
Starmerella sp. LESF 1293
Starmerella etchellsii LESF 1300
Starmerella meliponinorum LESF 1496
Wickerhamiella sp. LESF 1495
Wickerhamiella sp. LESF 1506
Wickerhamiella occidentalis LESF 1296
Yarrowia lipolytica LESF 1385
Sugiyamaella smithiae LESF 1336
Sugiyamaella carassensis LESF 1463
Sugiyamaella bonitensis LESF 1465
Sugiyamaella ligni LESF 1459
Sugiyamaella boreocaroliniensis LESF 1366
Sugiyamaella floridensis
Blastobotrys proliferans LESF 1481
Schizosaccharomyces pombe
Serinales
Pichiales
Phaffomycetales
Saccharomycodales
Saccharomycetales
Dipodascales
0.2
Acromyrmex coronatus
Mycetomoellerius tucumanus
Mycetophylax aff. auritus
Mycocepurus goeldii
Apterostigma goniodes